Master's thesis

NTNU
Norwegian University of Science and Technology
Faculty of Engineering
Department of Marine Technology

Emilie Grenth

Feasibility of a green corridor serviced by a battery-powered cargo ship

Master's thesis in Engineering and ICT
Supervisor: Sverre Steen
Co-supervisor: Benjamin Lagemann and YoungRong Kim
February 2024

NTNU
Norwegian University of
Science and Technology

Emilie Grenth

Feasibility of a green corridor serviced by a battery-powered cargo ship

Master's thesis in Engineering and ICT
Supervisor: Sverre Steen
Co-supervisor: Benjamin Lagemann and YoungRong Kim
February 2024

Norwegian University of Science and Technology
Faculty of Engineering
Department of Marine Technology

NTNU
Norwegian University of Science and Technology

NTNU Trondheim
Norwegian University of Science and Technology
Department of Marine Technology

MASTER THESIS IN MARINE TECHNOLOGY

Autumn 2023

FOR

Emilie Louise Mongstad Grenth

Feasibility of a green corridor serviced by a battery-powered cargo ship

Green corridors have been suggested as a way of introducing zero-emission technology to deep sea shipping, overcoming the problem of a lack of supply of zero-emission fuels stopping introduction of ships using such fuels and thereby stopping the development of a market for zero-emission fuels. So far, green corridors have been planned for use of ammonia, methanol or hydrogen as energy carriers. However, the well-to-wake energy requirements of those fuels, at least if green versions of the fuels are assumed, is believed to be very high. Due to the continued scarcity of renewable electric power to produce such fuels, one should look for alternatives. For really short distances, like fjord-crossing road ferries, battery power is becoming the standard, at least in Norway. The question to be explored in this master thesis is whether sensible green corridors for cargo ships running on battery power alone can be designed. It is suggested to do this as a case study, where both the battery capacity, the sailing speed and the distance between charging stations are treated as variables. The effect of weather shall be included in the calculation of power consumption.

In the thesis the candidate shall present her personal contribution to the resolution of problem within the scope of the thesis work.

Theories and conclusions shall be based on mathematical derivations and/or logic reasoning identifying the various steps in the deduction.

The thesis work shall be based on the current state of knowledge in the field of study. The current state of knowledge shall be established through a thorough literature study, the results of this study shall be written into the thesis. The candidate should utilize the existing possibilities for obtaining relevant literature.

The thesis shall be organized in a rational manner to give a clear exposition of results, assessments, and conclusions. The text should be brief and to the point, with a clear language. Telegraphic language should be avoided.

The thesis shall contain the following elements: A text defining the scope, preface, list of contents, summary, main body of thesis, conclusions with recommendations for further work, list of symbols and acronyms, reference and (optional) appendices. All figures, tables and equations shall be numerated.

The supervisor may require that the candidate, in an early stage of the work, present a written plan for the completion of the work. The plan shall include a budget for the use of laboratory or other resources that will be charged to the department. Overruns shall be reported to the supervisor.

The original contribution of the candidate and material taken from other sources shall be clearly defined. Work from other sources shall be properly referenced using an acknowledged referencing system.

NTNU Trondheim
Norwegian University of Science and Technology
Department of Marine Technology

The thesis shall be submitted electronically (pdf) in Inspera:

- Signed by the candidate
- The text defining the scope (this text) (signed by the supervisor) included.

Supervisor : Professor Sverre Steen
Advisors : Dr. Youngrong Kim and Dr. Benjamin Lagemann
Start : 15.09.2023
Deadline : 09.02.2024

Trondheim, 11.09.2023

Sverre Steen
Supervisor

Preface

This master's thesis is written as a part of my studies at the MSc program in Engineering and ICT at NTNU with a main profile in Marine Technology. The report is written during the fall semester of 2023 and the start of 2024. The report is written under the Department of Marine Technology and builds on the project thesis written during the spring semester of 2023.

The thesis has been investigating the feasibility of applying battery-powered cargo ships in a green corridor. The motivation has been to gain insight on applying battery-powered ships as a part of the solution for net zero in the shipping industry.

The thesis has been challenging both theoretically and programming wise. In the end, it has been rewarding to learn about battery technology and how batteries can be a part of the solution for reaching net zero.

Emilie Louise Mongstad Grenth

Emilie Louise Mongstad Grenth

Oslo, 9th February 2024

Abstract

International shipping is the main contributor of transported goods, transporting more than 80% of the transported goods. The International Maritime Organisation (IMO) has set a greenhouse gas (GHG) strategy to reach net zero in GHG emissions by 2050. NTNU has developed a computational model, the MariTEAM model, that can estimate power consumption for ships from the world fleet. This thesis will utilize the MariTEAM model by developing a code to estimate the needed battery capacity for a battery-powered cargo ship.

The MariTEAM model is designed to assess the power consumption for historical AIS and hindcast data. For this thesis, a Python code has been developed that fabricates the input data to simulate the desired route and simulate weather to get a probability distribution of needed battery capacity. The data obtained from the simulations has been processed and analyzed to investigate the battery capacities needed for different set power outputs and different operational speeds.

There were three case studies. Two cases estimate battery capacities for different operational speeds while the third case estimates the case ship range for different weather conditions and battery weights based on a percentage of dead weight tonnage (dwt) on two routes of different lengths. Furthermore, there are discussions on the optimal operational speeds for battery-powered cargo ships of this size. There are also discussions on balancing operational speed, probability of reaching destination, route length, and battery weight to find the best solution for battery-powered ships.

The thesis concludes that battery-powered cargo ships are feasible, however, there must be further studies optimizing speed and battery weight, and there must also be carried out a cost analysis and life cycle analysis of batteries to identify the optimal distances for battery-powered ships.

Sammendrag

Internasjonal skipsfart er hovedbidragsyteren til transporterte varer, og står for transport av mer enn 80% av de transporterte varene. Den internasjonale sjøfartsorganisasjonen (IMO) har satt en strategi for klimagassutslipp (Green house gas, GHG) for å nå netto null i GHG-utslipp innen 2050. NTNU har utviklet en beregningsmodell, MariTEAM-modellen, som kan estimere skip fra verdensflåten sitt energiforbruk. Denne avhandlingen vil bruke MariTEAM-modellen ved å utvikle en kode for å estimere den nødvendige batterikapasiteten for et batteridrevet lasteskip.

MariTEAM-modellen er designet for å vurdere energiforbruket for historiske AIS og vær-data. For denne avhandlingen er det utviklet en Python-kode som genererer inndata for å simulere den ønskede ruten og simulere været for å få en sannsynlighetsfordeling av nødvendig batterikapasitet. Dataene fra simuleringene er blitt behandlet og analysert for å undersøke batterikapasitetene som er nødvendige for forskjellige gitte effekter og ulike operative hastigheter.

Det ble gjennomført tre casestudier. To studier anslår batterikapasiteter for forskjellige operative hastigheter, mens det tredje studiet estimerer rekkevidden for casesskipet for forskjellige værforhold og batterivekter basert på en prosentandel av dødvekttonnasje (dead weight tonnage, dwt) på to ruter av forskjellig lengde. Videre diskuteres optimale operative hastigheter for batteridrevne lasteskip av denne størrelsen. Til slutt diskuteres det hvordan man må balansere operativ hastighet, sannsynlighet for å nå destinasjonen, rutelengde og batterivekt for å finne den beste løsningen for batteridrevne skip.

Avhandlingen konkluderer med at batteridrevne lasteskip er gjennomførbare, men det må utføres ytterligere studier for å optimalisere hastighet og batterivekt, det må utføres kostnadsanalyser og livssyklusanalyse av batterier for å kunne identifisere optimale distanser for batteridrevne skip.

Acknowledgments

Several people have played a prominent role in the completion of this thesis. I would therefore like to thank the most central people during this fall/winter.

Firstly I would like to thank my supervisor, Sverre Steen, for his support, investment, and engagement. All our meetings during the project thesis and master thesis have been valuable. His insights into hydrodynamics and statistics have been very valuable, and he has helped me every step of the way and I couldn't have done it without him.

I would like to thank my co-supervisor Benjamin Lagemann, for his investment in the thesis and for always giving me quick and valuable feedback on my updates.

I would also like to thank my second co-supervisor YougRong Kim, who helped me in the early stages of understanding the MariTEAM code which he developed in his PhD.

I would like to thank my roommate and office mate Ida Emilie Myhre for never getting tired of me and making this semester enjoyable.

Lastly, I would like to thank my family and all my other friends for always being a great support and making everything in life fun.

Thank you!

Table of Contents

List of Figures

List of Tables

Abbreviations

Hull and Propeller Characteristics

B	-	Ship breadth
C_b	-	Block coefficient
C_M	-	Midship section coefficient
C_P	-	Prismatic coefficient
dwt	-	Deadweight
D_p	-	Propeller diameter
LCB	-	Longitudinal center of buoyancy
ldt	-	Light displacement tonnage
L_{oa}	-	Length over all
L_{os}	-	Length of surface
L_{pp}	-	Length between perpendiculars
L_{wl}	-	Length of waterline
n	-	Propeller rpm
S	-	Wetted surface area
T	-	Ship draught
TA	-	Ship draught at aft
TP	-	Ship draught at perpendicular
∇	-	Volume displacement
V_D	-	Design speed of ship

Resistance

C_A	-	Correlation allowance
C_{AA}	-	Air resistance coefficient
ΔC_F	-	Hull roughness correction
C_F	-	Frictional resistance coefficient
C_R	-	Residuary resistance coefficient
C_T	-	Total resistance coefficient
F_n	-	Froude number
g	-	Constant of gravity
$H_{1/3}$	-	Significant wave height
h	-	Water depth
k	-	Form factor
R_{calm}	-	Calm water resistance
R_T	-	Calm water resistance
R_{waves}	-	Added resistance due to waves
R_{wind}	-	Added resistance due to wind
V	-	Ship speed
v	-	Sea water kinematic viscosity
ρ	-	Sea water density

Propulsion

η_d	-	propulsive efficiency
P_{tot}	-	Power prediction

Abbreviations

DoD	-	Depth of discharge
GT	-	Gross tonnage
Hs	-	Significant wave height
IMO	-	International Maritime Organisation
ITTC	-	International Towing Tank Conference
LCA	-	Life cycle analysis
LNG	-	Liquefied Natural Gas
NTNU	-	Norwegian University of Science and Technology
Tp	-	Peak period
WTW	-	Well-To-Wake

Chapter 1

Introduction

1.1 Motivation

Currently, over 80 percent of transport work is being performed by ocean shipping. And 2-3 percent of the global greenhouse gas (GHG) emissions come from maritime transport, and these numbers are only estimated from the combustion of fossil fuel ships. It does not take into account indirect emissions that come from production from ships and the transport of ship fuels (IMO, 2023). The International Maritime Organisation (IMO) set a greenhouse gas strategy which was recently revised in 2023 to reach net zero GHG emissions by 2050 for international shipping (IMO, 2023). For this to be possible a lot of private and public actions need to be made.

In recent years, the concept of green corridors has become increasingly prominent in discussions regarding zero-emission shipping in the industry. Green corridors are typically defined as ”specific shipping routes where the feasibility of zero-emission shipping is catalyzed by a combination of public and private actions” (GMF, 2022a).

There are challenges surrounding the availability of zero-emissions fuels in shipping since the world fleet is diverse, and since there is a general scarcity of renewable energy. Different vessels have different requirements which means different fuels can suit different types of ships and trades. Manufacturers hesitate to scale up the production of zero-emission fuels as long as demand and the market remain limited. Also, alternative fuels require research, development, and infrastructure investments. Alternative fuels have lower energy density than conventional fossil fuels, which means the ship has to refuel more often, having probably a different optimal route than the one being deployed today (DNV, 2023). Green corridors are suggested as an enabler to facilitate a coordinated transition process where both demand and supply are increased simultaneously.

Currently, the green corridors being developed have planned for use of ammonia, methanol or hydrogen as energy carriers. One of the downsides with the green version of these fuels is that their well-to wake energy requirements is high (Lindstad et al., 2023). An alternative could be battery powered cargo ships, right now battery powered ships are being used on short distance transports such as ferries in Norway. With the improving battery technologies battery powered ships could be a solution towards reducing the emissions by 2050. From studies looking into the energy efficiency well-to-wake study by Lindstad (Lindstad et al., 2023) electricity has the lowest energy loss compared to the other green fuels. However, batteries have even lower energy density than other alternative fuels, typically requiring even more frequent refuelling.

1.2 Objective

The main objective of this master's thesis is to research the feasibility of green corridors serviced with cargo ships powered solely by battery technology. Throughout the study, the needed battery capacity, corresponding battery weight, and battery package ranges for different weather conditions will be investigated. The research will focus on a theoretical case ship navigating two distinct routes: one long and one short. To achieve these objectives, the determination of battery capacities will depend on factors such as speed, battery weight limits, weather conditions and power.

1.3 Scope

The scope of the thesis has been to:

- Perform a background and literature review to provide information about green corridors, and their necessity for cooperation between private and public sectors to ensure zero emission.
- To create an energy consumption probability distribution, weather conditions are simulated using a Monte Carlo simulation. This involves a Python script that generates input data, which is then processed by the MariTEAM software to estimate the ship's power consumption. These estimates are used to calculate the total energy consumption for the entire voyage
- Analyze the generated data on energy consumption to calculate the required battery capacity and the corresponding weight
- Using the MariTEAM code to estimate calm water power consumption, construct a probability distribution for reaching the destination at various speeds.
- Implement a Python code that can use a weather scatter diagram and ship particulars to estimate the range when given a percentage of dwt of ship and speed to sail to estimate the range for the same speed in different weather conditions.
- Compare results for different cases. Discuss different methods to estimate the range, and how a set speed or a set power output affects the needed battery capacity.

1.4 Previous work

This thesis is a continuation of the work to the project thesis started during the spring semester of 2023. The project thesis focused on estimating the required battery capacity in more extreme weather by considering the calm water resistance and adding the weather resistance as a percentage of the calm water resistance. The project thesis used less complex formulas to estimate power consumption instead of using the MariTEAM model. Hence, the motivation, most of the background theory, and one of the cases are based on the project thesis, but improved and in an expanded format.

1.5 Outline of Thesis

- **Chapter 1:** Introduction

  Introduce the thesis to the reader, describe the motivation, objective, and scope.

- **Chapter 2:** Background theory

  Provide relevant background information regarding green corridors, difficulties choosing zero emissions fuel, the MariTEAM model, and simulations.

- **Chapter 3:** Methodology

  Description of the methods used to estimate battery capacity, probability distributions, and battery capacity ranges.

- **Chapter 4:** Results and Discussion

  Presentation of the results and discussion of the results.

- **Chapter 5:** Conclusion

  Conclusion of the results and discussion.

- **Chapter 6:** Further work

  Recommendation for further studies.

Chapter 2

Background theory

2.1 Green Corridor

2.1.1 Introduction to green corridors

The concept of green corridors has become increasingly prominent in discussions regarding zero-emission shipping in the industry. Green corridors are designated trade routes connecting port hubs that have been or are being customized to accommodate current or prospective zero-emission solutions (Joerss, 2021). For instance, green corridors can be a catalyst for policymakers to create an enabling ecosystem with targeted regulations, financial incentives, and safety regulations (GMF, 2022a). Also, policymakers can also put conditions in place to facilitate green shipping on specific routes. In the end, green corridors will work as a incentive for reducing emissions (Joerss, 2021).

The need to reduce GHG emissions and combat climate change has led to a rise in interest in green shipping corridors. At the moment, most shipping fuels are fossil-based. With the shipping industry being a central figure in global trade, it is essential to reduce emissions in the shipping sector (EU, 2021). Unfortunately, selecting the optimal sailing path, choosing the new fuel, and coordinating between the private and public sectors are challenging. This is where the Clydebank Declaration comes in, providing a framework for guidance.

2.1.2 Clydebank declaration

The Clydebank Declaration was launched in November 2021 during the climate meeting in Glasgow. The Clydebank declaration support establishment of green corridors, and its primary aim is to make sure that the sector is on track to reach net zero by 2050 (gov.uk, 2022). The declaration is a call for action for the shipping industry, governments, and stakeholders to collaborate for decarbonization of the shipping industry, and reach the target of zero-emissions shipping by 2050.

All Signatories of the Clydebank Decleration pledge to:

- "Facilitate the establishment of partnerships, with participation from ports, operators and others along the value chain, to accelerate the decarbonisation of the shipping sector and its fuel supply through green shipping corridor projects." (gov.uk, 2022)
- "Identify and explore actions to address barriers to the formation of green corridors. This could cover, for example, regulatory frameworks, incentives, information sharing or infrastructure." (gov.uk, 2022)
- "Consider the inclusion of provisions for green corridors in the development or review of National Action Plans." (gov.uk, 2022)

- ”Work to ensure that wider consideration is taken for environmental impacts and sustainability when pursuing green shipping corridors.” (gov.uk, 2022)

Currently, 24 countries have signed the pledge, Norway being among them. The Clydebank Declaration’s framework includes the development of new technologies, energy efficient measures, and the use of low and zero emission fuels. It also calls for equal standards and incentives for all shipping companies to support the transition to zero-emission (gov.uk, 2022). And it gives stakeholders a path to follow on the way to an environmentally-friendly shipping industry.

2.1.3 Current initiatives

There are several current initiatives to accelerate the development of green shipping corridors and the reduction of environmental impact from the shipping industry. The EU has launched several initiatives, in the the Baltic Sea and North Sea. Outside of Europe, Japan has announced a project with Australia. The United States is also looking at green corridors as an action to reduce emissions from the shipping industry (GMF, 2022a).

In Figure 2.1 the initiatives that have been announced following the Clydebank Declaration are illustrated. As can be seen in Figure 2.1 there are some long and short routes, the short ones mostly being in the Baltic region. Three of the corridors being announced have a chosen green fuel. For the Australia - East-Asia iron Ore which is being planned for ammonia-powered bulk carriers by 2028, given further technological developments (GMF, 2022b). The Halifax - Hamburg corridor between Canada and Germany, planning further the hydrogen technology (Farguson, 2022). And the West - Norway - Netherlands for two methanol fueled cargo ships.

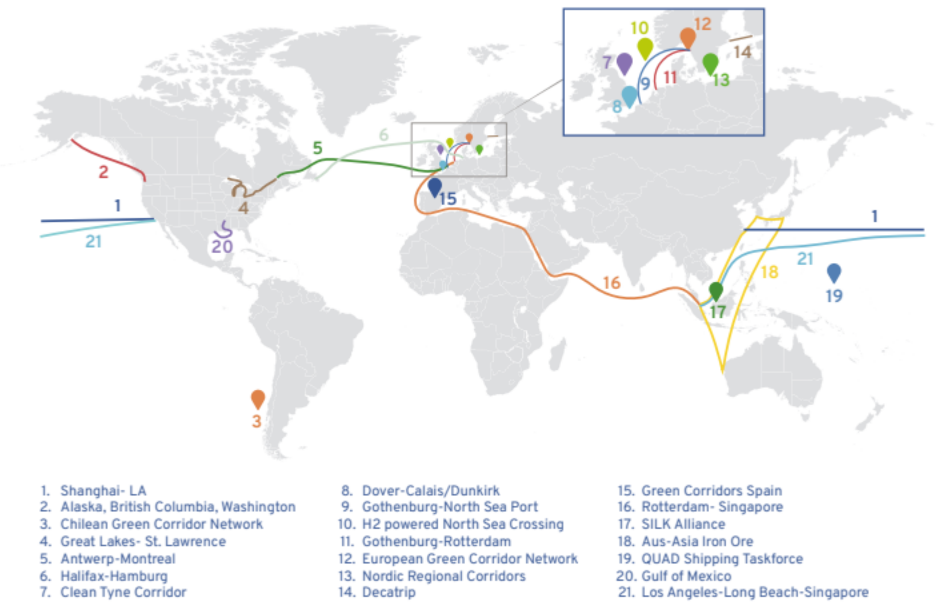

Figure 2.1: Illustration of the initiatives for green corridors in 2022, source: (GMF, 2022a)

2.1.4 Which fuel to apply in green corridors

The corridors connecting Rotterdam to West Norway, Halifax to Hamburg, and Australia to East Asia are planning to use three specific low-emission fuels: methanol, green hydrogen, and ammonia. The choice to incorporate multiple fuels stems from the varied needs of different ships navigating these routes. Experts are confronted with the task of determining the most suitable green fuel, considering the diverse requirements of different vessels. The scarcity of a universally suitable fuel further complicates the decision-making process, adding complexity to the search for a universal sustainable maritime energy solution.

2.2 Choosing the next green fuel

Deciding on a new fuel for the future zero emission shipping industry is difficult. Some of the more prominent options as the new fuels are ammonia, methanol, battery ships, and liquefied natural gas (LNG) (Nationalgrid, 2022). Why aren't the maritime industry or IMO choosing the zero emission fuel, so there are not multiple choices to choose between? It has proven difficult to choose zero emission fuel due to several factors that will be listed underneath (GMF, 2023).

Routes and Sea States
The selection of a zero-emission fuel for maritime vessels is intricately tied to the characteristics of their routes, encompassing considerations such as route length and prevailing sea states. These factors increase the complexity of the process in choosing the green fuel for achieving sustainable and efficient maritime operations (GMF, 2023). For instance, in selecting a zero-emission fuel for a transatlantic cargo vessel, longer route distances and variable sea conditions might make hydrogen fuel cells more suitable than battery power due to their higher energy density and quicker refueling capabilities, addressing the challenges of extended travel and the dynamic maritime environments (GMF, 2023).

Vessel Size
The size of a vessel stands as a central deciding factor in the choice of zero-emission fuels. Distinct energy consumption and operational requirements associated with vessels of varying sizes necessitate a tailored approach, emphasizing the need for comprehensive assessments based on vessel size categories (GMF, 2021). For instance, a small coastal ferry might find battery technology more suitable due to its shorter routes and frequent docking opportunities for recharging. In contrast, a large container ship traversing long international routes might benefit more from hydrogen or ammonia-based fuels, which can provide the necessary energy for longer voyages without the frequent need for refueling.

Type of Vessel
A critical consideration in fuel selection is the specific category of the vessel, ranging from cargo ships to container ships and Roll-On/Roll-Off (RORO) ships. The diverse operational profiles and unique demands of each vessel type contribute to the complexity of identifying an optimal zero-emission solution (GMF, 2021). For example, a RORO ship, which typically operates on shorter, fixed routes and carries vehicles, might favor a fuel like bio-LNG for its balance of energy density and lower emissions. On the other hand, a container ship that has longer international journeys may find ammonia to be a more feasible zero-emission fuel, given its suitable for longer maritime transports due to higher energy density.

Operational Requirements
Informed decision-making regarding zero-emission fuels hinges upon a thorough understanding of a vessel's operational requirements. Parameters such as speed, range, and power consumption must be precisely analyzed to align fuel choices. For example, let's take a large cargo ship that travels long distances across oceans. For this kind of ship, using ammonia as a fuel could be a good choice.

Ammonia has high density, which means that it won't need to refill often. This makes it a practical option for ships that have longer shipping journeys GMF, 2023.

Global Demand Considerations
Given the enormous size of the shipping industry, it's crucial to consider a worldwide approach when choosing fuels. If we were to aim for every ship to use the same fuel, we have to figure out how to produce a lot of it to meet the massive demand across the globe. This global perspective is essential for making sustainable and practical decisions about the types of fuels used in the shipping sector(GMF, 2023). For instance, if ammonia were chosen as the standard fuel for the global shipping industry, it would necessitate a massive scale-up in ammonia production worldwide. This would mean not only establishing large-scale facilities to produce green ammonia, but also creating a global network of distribution and refueling stations at major ports.

Infrastructure Accessibility
To be able to fuel a ship the fuel has to be accessible at the ports. A vital part of implementing zero-emission fuels is to manufacture enough and be able to distribute to the different ports it is needed. Whether it's practical and doable to use a particular fuel depends a lot on whether the necessary facilities and infrastructure are in place and what the necessary changes are needed. So, having the right setup in terms of infrastructure is vital for deciding which zero-emission fuel is feasible GMF, 2021. For example, if we consider hydrogen as a potential zero-emission fuel for the shipping industry, its feasibility heavily depends on the availability and development of hydrogen production, storage, and distribution infrastructure. If there aren't enough hydrogen production plants, or if ports around the world lack the facilities to store and supply hydrogen to ships, then despite its environmental benefits, hydrogen might not be a practical choice. Therefore, infrastructure is a key factor in determining whether hydrogen or any zero-emission fuel, is a possible solution for the shipping industry.

Considering all these complex factors, the selection of the next green fuel is difficult. The fuel needs to be chosen balancing different factors of technological feasibility, economic growth, environmental impact, and long term sustainability. This is where the green corridors are vital, they instigate collaboration between private stakeholders, governments, and research institutions towards zero emission.

2.2.1 Choosing the next green fuel for this thesis

The selection of the next green fuel is challenging, as previously discussed. This thesis explores the potential of battery-powered ships, influenced by their energy efficiency from a Well-to-Wake (WTW) perspective, as highlighted by (Lindstad et al., 2023). It evaluates the environmental impact from fuel extraction to consumption, with renewable electricity and batteries shown to have the lowest WTW energy use, as depicted in Figure 2.2.

The thesis focuses on battery-powered ships due to electricity having the lowest energy loss in the WTW analysis. There were considerations to look into the pricing of the different fuels, but unpredictable prices in the last years and different prices for different countries/areas make it hard to compare the fuels, therefore it was chosen to look at from an energy efficiency perspective.

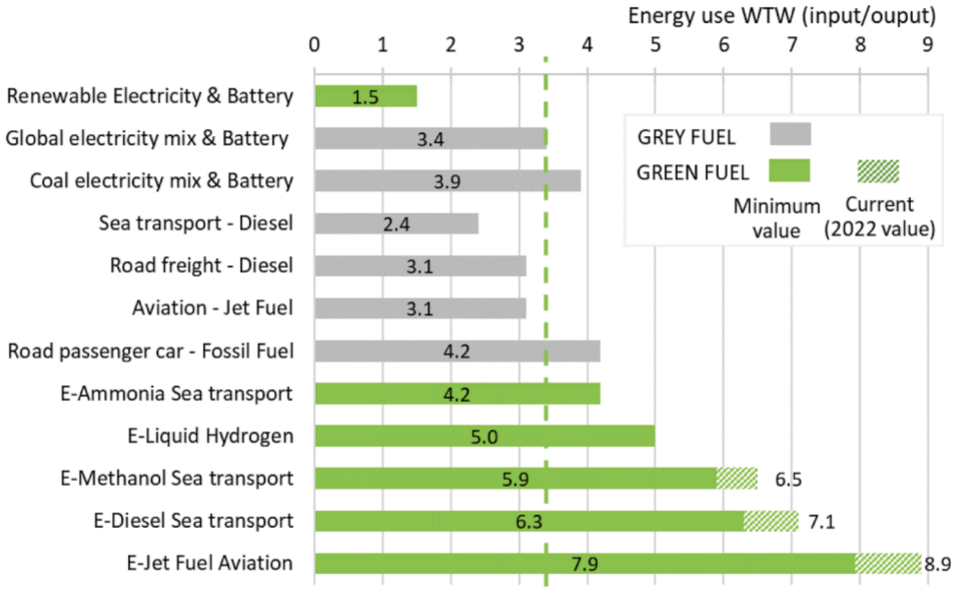

Fig. 5. WTW Energy use as a function of fuel and transport mode.

Figure 2.2: WTW Energy use as a function of fuel and transport mode from (Lindstad et al., 2023)

There are some other benefits with battery ships that are also why this thesis is looking into battery ships which are mentioned below:

- **Reduced emissions:** In use battery-powered ships produce zero emissions. This reduces greenhouse gas emissions and air pollution, especially in ports and coastal areas.
- **Propulsion system:** Electric propulsion systems are generally more energy-efficient than traditional internal combustion engines. The electric propulsion systems generally have higher efficiency at lower speeds, this is beneficial for ships that operate at variable speeds during journeys.
- **Noise reduction:** Electric propulsion systems make less noise than traditional engines, therefore reducing noise pollution and bettering the well-being of the marine ecosystem and nearby communities.
- **Fuel diversity:** Battery-powered ships can be charged using a variety of energy sources. This is a flexibility that makes a foundation for the transition to renewable energies.

2.3 Maritime batteries

Battery-powered ships, most commonly known as battery ships are a promising solution for zero-emission, but so far only for short distances due to the low energy density of batteries. Battery ships rely on advanced battery technology to store and deliver energy during navigation. At present the batteries are lithium-ion batteries. Some of the benefits of a battery ship are the reduction of noise, being capable of silent operations, and clean operations by reducing noise and air pollution (DNV, 2022).

2.3.1 Maritime batteries challenges

Currently battery technology is being used for short-distance sailings and routes where the vessel can charge regularly. The reason for battery ships not being used for long distances is that the batteries would be so heavy the ships would not have enough space for trade gods to make a profit. Another problem is that it takes longer time to charge maritime batteries compared to fueling other fuels. There are being looked into new solutions for charging battery ships. Some of the new solutions that are being mentioned are:

Charging vessel
This solution involves the deployment of specialized vessels equipped with charging capabilities. These charging vessels can connect with battery-powered ships during their voyage, providing an opportunity for swift and efficient recharging. This approach aims to minimize downtime at the port and maximize the operational range of battery-powered ships (this concept was explained to me by professor Medhi Zadeh during a meeting in spring 2023).

Swapping batteries
The concept of battery swapping involves the rapid exchange of depleted batteries with fully charged ones at designated ports or facilities. This solution eliminates the need for time-consuming recharging and allows vessels to maintain continuous operation by simply exchanging batteries, optimizing efficiency, and reducing turnaround time (Siamak Karimi and Suul, 2020).

Charging stations at sea
Exploring the feasibility of charging stations at sea is an innovative approach. Floating charging stations would be strategically positioned along major maritime routes, allowing battery-powered vessels to replenish their energy reserves during the voyage. This solution aims to address the spatial constraints batteries with longer ranges will uptake of the payload. It could be possible to have a wind turbine park at sea where ships can charge, this will also lessen port charges (Vard, 2013).

The different charging solutions are illustrated in Figure 2.3. These solutions reducing the charging time at the port could have a significant impact on making battery-powered ships more feasible.

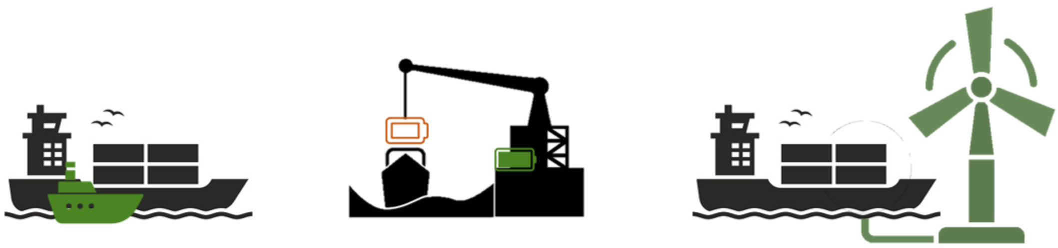

Figure 2.3: Possible future charging solutions

2.3.2 Battery Capacity

Battery capacity is a measure of the total amount of energy a battery can store, often measured in kilowatt-hours (kWh). The capacity of maritime batteries is extensive, but higher capacity means heavier batteries, even if the battery technology is ever-evolving. Modern maritime battery technology is most often lithium-based systems, therefore offering extensive battery capacity. These high-capacity batteries can be instrumental in powering not only the propulsion systems of electric and hybrid vessels but also the auxiliary functions, such as lighting, heating, and electronic navigation systems on the vessel (DNV, 2020).

The maritime industry is experiencing ambitious and necessary regulations to reach zero emission by 2050, and the role batteries with higher capacities can have becomes more prominent. Benefits during sailing are multiple, they have reduced operational costs and enhanced energy security (Mo, 2019).

For example, the use of high-capacity batteries allows for the exploitation of shore power, reducing the need for engines to run idle while being docked. Hence reducing noise and air pollution in ports. Moreover, advancements in battery technology have seen the development of batteries with not only higher capacities but also faster charging times and longer life cycles, which is central to their economic lifespan in commercial operations (DNV, 2020).

Furthermore, the scalability of maritime batteries offers the flexibility to tailor energy storage systems to a vessel's specific needs. Ships with larger energy demands, such as cruise liners or container ships, can integrate multiple high-capacity battery units to form a great collective energy reserve. This scalability ensures that vessels of different sizes and operational profiles can achieve their energy requirements. If the electricity the ship is powered with is generated by renewable energy sources, such as solar or wind power, maritime batteries can provide a consistent and reliable green energy supply, thereby playing a pivotal role in the journey towards a sustainable maritime future (Mo, 2019).

2.3.3 Charging time

The charging time of maritime batteries is a crucial factor influencing the operational efficiency of electric and hybrid vessels. It is defined by the rate at which a battery can be brought from a state of depletion to full charge. Technological advancements have led to the development of rapid charging capabilities, allowing batteries to receive a considerable amount of energy within a relatively short period. This technology development is important for maintaining the continuous operations of commercial vessels, particularly those on tight schedules (DNV, 2020). The charging time is dependent upon multiple factors, including the battery's capacity, the energy source's output, and the charging technology employed. Theoretical models of charging dynamics suggest that with appropriate infrastructure and power management, the downtime, and time in dock charging, for battery-powered vessels can be minimized, increasing their competitiveness against more conventional fuels (DNV, 2020).

How to calculate charging time depends on the charging current. The formula for estimating charging time is described in Equation 2.1.

$$Charging\ time = \frac{Battery\ capacity[kWh]}{Charging\ current[kW]} \tag{2.1}$$

An example: If the charging current is 10 MW, and a battery of 25000 kWh needs to be fully charged we get a charging time of 2.5 hours using Equation 2.1.

$$\text{Charging time} = \tfrac{25000}{10000} = 2.5$$

The depth of discharge (DoD) of a battery refers to the extent to which a battery is used relative to its total capacity (Mo, 2019). A deep discharge, where a significant percentage of a battery's energy is utilized before recharging, can affect the battery's overall lifespan. Maritime batteries are often designed to withstand varying DoD levels, with some modern batteries capable of operating effectively at high DoD. The ability to use a greater depth of discharge without compromising the battery's lifespan or performance is a key consideration in maritime applications. where long periods of operation without access to charging facilities are common. Theoretical analyses indicate that lower DoD will prolong a battery's life, the trade-off often lies in the under-utilization of the available capacity (DNV, 2020). This indicates that it is important to find a balance between operational demands and long-term battery health.

Battery lifespan in maritime applications is influenced by the frequency and the way of usage, and also by the charging patterns. Repeated cycles of discharging and charging can lead to a gradual decline in battery capacity, a phenomenon known as battery degradation (DNV, 2020). Theoretical frameworks for battery life estimation include factors such as the number of charge-discharge cycles, the temperature during operation and charging, and the rate of charging and discharging. High temperatures and rapid charging rates are typically associated with increased aging of battery components. Therefore, battery management systems are employed to optimize charging regimes and usage patterns with the objective of maximizing the lifespan of maritime batteries. These systems are instrumental in ensuring that the full benefits of maritime battery technology are executed over the operational lifetime of the vessel (DNV, 2020).

2.3.4 Future of maritime batteries

As the maritime industry progresses toward sustainability, innovative solutions for battery charging are being explored to enhance the feasibility of battery-powered vessels. Battery swapping, a concept borrowed from the electric vehicle industry, is one such solution that has the potential to drastically reduce turnaround times. Instead of waiting for batteries to charge, depleted batteries could be exchanged for fully charged ones, enabling ships to depart almost immediately after docking. This approach necessitates substantial infrastructure investment and standardized battery modules across different vessels but could revolutionize energy management in maritime logistics (Siamak Karimi and Suul, 2020).

Continuing the development of maritime battery technology, the industry is not only advancing in the capacity and efficiency of the batteries themselves but also in the methodologies applied to charging. Battery swapping is a particularly innovative approach that is being considered, which could drastically streamline the recharging process (DNV, 2020). By simply replacing depleted batteries with charged ones, vessels could minimize downtime and maintain more consistent operating schedules. This system would require standardized batteries and the necessary infrastructure at ports. If battery swapping becomes possible on a large scale, it can offer a path to a very agile "re-charging" process for battery-powered ships.

In parallel, the concept of using remote charger vessels presents a dynamic charging solution that aligns with the demands of modern shipping. These charger vessels would meet ships as they approach or depart from ports, providing charge without necessitating a full stop for the primary vessel. This "charge-on-the-go" system could significantly cut down on port charging times and is being researched as a viable method for keeping battery-powered ships operational with minimal disruption. These advancements in charging technology, when combined with increasing battery capacities, are anticipated to be instrumental in the maritime industry's transition to zero-emission operations.

2.4 The MariTEAM model

To calculate the power prediction the MariTEAM model python code is used, which is developed by Young-Rong Kim (Kim et al., 2023). The MariTEAM model uses Automatic Identification System (AIS) data, Ship technical information, and historical weather hindcast data to estimate a ship's power prediction.

The MariTEAM model is developed by the interdisciplinary research program IndEcol and the Department of Marine Technology at NTNU specializing in environmental analysis. The methods in the MariTEAM model are acknowledged empirical methods which are described in Figure 2.4.

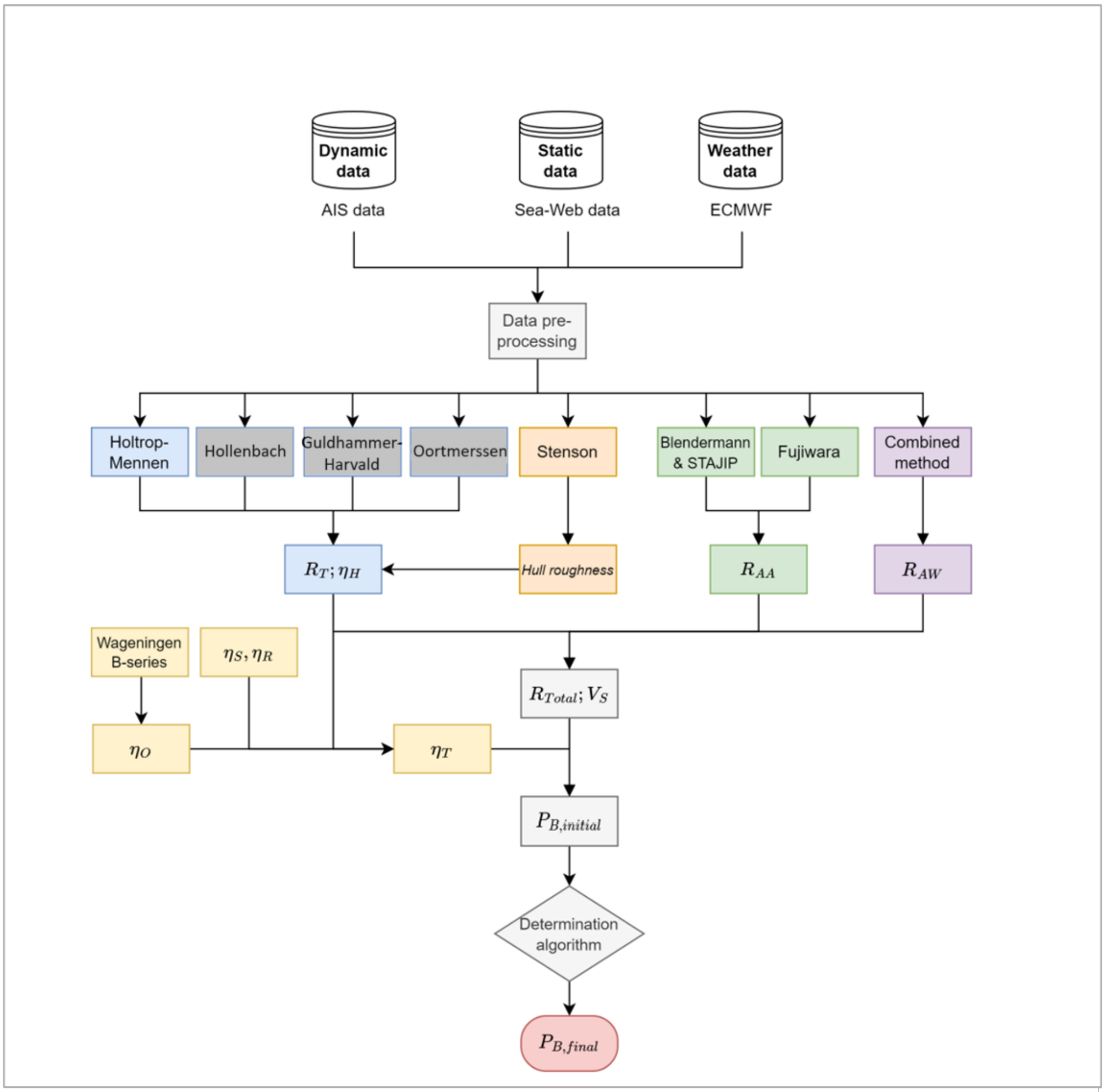

Figure 2.4: Schematic diagram of what parts of the MariTEAM model is used to calculate the power prediction, figure from (Kim et al., 2023) with modifications of colors

The model's development and implementation involve a bottom-up approach, incorporating data on fleet composition and trading patterns. It employs a comprehensive methodology that includes data pre-processing, estimation of ship resistance, and evaluation of propulsion efficiency. This is achieved using the Maritime Transport Environmental Assessment Model framework (Kim et al., 2023).

The model's effectiveness is further validated through comparisons with full-scale measurements from operating ships and annual fuel consumption and emissions data, demonstrating its accuracy and reliability in practical applications. This positions the MariTEAM model as a valuable asset in advancing the understanding of ship emissions and aiding in the development of effective strategies for emission mitigation in the maritime sector (Kim et al., 2023).

In this thesis, the MariTEAM model is employed for power prediction by simulating the route and weather conditions, rather than utilizing historical hindcast data. This is achieved within a simulation framework that generates weather conditions through a Monte Carlo simulation, allowing for the examination of various weather scenarios and their impact on power consumption. This method provides a comprehensive insight into the influence of different weather conditions on power needs and aids in understanding the required battery capacities more thoroughly.

The MariTEAM model processes a pandas DataFrame containing data on the vessel's specifications and weather parameters. A Python script has been developed to simulate these weather parameters, thereby facilitating the estimation of necessary power. This estimated power is then used to calculate energy consumption, with the results presented in graphical visualizations. The complete code developed for this analysis is documented in Appendix H and included with the thesis submission in Inspera.

The MariTEAM code is restricted in this thesis and only uses Holtrop-Mennen to calculate the calm water resistance. How the power prediction is calculated for this thesis can be described in Figure 2.4. The MariTEAM model serves as a tool for estimating the power consumption and resistance of ships part of the global fleet. This model is particularly significant in the context of assessing global shipping emissions and exploring various emission reduction scenarios (Kim et al., 2023).

2.5 Simulation

A simulation is an imitation of a real-world process, and it should account for uncertainty and stochastic natural processes such as weather and time of failures (Twi, 2023). It serves as a predictive tool, enabling researchers and practitioners to observe outcomes without physically enacting the conditions in real life. In maritime operations, simulations can model oceanic conditions, ship responses, and navigational strategies. This is particularly valuable given the dynamic and often unpredictable nature of maritime environments. Simulations help in decision-making, risk assessment, and planning, by providing a virtual environment in which to test and refine processes and responses to a wide range of maritime situations (Twi, 2023).

2.5.1 Monte Carlo simulation

The Monte Carlo simulation is a computational technique that integrates randomness and statistical analysis to model systems with inherent uncertainty (IBM, 2023). When applied to maritime contexts, this simulation method can effectively emulate various weather conditions such as significant wave height (Hs), peak spectral wave period (Tp), and wave direction. It utilizes statistical probabilities for different combinations of Hs and Tp, generating a multitude of potential weather scenarios. This probabilistic modeling provides a detailed forecast of possible maritime weather patterns, allowing for a comprehensive understanding of the environmental conditions that a ship might face.

By considering historical data and statistical probabilities, Monte Carlo simulations can predict the likelihood of various wave heights, helping in the structural design of vessels to ensure they can withstand diverse sea states. It also evaluates the frequency and duration of wave periods, aiding in the development of effective navigational and operational strategies. Furthermore, by factoring in the randomness of wave direction, the simulation can assess the impact of waves hitting the ship from various angles.

The strength of the Monte Carlo simulation lies in its capacity to produce a wide array of weather scenarios, thereby equipping us with the information needed to navigate the dynamic conditions that occur at sea. This approach enhances decision-making by saving time, instead of gathering historical data for a large number of scenarios over a long period of time, a probability distribution can be made by having many simulations.

Determining the optimal number of Monte Carlo simulations necessary for accurate weather simulation in maritime contexts depends on various factors, including the complexity of the weather model and the desired accuracy of the results. Generally, a higher number of simulations will provide reliable insights, particularly in capturing the stochastic nature of maritime weather conditions. In this thesis, 10 000 simulations will be used as 10 000 simulations are considered sufficient for Monte Carlo simulations (IBM, 2023).

2.6 Theory of ship powering

Traditionally, ship resistance is defined within the framework of hydrodynamics, assuming a calm water sea state. Ships are typically optimized for such conditions, even though real-world operations frequently involve the presence of wind, waves, and currents. The effects of unfavorable weather conditions on resistance are significant, therefore added resistance to wind and waves must be taken into account.

This section aims to establish the key aspects of ship resistance and propulsive efficiency for estimating ship powering.

2.6.1 Calm water resistance using Hollenbach

Calm water resistance is the initial resistance a ship experiences when navigating undisturbed waters, excluding external forces such as wind, currents, and waves. In naval architecture calm water resistance gives insight into baseline drag forces in idealized conditions.

Calm water resistance is estimated using the Hollenbach method (Hollenbach, 1998). The method is a sufficient choice for a first estimate, especially for ships with moderate speed, and modern ships, and only requires main dimensions.

Hollenbach's formula for calm water resistance is described by Equation 2.2, and its variables are described in Table 2.1.

$$C_{Ts} = (C_{Fs} + \Delta C_F) \cdot (1 + k) + C_R + C_A \quad (2.2)$$

Symbol	Parameters
C_{Ts}	Total resistance coefficient
k	Form factor
ΔC_F	Added frictional resistance due to roughness
C_R	Residual resistance coefficient
C_A	Correlation factor from analysis of trial results

Table 2.1: Table describing parameters in Hollenbach's calm water resistance

And the wetted area S is defined by the Mumford formula:

$$S = 1.025 \cdot (\frac{\nabla}{T} + 1.7 \cdot L_{pp} \cdot T) \quad (2.3)$$

The calm water resistance is found using Equation 2.4, and its parameters are described in Table 2.2.

$$R_T = \frac{1}{2} \cdot \rho \cdot V^2 \cdot S \cdot C_{Ts} \tag{2.4}$$

Symbol	Parameter
ρ	Water density
V	Ship speed
S	Wetted surface
C_{Ts}	Total resistance coefficient from Equation 2.2

Table 2.2: Table describing parameters for calm water resistance

2.6.2 Wind Resistance

Wind resistance, alternatively termed air resistance or drag, is the force that acts in opposition to the motion of an object. In the case of a ship, this resistance results from the interaction between the ship's portion above water and the wind. The calculation of wind resistance involves the use of Equation Equation 2.5, as outlined in the resistance compendium TMR4220 - Naval Hydrodynamics.

$$R_{AA} = C_{air} \cdot \frac{\rho_{air}}{2} \cdot V_{rel}^2 \cdot A_p \tag{2.5}$$

Symbol	Parameter
C_{air}	Air resistance coefficient
A_p	Transverse projected area
V_{rel}	Relative wind velocity ($V_{wind} + V_{shipspeed}$ in head wind)
ρ_{air}	Air density

Table 2.3: Table describing parameters for calculation of air resistance

2.6.3 Wave resistance using STAWAVE-1

Wave resistance on a ship refers to the energy loss because of the ship's generation of waves as the ship moves through water. To validate the implementation of the code we will be assessing head waves, where Wave resistance is estimated using STAWAVE - 1 from (ITTC, 2014) using Equation 2.6, parameters are described in Table 2.4.

$$R_{wave} \approx R_{AWL} = \frac{1}{16} \cdot \rho g H_{\frac{1}{3}}^2 \cdot B \sqrt{\frac{B}{L_{BWL}}} \tag{2.6}$$

Symbol	Parameter
ρ	Water density
$H_{\frac{1}{3}}$	Significant wave height
B	Beam of ship
L_{BWL}	Length of the bow on the water line

Table 2.4: Table describing parameters for calculation of wave resistance

2.6.4 Power prediction using STEAM3

Power prediction on a ship is the process of determining the amount of power needed for the ship to travel. The process involves finding the required propulsive power for a ship to achieve desired speeds and destinations. The power prediction can be hand calculated using Equation 2.7 by (Johansson, 2017), parameters are described in Table 2.5.

$$P_{tot} \approx \frac{1}{\eta_D} \cdot (R_{calm} + R_{wind} + R_{wave}) \cdot V \quad (2.7)$$

Symbol	Parameter
V	speed of ship in m/s
R_{calm}	Calm water resistance
R_{wind}	Added resistance from wind
R_{waves}	Added resistance from waves
η_D	Propulsive efficiency by Emerson's formula from Equation 2.8

Table 2.5: Table describing parameters for calculation of power prediction

The propulsive efficiency is determined by Emerson's formula in Equation 2.8, and its parameters are described in Table 2.6.

$$\eta_D = 0.84 - \frac{n\sqrt{L_{pp}}}{1000} \quad (2.8)$$

Symbol	Parameter
n	Propeller rate of revolutions
L_{pp}	Ship length between perpendiculars

Table 2.6: Table describing parameters for calculation of propulsive efficiency

Chapter 3

Method

3.1 Step-by-step approach

For this thesis, the MariTEAM code is being used to calculate power consumption for a case ship. Usually, the code is given historical weather data to calculate the power consumption, but for this project, a Monte Carlo simulation is deployed to simulate weather parameters. From the power consumption, the energy consumption probability distribution is calculated.

The essential weather parameters for MariTEAM include significant wave height (Hs), wave period (Tp), wind speed, and wind and wave direction. Utilizing global wave statistics data (Hogben, 1986), observations for various Hs and Tp combinations, along with their respective directions, are obtained for a year. Through Monte Carlo simulation, Hs, Tp, and wave direction are randomly selected, considering their occurrence probabilities. Wind speed is estimated from Hs, assuming alignment between waves and wind direction (DNV, 2010).

Since we are simulating different weather conditions the route is split into different legs which each has discrete independent weather conditions. The routes consist of one leg for the shorter distance and four legs for the extended journey. When using historical hindcast data, the MariTEAM model computes the power consumption across all AIS points. However, in the context of Monte Carlo simulation for weather forecasting, several points will give similar energy consumption outcomes for the simulations. Limiting the number of weather conditions impacting a single simulation preserves the distinctiveness of extreme weather scenarios, including both calm conditions and storms, which might otherwise be lost if the route is segmented into numerous legs. The route is simulated 10,000 times, usually, this is considered a sufficient amount of simulations to get a good representation.

The resulting power consumption data is categorized into 1000 kWh intervals, and a cumulative probability distribution is established for the route's energy consumption. From the energy consumption probability, different batteries weights can be estimated for different energy consummations.

Then, the MariTEAM code is used to calculate the energy consumption in calm water conditions. This is used to find the optimal speed when given a power output and battery capacity. This is being used to make a speed probability distribution for the case ship, and voyage time distribution.

Furthermore, MariTEAM is employed to create an interactive matrix with visualizations illustrating ship range for different Hs and Tp combinations, with ship speed and percentage of deadweight tonnage(dwt) for battery packages as variable parameters.

The step-by-step methodology is outlined in the flowchart presented in Figure 3.1

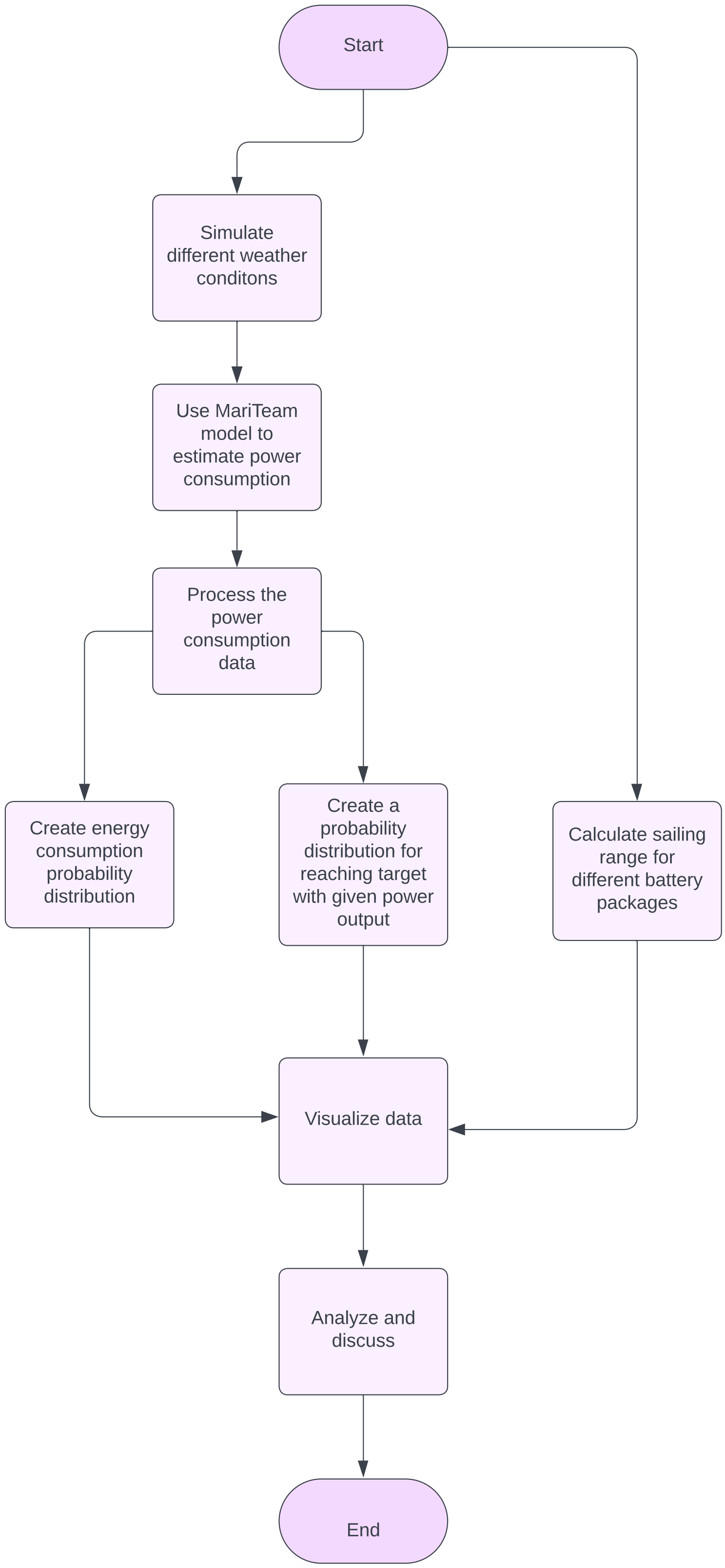

Figure 3.1: Flowchart of methods used in this master thesis

3.2 Data from global wave statistics

Before making a probability distribution for the energy consumption there has to be done some data prepossessing. Different Hs and Tp combinations are gathered from Global wave statistics (Hogben, 1986), where you get all the Hs and Tp observations for a year. In this thesis we look into the observed Hs and Tp observations for nautic zone 11, all the nautic zones is described in Figure 3.2. The observations for zone 11 are described in Figure 3.3.

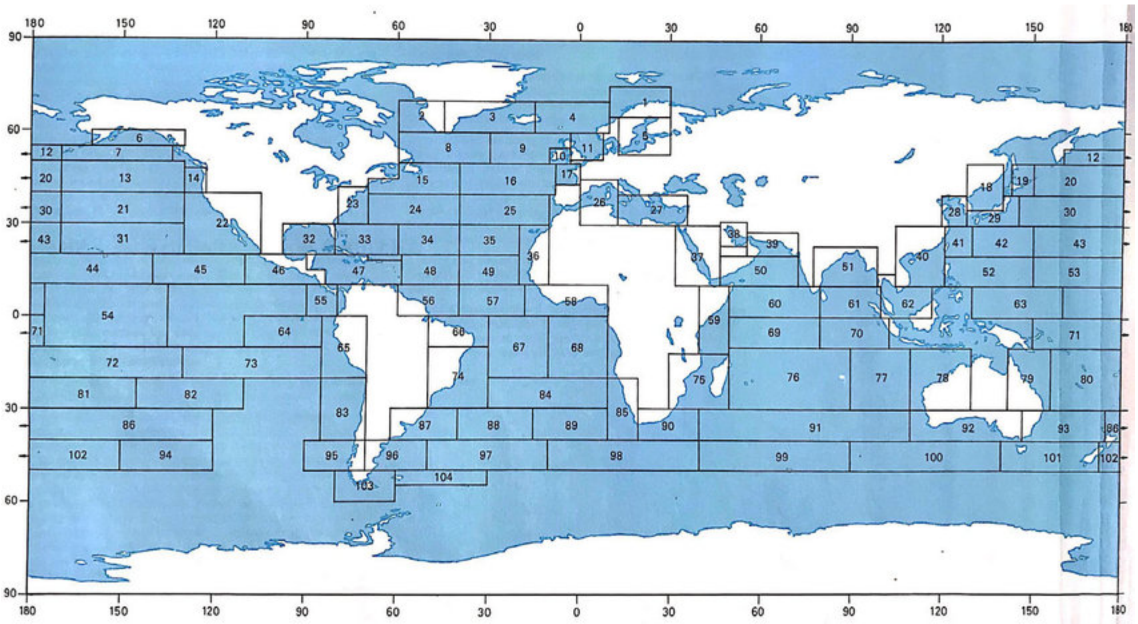

Figure 3.2: Ocean areas as defined by Ocean Wave Statistics (Hogben, 1986)

Hs											
15	0	0	0	0	0	0	0	0	0	0	0
14	0	0	0	0	0	0	0	0	0	0	0
13	0	0	0	0	0	0	0	0	0	0	0
12	0	0	0	0	0	0	0	0	0	0	0
11	0	0	0	0	0	0	0	0	0	0	0
10	0	0	0	1	1	0	0	0	0	0	0
9	0	0	0	1	1	1	0	0	0	0	0
8	0	0	1	2	2	1	1	0	0	0	0
7	0	0	2	4	4	2	1	0	0	0	0
6	0	1	4	9	7	4	1	0	0	0	0
5	0	2	11	19	14	6	2	1	0	0	0
4	0	6	27	39	26	10	3	1	0	0	0
3	1	17	63	73	40	13	3	1	0	0	0
2	3	49	121	99	40	10	2	0	0	0	0
1	19	89	94	41	10	2	0	0	0	0	0
Tp	4	5	6	7	8	9	10	11	12	13	14

Figure 3.3: Scatter diagram for zone 11 from Figure 3.2

In the Global Wave Statistics book the observations are divided into the directions the observed waves are coming from. The directions for the observations, and their percentage of total observations are in Table 3.1, but from the Global Wave Statistics, the observations give a total of 97.6%.

For the code simulating the wave directions, it is necessary with a 100% distribution to make the Monte Carlo simulation of wave direction later. Therefore were all directions divided by 0.976 to get a 100 percentage distribution, the new percentage of occurrences is as described in Table 3.2.

Direction	Degree	Occurrence
North	0	11.34 %
North-east	45	8.47 %
East	90	9.15 %
South-east	135	10.08 %
South	180	14.12 %
South-west	225	15.79 %
West	270	15.85 %
North-west	315	12.8 %
	Total percentage:	**97.6 %**

Table 3.1: Wave directions observed from global wave statistics for zone 11

Direction	Degree	Occurrence
North	0	11.6 %
North-east	45	8.7 %
East	90	9.4 %
South-east	135	10.3 %
South	180	14.5 %
South-west	225	16.2 %
West	270	16.3 %
North-west	315	13.0 %
	Total percentage:	**100 %**

Table 3.2: Wave directions observed from global wave statistics for zone 11 (Occurrence values divided by 0.976)

3.3 Simulations

In this thesis, a simulation approach is adopted as a method for assessing power consumption in maritime operations. Rather than relying on hindcast data and historical AIS data, an artificial data set is generated through Monte Carlo simulation.

This choice is motivated by efficiency considerations, as Monte Carlo simulation enables a more rapid data generation. Additionally, utilizing simulated data allows for a more extensive dataset, addressing the limitation of relying solely on historical AIS data, especially when the target ship has not traversed the specific route as many times as we are simulating. The inclusion of a broader range of possible weather conditions and different traversing speeds for the ship, other than just those encountered by the ship historically, enhances the analysis. This method helps us better understand the needed energy consumption for the ship in different and typical weather situations.

With probabilities for Hs and Tp combinations and wave directions, they are chosen randomly using a Monte Carlo model for creating artificial data sets for a route.

3.3.1 Simulation of weather data

Hs and Tp
The selection of significant wave height (Hs) and wave period (Tp) for the artificial dataset is fabricated by employing a Monte Carlo model. The available range of Hs and Tp values is derived from the scatter diagram specific to ocean zone 11, as can be seen in Figure 3.2. This scatter diagram is transformed into a probability matrix, which becomes an integral component of 10 000 Monte Carlo simulations. By doing so, the simulation considers the likelihood associated with various combinations of Hs and Tp, increasing the dataset to be more accurate to real life.

Wind and wave direction
Wave direction is determined through a Monte Carlo simulation, considering the eight directions outlined in Table 3.2. Given the assumption of a correlation between wind and waves, wind and wave direction is inline (DNV, 2010).

Wind speed
Wind is an important factor when estimating the energy consumption. Assuming that there are correlation between significant wave height and wind speed Equation 3.1 from (Stewart, 2008) is used to estimate the wind speed given a significant wave height from the Monte Carlo simulation.

$$V_{WTref} = \sqrt{\frac{gH_s}{0.22}} \tag{3.1}$$

Symbol	Parameter
H_s	Significant wave height
g	Acceleration due to gravity

Table 3.3: Parameters for Equation 3.1

3.4 Battery capacity and weight

The Corvus Blue Whale maritime battery is being used to estimate the battery weight. Corvus Blue Whale specifies that for every kWh the motor needs a battery weight of 8.9 kg. It is assumed that the depth of discharge is 50 percent, meaning the battery capacity has to be double what is the minimum needed. In practice, this means that for every kWh needed the battery weight is 17.8 kg. This is practiced so the battery never needs to be fully discharged, this will help maintain battery capacity over time.

Equation 3.2 is how to calculate the battery weight for a given energy consumption.

$$Batteryweight = \frac{1}{DoD} \cdot 8.9 \cdot E_{tot} \tag{3.2}$$

Symbol	Parameter
DoD	Depth of discharge
E_{tot}	Total energy consumption [kWh]

Table 3.4: Parameters for Equation 3.2

3.5 Power consumption using The MariTEAM model

Since the MariTEAM model initially uses historical data to estimate the power consumption, there has been made a code to simulate different weather conditions to calculate the different power consumption. This is done because the historical data can be unreliable and there would have been fewer voyages from real life than the amount that can be simulated, in this case 10 000 simulations.

The MariTEAM code calculates both the power consumption and emissions. There are parts of the input to the code that are required for the emissions part, and parameters is only required for emissions calculations will be set to zero since the part of the code that calculates emissions won't be used. The MariTEAM model gets a pandas DataFrame with information about different parameters which is described in Table 3.5.

Parameter	What the parameter is in the input file
bearing	Direction ship is sailing
draught	Draught of ship
delta_dist_km	Length ship is sailing with further given weather conditions
delta_time_s	Time used sailing between coordinates
eca_exists	Emissions control area
x_coor	Latitude coordinate
y_coor	Longitude coordinate
time	Time of voyage
wave_height	Significant wave height
wave_direction	Direction of wave
u10	East-west wind component
v10	North-south wind component
mwp	Maximum wave period
wind_speed	Wind speed
wind_direction	Wind direction
beaufort	Beaufort value for the wind speed
unixtimestamp	Time in unixt format
origin	For historical data this is 1 to recalculate the speed, therefore 0

Table 3.5: Explanation to what the data frame input is in the MariTEAM code

As mentioned a Monte Carlo simulation is used to simulate the weather conditions (Hs and Tp) and the wind and wave direction (both assumed inline). The selection of other variables is guided by available ship data, route direction, and the specific requirements of the code implementation.

A description of the input parameters for the MariTEAM model, including their respective units and the basis for their selection or simulation, is provided in Table 3.6.

Parameter	Unit	Description of the data and how it is fabricated or chosen
bearing	Degrees	South
draught	m	Draught of ship
delta_dist_km	km	Length of leg
delta_time_s	-	Used for emission calculations, set as 0
eca_exists	-	Used for emission calculations, set as 0
x_coor	-	Latitude coordinate for where ship starts
y_coor	-	Longitude coordinate for where ship starts
time	-	Not historical data, set as 0
wave_height	m	Chosen using Monte Carlo simulation
wave_direction	Degree	Chosen using Monte Carlo simulation
u10	m/s	Calculated from wind speed and wind direction
v10	m/s	calculated from wind speed and wind direction
mwp	Second	Chosen using Monte Carlo simulation
wind_speed	m/s	Calculated from wave_height
wind_direction	Degree	set as equal as wave_direction
beaufort	-	Calculate the Beaufort value from wind speed
unixtimestamp	-	Not historical data, set as 0
origin	-	1 for historical data, set as 0

Table 3.6: Input to the MariTEAM code

First the power consumption is calculated for the route for all speeds between 5-15 knots each having 10 000 simulations, we do not look at speeds higher than 15 knots because the case ship is based on a ship with a design speed of 15 knots. After the power consumption is calculated using the MariTEAM model the energy consumption for the whole route is calculated. Using Equation 3.3 the energy consumption is calculated and transferred into a CSV file, which later is used to analyze and visualize the data.

$$E = (P_{mot} + P_{aux}) \cdot t \tag{3.3}$$

Symbol	Parameter
P_{mot}	Power for motor
P_{aux}	Power for auxiliary machinery
t	sailing time for the ship calculated using Equation 3.4

Table 3.7: Parameters for Equation 3.3

$$t = \frac{d}{V} \tag{3.4}$$

Symbol	Parameter
V	velocity in km/t
d	distance in km

Table 3.8: Parameters for Equation 3.4

3.5.1 Checking if the MariTEAM model is implemented correctly

To validate that the implementation of the MariTEAM code is correct there have been hand calculations to verify that the code gives good estimates for power prediction. The methods to calculate the resistance and then the power prediction is described in Section 2.6.

The MariTEAM is a more thorough way to estimate power and emissions predictions for the world fleet, so when hand calculating the power prediction there are simplifications made.

The simplifications to hand calculate the power prediction:

1. Draught at AP and Draught at FP is in this estimation equal to T, meaning $AT = AP = T$
2. Hull roughness, k, is set to 150. A typical value for ship resistance calculations.
3. Block coefficient set as 0.67
4. Wetted surface is found using (Kristensen, 2017) method for a RO-RO ship, formula as in Equation 2.3

After hand calculating the power predictions the power prediction is 6.8% more for the MariTEAM code, and the code is assumed to be giving correct results. Comparisons of calm water, wind and wave resistance and power prediction is described in Table 3.9 and complete hand calculations can be seen in the appendix in Appendix F.

Symbol	Description	Hand calculations	MariTEAM code	Difference
R_T	Calm water resistance	116 kN	113 kN	2.7 %
R_{AA}	Wind resistance	15.1 kN	12.7 kN	18.9 %
R_W	Wave resistance	53.6 kN	46.8 kN	14.5%
P_{tot}	Power prediction	1410.7 kW	1506 kW	6.8 %

Table 3.9: Results from validation of the results from the MariTEAM code

3.6 Speed distribution for given power

In Section 3.5 the energy consumption is calculated on the assumption that the ship sails at a set speed continuously through the whole voyage. Often in maritime voyage planning the power output is assumed fixed, not the speed. Therefore, in this section, we will modify the methodology to account for a fixed power.

The fixed power output is set equal to the needed power consumption for sailing at the design speed, 15 knots, in calm water conditions. An increase or reduced resistance due to weather will affect the speed. By setting the fixed power output and assuming a given battery capacity, we can construct a probability distribution to analyze if the ship will reach its destination at various speeds and weather conditions. The battery capacity is set to a level corresponding to the given route, the fixed power output for a sailing speed of 15 knots in calm water conditions. The simulations will result in different speeds, affected by the weather, and hence provide a derived distribution of probable voyage times.

To construct the probability distribution, data from previous simulations of power consumption are utilized. Initially, the portion of power consumption attributable to calm water resistance is determined. Subsequently, the remaining power usage is ascribed to weather-related factors.

Utilizing the MariTEAM model, the power consumption at speeds ranging from 5 to 15 knots under calm water conditions is estimated. The maximum speed at which the ship can operate given its power output is then identified by selecting the combination of calm water power consumption and weather-induced power consumption that most closely matches the available power output.

The maximal power consumption from calm water resistance is found using Equation 3.5 with parameters described in Table 3.10.

$$P_{R_{Cmax}} = P_{R_{lim}} - (P_R - P_{R_C}) \tag{3.5}$$

Symbol	**Parameter**
P_R	Initial power consumption in simulation
P_{R_C}	Power consumption for calm water
$P_{R_{Cmax}}$	Power to not exceed maximum power
$P_{R_{lim}}$	Set power consumption limit

Table 3.10: Parameters for Equation 3.5

3.7 Payload allocation needed for equal energy efficiency between different fuels

In this thesis, instead of speculating about cargo earnings, there will be an assessment of the limits of battery capacity in relation to vessel payload. This approach involves the application of the energy use WTW factors outlined by Lindstad (Lindstad et al., 2023), providing a framework for understanding how battery usage interacts with payload capacity from an energy perspective.

This methodology enables an assessment of the trade-offs between battery weight and payload, in comparison to traditional diesel-powered systems. The energy use WTW factors used can be seen in Figure 3.4.

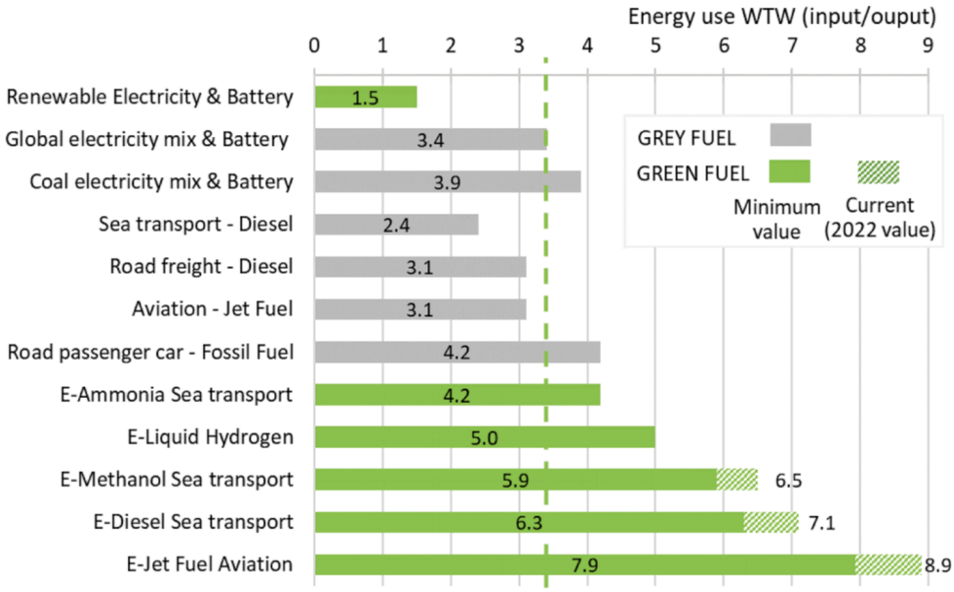

Fig. 5. WTW Energy use as a function of fuel and transport mode.

Figure 3.4: WTW Energy use as a function of fuel and transport mode from (Lindstad et al., 2023)

To calculate the the percentage of the payload that needs to be available as a percentage of dwt we use Equation 3.6, which describes the transport efficiency, to estimate the relation between E-diesel and other fuels. This is done by putting the transport factor η equal for the same ship, sailing the same route that uses different fuels (Therefore different Energy use WTW factors). UsingEquation 3.7 the payload necessary capacity needed is calculated for the transport efficiency to be equal.

$$\eta = \frac{p \cdot d}{E} \tag{3.6}$$

Symbol	Parameter
p	Estimated to be deadweight of the ship
d	Distance the ship is sailing
E	Fuel factor from (Lindstad et al., 2023)

Table 3.11: Parameters for Equation 3.6

To find out how much percentage of the payload can be utilized by the same ship with different fuels Equation 3.7 is used derived from the putting the transport efficiency to be equal for the same ship with different fuel.

$$p_j = \frac{p_i \cdot E_i}{E_j} \approx \% \cdot p_i \tag{3.7}$$

Symbol	**Parameter**
p_i	Estimated to be deadweight of ship i
p_j	Estimated to be deadweight of ship j
E_i	Fuel factor from (Lindstad et al., 2023) for ship i
E_j	Fuel factor from (Lindstad et al., 2023) for ship j

Table 3.12: Parameters for Equation 3.7

Underneath follows an example of how to estimate needed payload allocation between two fuels for a ship for equivalent energy consumption:

To put into context, assume we have a ship, denoted as ship j, which operates using e-diesel, let us consider a payload represented by the deadweight tonnage $p_i = 1000$ tons. Referring to the findings presented by Lindstad (Lindstad et al., 2023), we utilize the energy use WTW factor for battery-powered ships, denoted as E_i, which equals 1.5, and for e-diesel-powered ships, denoted as E_j, which equals 6.3. Applying the payload percentage equation (3.7), we derive the following expression:

$$p_j = \frac{p_i \cdot 1.5}{6.3} \approx 0.24 \cdot p_i = 240$$

This calculation implies that a payload allocation of 24% for the battery ship is required to ensure an equivalent energy consumption for both battery-powered and e-diesel-powered ships of same size. In theory this implies that the battery can uptake 76 % of the dwt.

3.8 Range calculations

Weather conditions significantly influence the resistance a ship encounters, playing a big role in determining the necessary battery weight for electric vessels. This thesis explores the impact of allocating a certain percentage of a ship's dwt for battery usage and how this affects the vessel's range under varying weather conditions. To visualize these effects, a matrix using Hs and Tp will be utilized. The matrix will only feature combinations of Hs and Tp that have been observed. Not calculating the battery range for weather conditions outside the observed combinations from the scatter diagram (Figure 3.3) is chosen because they are highly unlikely and are to be considered more extreme weather conditions where the battery ship range would be short.

The MariTEAM code is used to calculate the power consumption used by the ship for the observed Hs and Tp combinations. It is assumed that wind and wave directions are inline, but opposite to the ship's bearing. The range calculations are conducted using Equation 3.8.

To be able to explore different ranges for different speeds and different battery weights an interactive visualization tool in the form of a slider is developed. A slider is an interactive feature that allows users to easily adjust and visualize changes in data by moving a handle along a bar. This allows for the exploration of the ship's range at various speeds and battery capacities, which are expressed as a percentage of the ship's dwt.

$$Range = \frac{dwt_p \cdot V}{8.9 \cdot 10^{-3} \cdot \frac{1}{DoD} \cdot P_{tot}} \tag{3.8}$$

Symbol	Parameter
DoD	Depth of charge
dwt_p	Percentage of dwt used
V	Velocity of ship in m/s
P_{tot}	Power consumption
$8.9 \cdot 10^{-3}$	$\frac{kg}{kWh}$

Table 3.13: Parameters for Equation 3.8

Chapter 4

Results and discussion

The goal of this chapter is to assess what battery capacity and weight are needed for two shipping routes and the range of ships with a given battery capacity and power output. This includes simulating the weather for each route 10 000 times using a Monte Carlo simulation for Hs, Tp, and wind and wave direction. For the simulated weather of the routes power predictions for the given weather are calculated. The power prediction is done for different speeds of the ship, to see how the different speeds affect the power demand. From this we get an energy consumption probability distribution for the weather, seeing the energy consumption needed for different sailing conditions.

4.1 Case studies

The objective of the case studies is to determine the energy consumption and, consequently, the required battery capacity and weight for a specific maritime route. Additionally, the operational range of ships with various battery capacities under different weather conditions will be explored. The case ship used is a ship with similar main particulars and which sails the same route today as the planned ships for 2024 for the West-Norway - Netherlands green corridor. So the case ship is representative of the ship that could be applied to the route. The assessment has some assumptions given that battery-powered cargo ships are not in operation currently, these will be mentioned in Section 4.3.

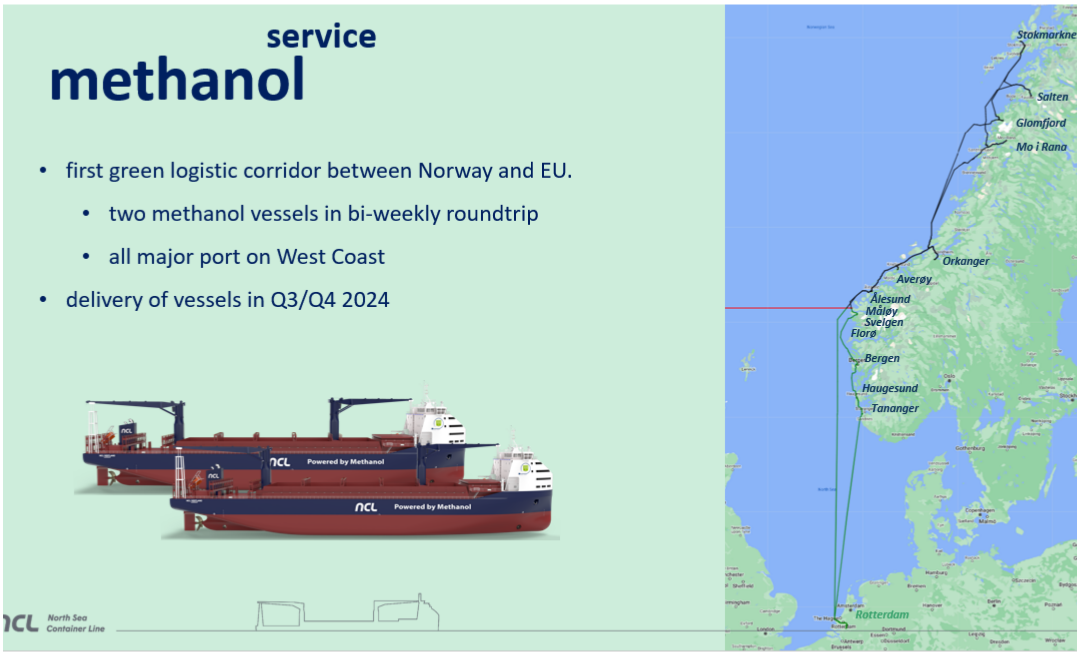

Figure 4.1: Image with planned ports, source: email from Bente Hetland, the managing director in NCL.

There is a planned green corridor between west Norway and Rotterdam. The route is illustrated in Figure 4.1, so the plan is to visit the major ports on the west coast of Norway, and the longest sailing route is between Tananger and Rotterdam. NCL is currently building two methanol ships, which are planned to be ready in the second half of 2024.

In the first case the route goes from Tananger to Harlingen in the Netherlands, Harlingen was chosen for simplicity of the route going in a straight line from north to south, the route is 593 km.

In the second case the route goes from Kristiansand in Norway to Ringkøbing in Denmark, the route is 159 km . With the knowledge that there are severe limitations to battery-powered ships from the project thesis, a route between Norway and Denmark is explored checking the feasibility of a shorter distance where there could be a possible charging stop.

The routes used in the first two cases are illustrated in Figure 4.2

Later the same case ship will be used to estimate the needed power consumption and energy consumption for calm water resistance. This data will later be used to estimate the range for the case ship when given a speed and battery weight as a percentage of dwt.

Figure 4.2: The different case routes: black: Tananger - Harlingen, red: Kristiansand - Ringkøbing

4.2 Battery pack data

For this case, the Corvus Blue Whale battery will be used as the battery in the case ship, and its particulars.

The Blue Whale battery is a large-scale energy storage system designed for use in the maritime industry, particularly in larger vessels like cruise ships and cargo carriers. Characterized by its high energy capacity, the battery is engineered to support extended operations on electric power, aiming to reduce reliance on traditional fuels and lower emissions. Its high energy density is a key feature, enabling substantial storage capacity within a limited space, an essential factor for large vessels. The modular design of the Blue Whale allows for flexible integration into various ship designs, accommodating to different power requirements (Corvus-Energy, 2022).

From an environmental perspective, the Blue Whale battery contributes to the maritime industry's shift towards more sustainable practices. It supports the transition to hybrid and fully electric propulsion systems, aligning with global efforts to reduce greenhouse gas emissions in marine transport. The battery system includes an advanced management system for efficient operation, monitoring, and maintenance, ensuring both performance and life cycle. Corvus Energy's development of the Blue Whale battery is reflective of the broader industry trend towards incorporating green technology in maritime operations, aiming to balance operational efficiency with environmental considerations (Corvus-Energy, 2022).

In the case studies the theoretical battery ship will be powered by the Corvus Blue Whale maritime batteries. The Corvus Blue Whale is light and small while being intended for bigger vessels (Corvus-Energy, 2022). Based on Figure G.1 in appendices 8.9 kg/kWh is used for finding the weight of the battery for the given total energy consumption, but as mentioned in chapter 3 since the depth of charge is 0.5 the battery weight is practically 17.8 kg/kWh to maintain the batteries.

Battery weight	8.9 [kg/kWh]
Depth of charge	0.5

Table 4.1: Particulars for Corvus Blue Whale batteries

4.3 Assumptions

Several assumptions are being made to estimate resistance and battery capacities:

1. Draught at aft perpendicular and draught at forward perpendicular is in this estimation equal to draught, zero trim
2. Wave direction and wind direction is inline
3. Wind can be estimated from significant wave height
4. The depth of discharge is set as 0.5
5. Don't take into account the shape of the battery packages, but look at the total weight as a percentage of dwt.

4.4 Case vessel data

Since the ships planned for 2024 aren't available yet, a substitute ship currently operating on the same route and exhibiting similar qualities is being used for this study. The case ships main particulars are found in Table 4.2. The cases will estimate the power consumption of two routes, between west Norway and the Netherlands, and another shorter route between Norway and Denmark. Later the case ship will be used to calculate the range for the case ship given different battery weights.

Length	120	m
Length BP	117.6	m
Breadth	20.8	m
Draught	6.2	m
Built	2015	-
Service speed	15	knots
dwt	4900	tons
ldt	4519	tons
teu	none	-
Auxiliary engine	820	kWh
Main engine	3940	kWh
Main engine rpm	750	rpm
Main engine stroke	4	-
Main engine cylinders	9	-
Ship type	Ro-Ro	-
Ship type detailed	Ro-Ro Cargo ship	-

Table 4.2: Main particulars for case ship

4.5 Case: Norway - Netherlands

The objective of this case is to check if the battery powered ships will be applicable on a ship sailing the Rotterdam - West coast of Norway's green corridor. It is assumed that there are four specific weather conditions encountered along the route, this means that there are four Monte Carlo simulations for the weather parameters. To calculate the power predictions using the MariTEAM the data in Table 4.3 is given to the code as a pandas DataFrame.

From: Tananger, Norway
To: Harlingen, Netherlands
Start coordinates: 58.9N, 5.4 E
End coordinates: 53.2N, 5.4E
Length of route: 593 km

Parameter	Description of how the data is fabricated or chosen
bearing	180 degrees
draught	6 m
delta_dist_km	143 km, one fourth of the whole leg
delta_time_s	0, used for emission calculations
eca_exists	0, used for emission calculations
x_coor	58.9
y_coor	5.4
time	0, not historical data
wave_height	Chosen using monte carlo simulation
wave_direction	Chosen using monte carlo simulation
u10	calculated from wind speed and wind direction
v10	calculated from wind speed and wind direction
mwp	Chosen using monte carlo simulation
wind_speed	Calcluate from wave_height
wind_direction	set as equal as wave_direction
beaufort	Calculate the beafort value from wind speed
unixtimestamp	0, not used
origin	0, often 1 for historical data

Table 4.3: Input to the MariTEAM code

First, the power consumption of the 10 000 simulations for each speed between 5- 10 knots is calculated using the MariTEAM code. Then from the power prediction, the energy consumption is calculated for the route. Then the energy consumption is split into energy bars of 1000 kWh each. From that, we get the energy consumption, which is illustrated in Figure 4.3, which is the energy consumption for 10 knots, histogram for energy consumption for all other speeds can be seen in Appendix A.

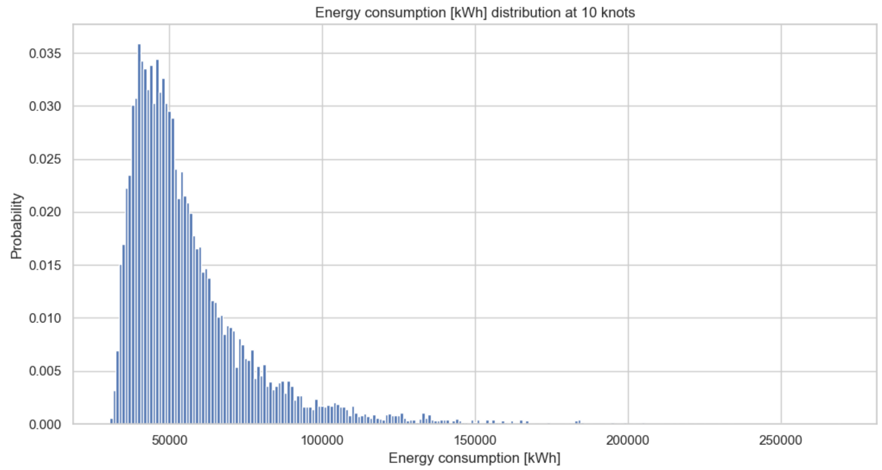

Figure 4.3: Energy consumption distribution for ship sailing Tananger - Harlingen with speed 10 knots

Then a cumulative probability distribution is calculated using Equation 4.1 for the energy consumption for the different speeds, where $P(X_i)$ is the probability of the bar. The cumulative energy consumption probability distribution for Tananger- Harlingen is plotted in Figure 4.4.

$$F(X) = \sum_{i=0}^{j} P(X_i) \tag{4.1}$$

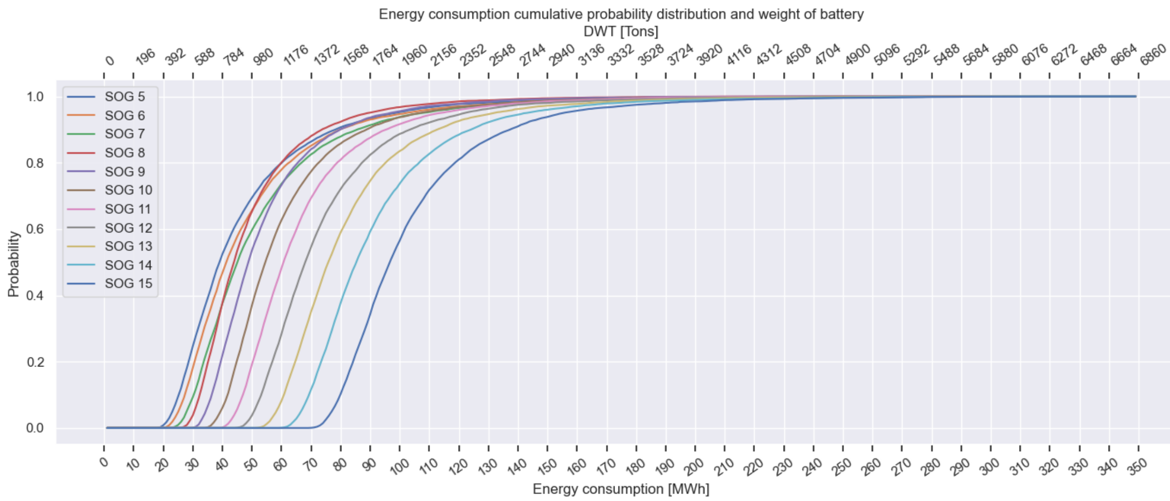

Figure 4.4: Cumulative energy consumption for Tananger - Harlingen, 4 legs

Speeds between 5-9 knots

For the case between Norway and the Netherlands, the results of the energy consumption's cumulative probability distribution for all speeds between 5-15 are presented in Figure 4.4. From the cumulative probability distribution, it is observed that for speeds between 5 and 9 the curves of the probabilities of energy consumption are between 40-60 MWh, and they are being intersected. The curves also converge around the same range at 120-130 MWh. This suggests that at lower speeds, weather conditions play a more significant role in influencing energy consumption. This is also confirmed by looking at Figure 4.5.

In Figure 4.5a and Figure 4.5b, the analysis confirms that the peak probability of energy consumption is centered approximately at 50 MWh for both speeds, 5 and 9 knots. Furthermore, a parallel decline in probability is observed for higher levels of energy consumption in each instance. This consistency suggests a comparable power consumption pattern at these operational speeds between 5-9 knots, this implies that investigations into slow steaming strategies for this type of ship should focus on speeds of 9 knots and above.

All histograms for energy consumption are found in Appendix A.

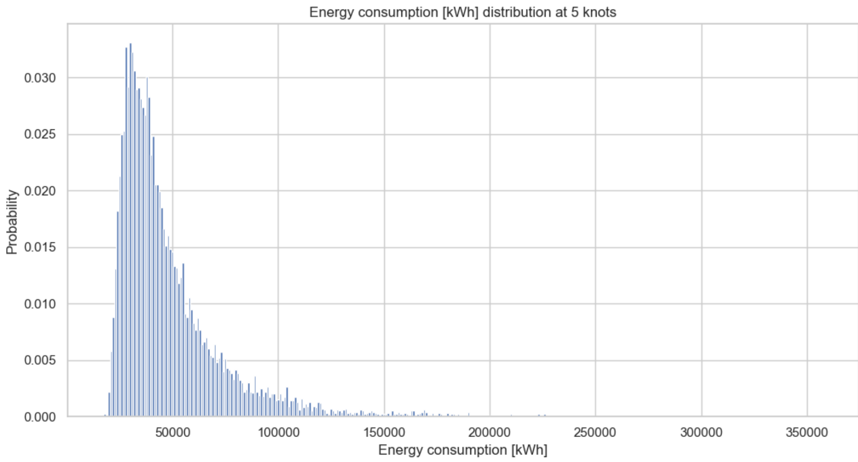

(a) Speed: 5 knots

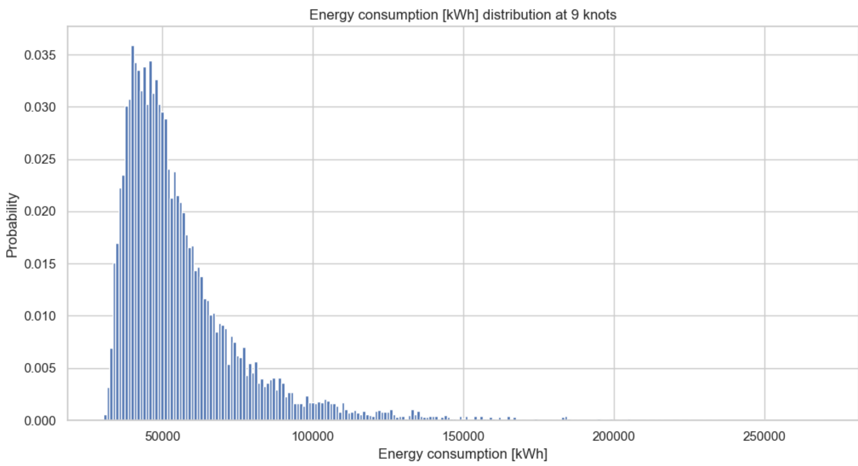

(b) Speed: 9 knots

Figure 4.5: Energy consumption histograms for the ship sailing from Tananger to Harlingen at different speeds.

Speeds between 10-15 knots

When analyzing the energy consumption probability distribution curves presented in Figure 4.4 for speeds ranging from 10 to 15 knots, it is observed that these curves do not intersect with each other, and the increase in energy consumption becomes more pronounced between the higher speeds, in contrast to the behavior observed at lower speeds. This suggests that the rise in energy consumption attributable to increased speed is more significant from 10 knots upwards.

Since speeds from 10 knots and above affect the battery capacity more severe speed will be a important factor when considering the necessary battery capacity for higher speeds. It will also be important to find a balance between battery weight and needed payload allocation. Further studies will be necessary to find out to which extent shipping companies are willing to compromise on the allocated payload for increased battery capacity if the ships are going to sail at higher speeds. Looking at needed payload allocation from a energy perspective will be explored later in Section 4.7.

4.5.1 Different number of legs

The decision to split the route into four legs came from the consideration that in a real-life voyage, the weather does not stay the same during the whole journey. By splitting up the journey into four legs, this approach significantly reduces the probability of encountering successive extreme weather conditions, as the likelihood of simulating four consecutive extreme weather scenarios is very low. To evaluate the impact of segmenting the journey was simulated with fewer numbers of legs. Initially, the journey was split into two legs, and one single leg.

The results from the two-legged journey are presented in Figure 4.6. The outcomes of the simulation with one leg are presented in Figure 4.7.

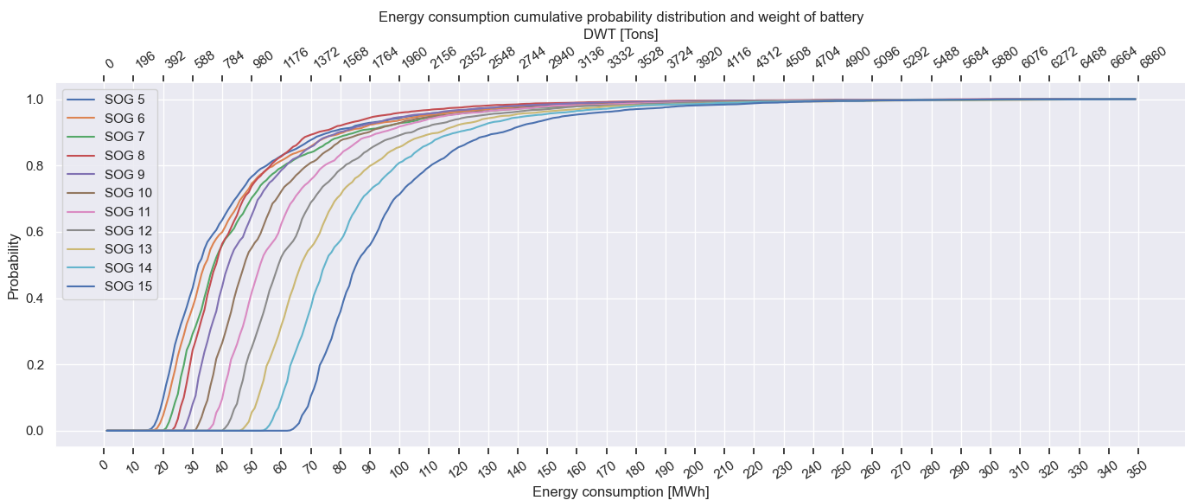

Figure 4.6: Cumulative energy consumption for Tananger - Harlingen, 2 legs

In Figure 4.6 the journey is split into two legs, and gives a similar energy distribution probability distribution as for four legs. It's observed that energy consumption is slightly lower at lower probabilities, which may be attributed to the fact that journeys with more segments are less likely to have the lowest capacities. This is because the likelihood of encountering segments with higher weather-related energy contributions increases with the number of segments.

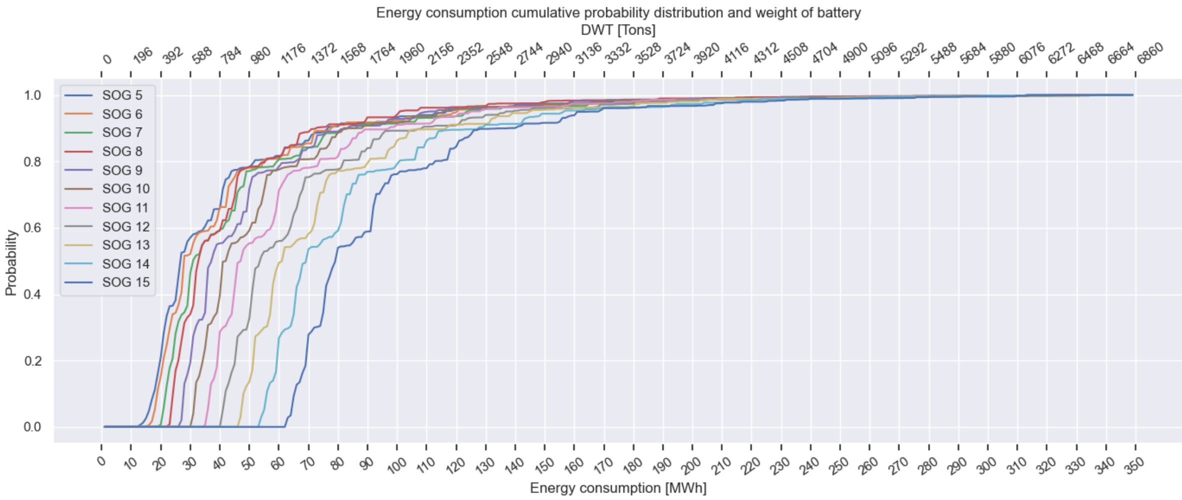

Figure 4.7: Cumulative energy consumption for Tananger - Harlingen, 1 leg

In the simulation where the voyage is split into a single leg, as observed in Figure 4.7, the cumulative probability curves are uneven. This irregularity occurs because of discretification in the scatter diagram being too coarse. In a simulation of 10,000 iterations, these discrete measurements lead to a repetition of certain values, thereby causing the curve to become uneven and choppy. This can also be seen from the histogram visualization showing the distribution of the energy consumption distribution in Figure 4.8. The pattern observed in the curve reflects the impact of significant fluctuations in the scatter diagram's values. This observation was validated through a supplementary simulation using a different but similar scatter diagram, with similar discretification. The results of this additional simulation can be observed in Figure 4.9, confirming that the discretification are responsible for the uneven nature of the probability curves.

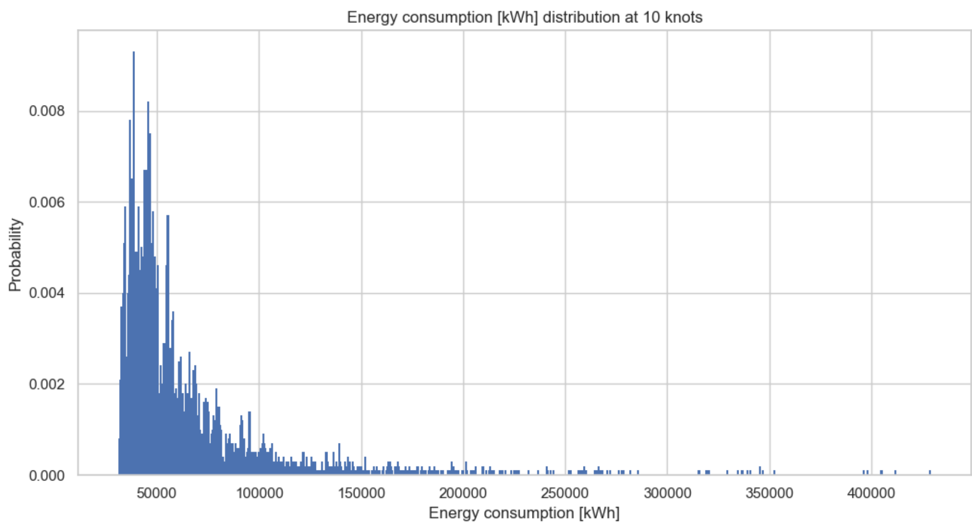

Figure 4.8: Energy consumption distribution for Tananger - Harlingen, 1 leg - 10 knots

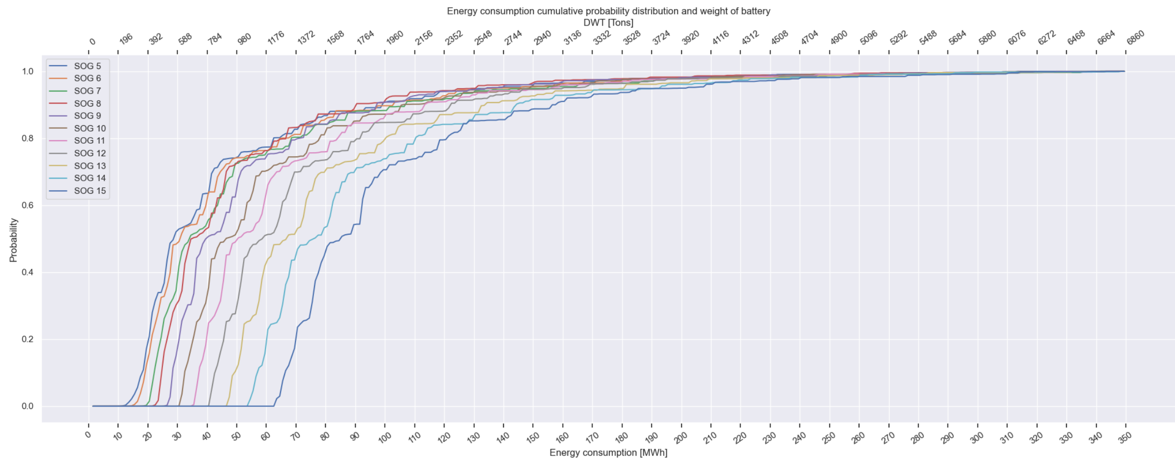

Figure 4.9: Cumulative energy consumption for Tananger - Harlingen, 1 legs - different scatter diagram

4.5.2 Percentage of dwt the battery will occupy for different probabilities of reaching destinations

From the cumulative probability, different battery weights are calculated for different percentages of sailing availability.

To illustrate, a probability of 95% means that there is a 95% chance that the ship will not use more than this amount of energy, which again means a 95% chance the ship will be able to reach its destination with a battery pack with that amount of available energy. Meaning that the higher the probability of the ship being able to reach destination the heavier the battery will most likely become.

The different battery weights in the form of a percentage of the dwt of the ship for given sailing probabilities can be seen in Table 4.4, the given dwt of the ship is 4900 tons.

SOG/ Probability	0.90	0.91	0.92	0.93	0.94	0.95	0.96	0.97	0.98	0.99
5	28.5	29.4	30.8	32.2	33.9	35.8	38.0	41.1	46.3	57.5
6	28.9	30.1	31.2	32.7	34.8	37.2	39.9	43.6	49.6	61.2
7	31.1	32.5	33.8	34.9	36.7	38.3	42.0	45.7	51.5	62.2
8	26.8	27.7	28.7	29.7	30.8	32.4	34.5	37.0	41.3	49.2
9	29.0	29.9	31.0	32.1	33.1	35.2	37.3	39.6	44.4	51.4
10	32.2	33.1	34.3	35.4	36.9	38.8	41.4	44.8	49.3	58.4
11	34.7	35.7	36.7	38.1	39.4	40.9	43.7	46.9	51.4	63.7
12	37.7	38.6	39.8	41.0	42.7	44.4	46.5	49.2	54.1	63.7
13	40.9	41.9	43.0	44.1	45.9	47.8	50.5	53.4	59.6	68.3
14	45.1	46.0	46.9	48.2	49.8	51.8	54.6	57.9	62.9	73.3
15	49.8	50.9	51.9	53.2	54.8	56.4	59.0	63.2	68.8	78.3

Table 4.4: Weight of battery as percentage of dwt, route: Tananger - Harlingen

From Table 4.4 it is observed that attaining a 0.99 probability requires heavy batteries, with weights ranging between 49.2% and 78.3% of the dwt. The need for such high battery weights comes from the requirement for ships to navigate through more extreme storms at this probability level. However, the required battery weight for 9 knots decreases significantly from 51.4% to 37.3% of dwt when the probability is adjusted from 0.99 to 0.96, representing a 14.1% reduction. By setting a lower probability for weather conditions, the battery weight can be significantly reduced.

Considering that battery-powered ships will need time for charging, effective weather planning and optimization can ensure that periods of downtime due to weather are utilized for recharging the batteries.

Table 4.4 indicates that at higher speeds, particularly between 13-15 knots, the required battery weight becomes significantly heavy. With a probability of 0.90, the battery's weight ranges between 40.9% and 49.8% of dwt. This scenario is less ideal, as the battery occupies a considerable part of the payload, and the ship's sailing conditions are limited. The trend towards heavier batteries at higher probabilities is noticeable, making it unlikely for a battery-powered ship on this route to implement speeds above 12 knots with current battery technology, while still accomplishing a reasonable payload.

When looking at Table 4.4 it is interesting to see again that the needed battery weight is similar for the different probabilities and speeds between 5-9 knots, this matches the observations for the cumulative energy consumption probability distribution in Section 4.5. With a probability between 0.90 - 0.96, the battery weight is between 28.5%-42.0% of dwt for the slower speeds. Having the battery taking up 42% of the dwt is a lot, this indicates that this route may be too long if the ship is needed for higher-speed operations that demand more payload capacity.

4.5.3 Energy consumption in calm water conditions

The MariTEAM code was used to calculate the energy consumption for calm water conditions, meaning waves and wind is not being considered in this scenario, for speeds between 5-15 knots for the ship.

The energy consumption for the case ship in calm water for different speeds can be seen in Figure 4.10 and Table 4.5.

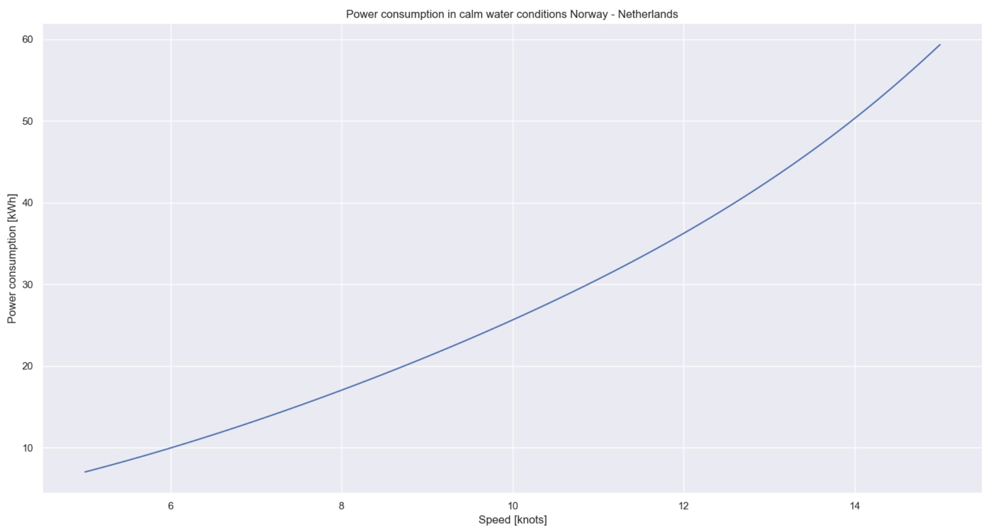

Figure 4.10: Energy consumption in calm water conditions, Norway - Netherlands in headwind and head waves

5	6	7	8	9	10	11	12	13	14	15
7035.6	9968.4	13316.9	17044.7	21140.4	25633.9	30611.6	36224.8	42688.5	50284.7	59327.3

Table 4.5: Energy consumption for the for ship in calm water conditions in kWh, Netherlands-Norway

Figure 4.10 illustrates that the energy consumption increases more and more the higher the speeds of the ship. These results are being used to estimate battery capacity and corresponding battery weight for the power output. This finding supports that for higher speeds, the influence of calm water conditions on power consumption becomes markedly pronounced.

4.5.4 Optimal speed given a specified power output

In this section, the power output of the ship is determined based on the power consumption in calm water conditions at a design speed of 15 knots. Furthermore, the battery capacity and corresponding battery weight are estimated from the power output based on sailing the route at 15 knots. This is then used to identify the optimal speeds for the case ship, ensuring it does not exceed the established power consumption limit.

With a power output of 2779, which is the needed power consumption for calm water conditions at 15 knots the needed battery weight is 21.6% of the dwt. To provide an understanding of the relationship between power consumption and voyage parameters such as speed and sailing time, the study further examines scenarios for different power outputs. The different power outputs and their corresponding battery weights are described in Table 4.6, all the different power outputs are chosen as a factor from the power consumption for 15 knots in calm water conditions.

The probability of achieving certain sailing speeds with the specified power outputs is illustrated in Figure 4.11 where you see the probability of the ship being able to sail the route for the given speed. For example, if you look at the dark red curve for 2223 kW the highest probability at 5 knots to reach the target destination is under 70% probability. This is of course not applicable because sailing at 5 knots is too slow and under 70% probability also too rarely.

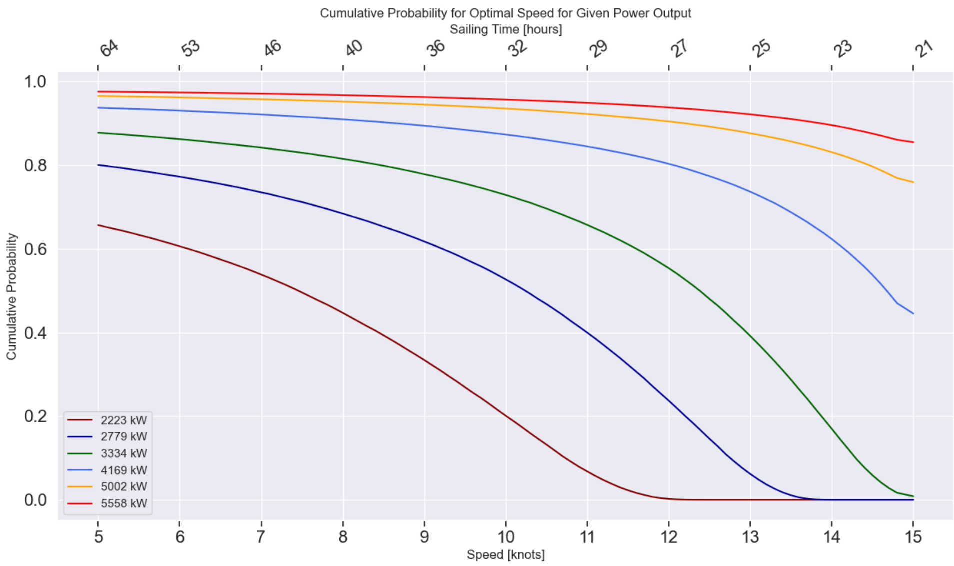

Figure 4.11: The optimal speeds with voyage time for the Norway - Netherlands given the power consumption needed for 15 knots in calm water

In Figure 4.11 the first three power output curves are not sufficient to be able to complete the route even if the ship sails at 5 knots for the entirety of the journey. For 3334 kW power output, which is the biggest power output of the first three, it can be observed that if the speed can be lowered to 5 knots there is a around 90% probability of sailing. But as mentioned before when choosing a sailing speed of 5 knots is too slow. From previous results, the minimum speed should be around 9 knots. When looking at the probability of sailing at 9 knots the probability is right under 80%, therefore the higher power outputs were chosen to look into.

When looking at the power output of 4169 kW, 5002 kW, and 5558 kW in Figure 4.11 4169 kW is still not enough power if the ship is to have a high probability to sail at a more reasonable speed. The probability curves for 5002 kW and 5558 kW both seem to be almost inline from 10 knots and lesser speeds and when looking at 9 and 10 knots it is observed that the probability of reaching the target destination is around 95%. The battery weight for the two highest powers are 38.8% and 43.1% of dwt.

By comparing the results of battery weight for 9 and 10 knots for a set power output with a set speed in any given probability in Table 4.4 from Section 4.5.2 the battery weights for similar speeds are slightly higher for set speed. This is a small indication that for a set speed, the battery weight is over-predicted. The reason this may occur is because is the size of the increments used in the analysis. Fixed speeds are considered in increments of 1 knot, whereas the speed probabilities are evaluated at more refined increments of 0.1 knot, seemingly leading to a more nuanced assessment in the latter case.

Power output [kW]	Battery weight [Tons]	% of dwt	Factor
2223	845	17.2	0.8
2779	1056	21.6	1.0
3334	1267	25.6	1.2
4169	1584	32.3	1.5
5002	1901	38.8	1.8
5558	2112	43.1	2.0

Table 4.6: Battery weight for the different power outputs, factor is the factor between the needed power for 15 knots in calm water and the power output

4.6 Case: Norway - Denmark

The objective of the case study is to determine the energy consumption and, consequently, the required battery capacity and weight for a specific maritime route. Additionally, the operational range of ships with various battery capacities under different weather conditions will be explored.

This case has chosen a shorter route to investigate the needed battery capacity needed if we were to have shorter stages between stops. A possible route between Norway and Denmark were chosen. Kristiansand was chosen as the port in Norway and Ringkøbing was chosen as the port in Denmark. Ringkøbing were chosen because there is a wind turbine park there so there may be possibilities for a charging station from renewable energies there in the future. It is assumed on this route that the weather conditions will be constant during the entirety of a voyage. To calculate the power prediction using the MariTEAM code the data in Table 4.7 is given to the code as a pandas DataFrame.

From: Kristiansand, Norway
To: Ringkøbing, Denmark
Start coordinates: 58.1N, 8.1E
End coordinates: 56.1N, 8.0E
Length of route: 159 km

Parameter	Description of how the data is fabricated or chosen
bearing	180 degrees
draught	6 m
delta_dist_km	159 km, the whole leg
delta_time_s	0, used for emission calculations
eca_exists	0, used for emission calculations
x_coor	58.1
y_coor	8.1
time	0, not historical data
wave_height	Chosen using monte carlo simulation
wave_direction	Chosen using monte carlo simulation
u10	calculated from wind speed and wind direction
v10	calculated from wind speed and wind direction
mwp	Chosen using monte carlo simulation
wind_speed	Calculate from wave_height
wind_direction	set as equal as wave_direction
beaufort	Calculate the Beaufort value from wind speed
unixtimestamp	0, not used
origin	0, often 1 for historical data

Table 4.7: Input to the MariTEAM code

First, the power consumption of the 10 000 simulations for each speed between 5- 10 knots are calculated using the MariTEAM code. Then the from the power prediction the energy consumption is calculated for the route and are put into histogram where the histogram bars are split into 1000 kWh each. From that, we get the energy consumption, which is illustrated in Figure 4.12, which is the energy consumption for 10 knots, all other speeds can be seen in Appendix B.

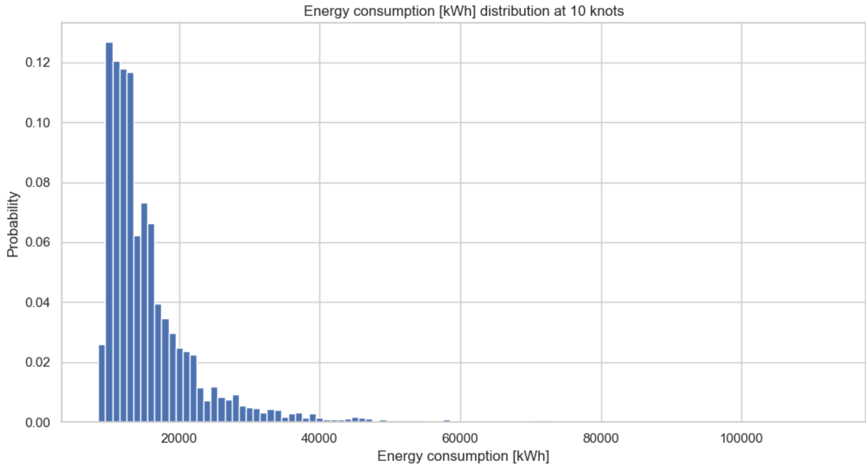

Figure 4.12: Energy consumption distribution for ship sailing Kristiansand - Ringkøbing with speed 10 knots

Then a cumulative probability is calculated using Equation 4.1 for all the energy brackets for the different speeds as in the previous case.

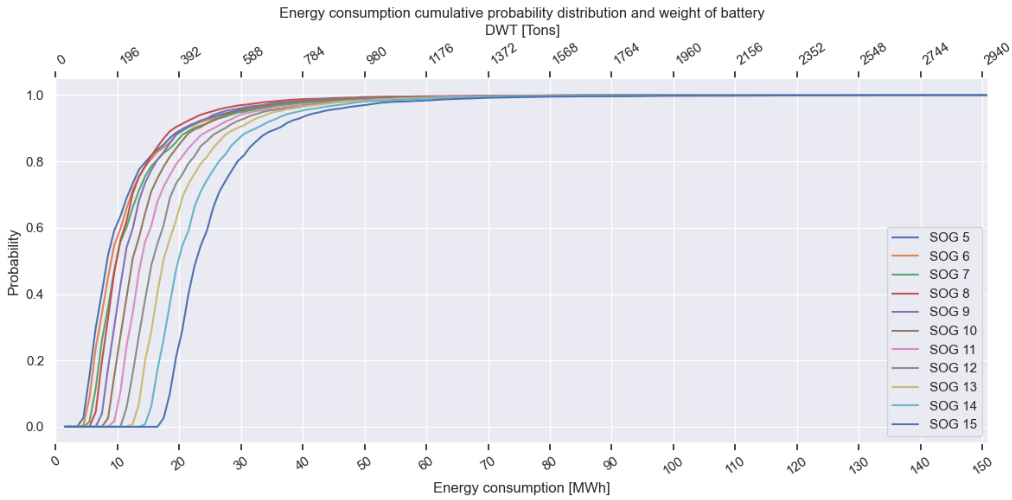

Figure 4.13: Cumulative energy consumption for Kristiansand - Ringkøbing, less x-axis values

Speeds between 5-9 knots

In the case of Norway and Denmark, the results of the energy consumption cumulative probability distribution for all speeds between 5-15 are presented in Figure 4.13. In Figure 4.13 the speeds between 5-9 knots converge around 40-50 MwH, this will give a battery package which will occupy between 16% - 20%. This is also observed in Figure 4.14a and Figure 4.14b where the energy consumption has a similar distribution in their histograms for 5 and 9 knots. This is an indication that speeds from 9 knots and above should be investigated further since the weather is such a prominent contributor to the needed battery capacity. A similar pattern is noted in the Norway-Netherlands case, indicating a consistent trend.

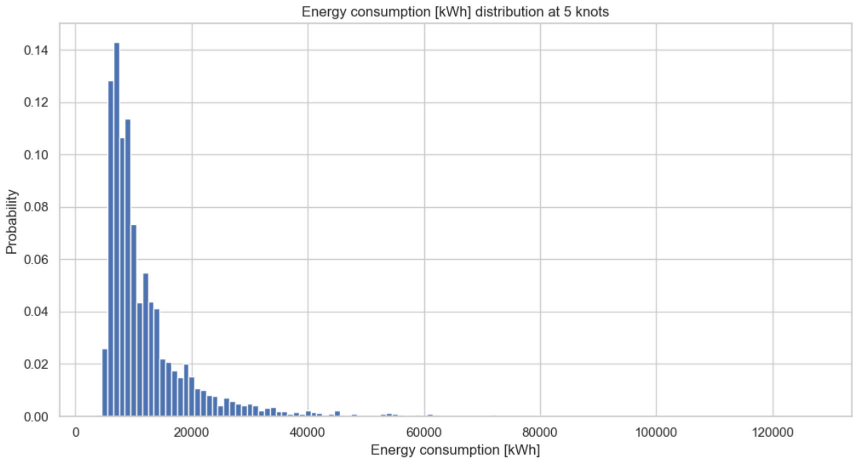

(a) Speed: 5 knots

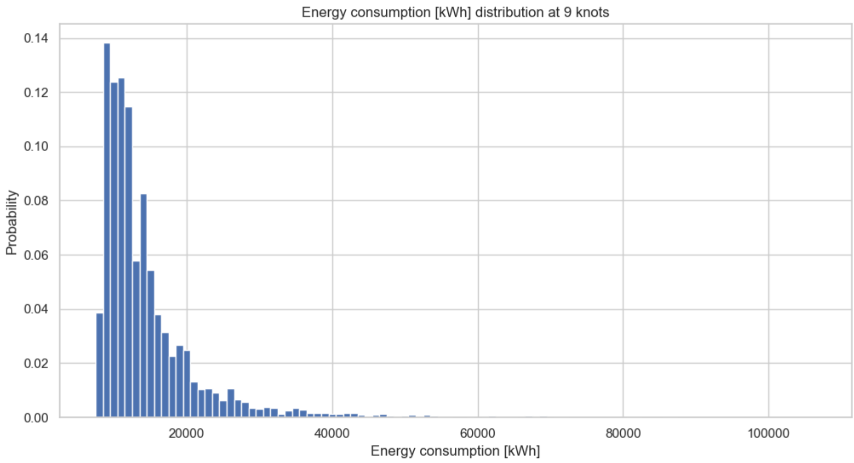

(b) Speed: 9 knots

Figure 4.14: Energy consumption histograms for the ship sailing from Kristiansand to Rinkøbing at different speeds.

Speeds between 10-15 knots

When analyzing the energy consumption probability distribution for higher speeds ranging from 10 to 15 knots in Figure 4.13 it is observed that the curves converge within the range of 50-60 MWh, this will give a battery weight that occupies around 20% - 24% of dwt. The tendency of the curves to cluster in this energy consumption range suggests that the vessel is likely to achieve good energy efficiency at higher speeds without substantially compromising payload capacity. Therefore, the operational profile of the ship appears to be possible to optimize at a higher velocity for this route compared to the longer route.

In comparing the energy consumption profiles of lower and higher velocities, it becomes evident that the implementation of higher sailing speeds is more appropriate for battery-operated ships of this size undertaking voyages of shorter lengths.

4.6.1 Percentage of dwt the battery will occupy for different probabilities of reaching destinations

From the cumulative probability, different battery weights are calculated for different percentages of sailing availability. The different battery weights in the form of a percentage of the dwt of the ship for given sailing probabilities can be seen in Table 4.8, the given dwt of the ship is 4900 tons. Compared to the previous case the battery weight is much lighter overall, and considerably when the ship sails slower than 11-12 knots.

SOG/ Probability	**0.90**	**0.91**	**0.92**	**0.93**	**0.94**	**0.95**	**0.96**	**0.97**	**0.98**	**0.99**
5	7.6	7.9	8.4	9.0	9.6	10.4	11.4	12.7	15.0	19.6
6	7.7	8.1	8.6	9.3	9.9	10.8	11.8	13.1	15.5	20.4
7	8.1	8.7	9.1	9.6	10.3	11.1	12.1	13.3	15.1	18.8
8	7.0	7.3	7.7	8.1	8.5	9.2	9.9	11.0	12.6	16.0
9	7.7	8.0	8.4	8.9	9.3	9.8	10.8	12.2	13.7	16.8
10	8.3	8.7	9.1	9.6	10.0	10.6	11.5	12.7	14.2	18.0
11	9.3	9.6	10.0	10.4	10.9	11.6	12.7	14.2	16.6	20.4
12	10.0	10.3	10.6	11.1	11.6	12.3	13.6	14.9	16.9	20.4
13	10.7	11.1	11.4	11.8	12.3	13.0	14.0	15.3	16.9	21.0
14	11.8	12.2	12.6	13.0	13.5	14.2	15.3	16.7	18.1	22.3
15	13.1	13.4	13.8	14.4	14.9	15.6	16.8	18.2	20.1	24.6

Table 4.8: Weight of battery as percentage of dwt, route: Kristiansand - Ringkøbing

Upon examining Table 4.8 it is interesting to observe that the needed battery weight for 0.99 probability never exceeds 25% of dwt. Analyzing all the speeds and the probabilities it seems plausible to assume it should be feasible to have battery-powered ships at design speed if the shipping companies are willing to sacrifice some payload. The priority for shorter journeys should shift towards optimizing cost efficiency through increased payload capacity rather than expected sailing times.

By combining the slow steam approach and shorter journeys the battery capacity could be severely decreased. An acceptable speed could be 9-10 knots with a probability threshold of 0.97, where the necessary battery weight is 12.2%-12.7% of dwt.

4.6.2 Optimal speed given an power output

As in the previous case the power consumption of the ship is determined based on its efficiency in calm water conditions at a design speed of 15 knots. This is then used as a benchmark in to identify the optimal speeds for the case ship, ensuring it does not exceed the established power output limit.

With a power output set at 2779, the necessary power output for maintaining 15 knots in calm conditions, the required battery weight is identified as 5.8% of the dwt. This specific battery capacity is selected to support sailing at 15 knots with the given power output over the designated route. To further explore the dynamics between power output and voyage factors such as speed and duration, the study investigates various power output scenarios. These scenarios, along with their associated battery weights, are detailed in Table 4.9, all the different power outputs are chosen as a factor from the power consumption for 15 knots in calm water conditions.

The probability of achieving certain sailing speeds with the specified power outputs is illustrated in Figure 4.15 where you see the probability of the ship being able to sail the route for the given speed. For example, if you look at the dark red curve for 2223 kW the highest probability at 5 knots is around 70% probability. This is not applicable, because of low reach of destination probability and long voyage time.

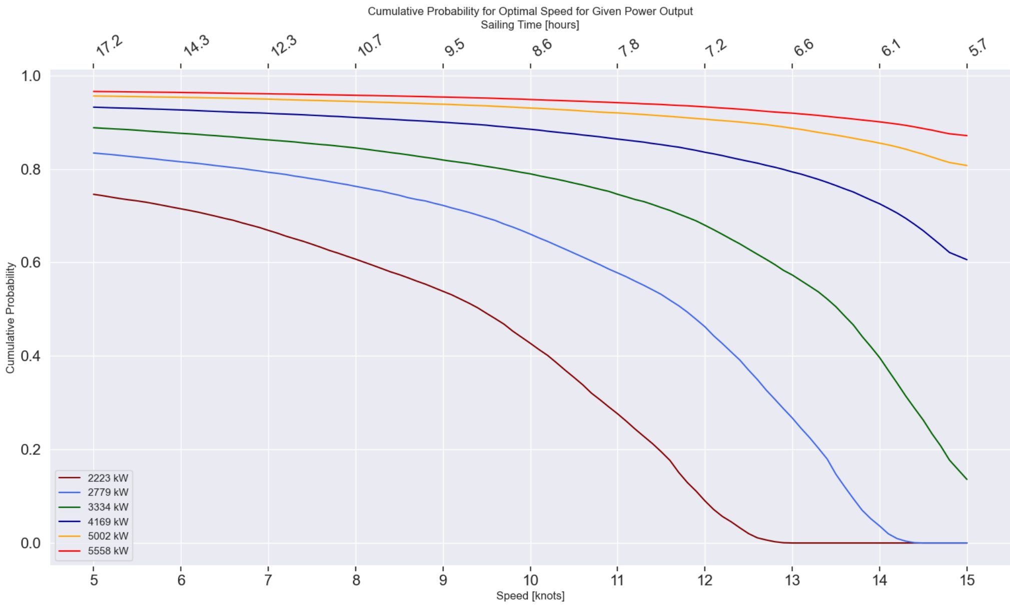

Figure 4.15: The optimal speeds with voyage time for the Norway - Netherlands voyage given the power output needed for 15 knots in calm water

Figure 4.15 shows that the first three power outputs are too low to be able to complete the route even if the ship sails at 5 knots for a big share of the journeys. For 3334 kW power output, it is observed that if the speed can be lowered to 5 knots there is a around 90% probability of sailing. But as mentioned before a sailing speed of 5 knots is too slow.

From previous results, the minimum speed should be around 9 knots. When looking at the probability of sailing at 9 knots the probability is right under 80%, therefore as in the previous case higher power outputs will be investigated further.

When looking at the power output of 4169 kW, 5002 kW, and 5558 kW in Figure 4.15 4169 kW is still not enough power if the ship is to have a high probability of reaching the destination at a more reasonable speed. The curves for 5002 kW and 5558 kW both seem to be almost inline from around 10 knots and lesser, and when looking at 9 and 10 knots it is observed that the probability is around 95%, same as for the case of the Netherlands case. The battery weight for the two highest power outputs are 10.4% and 11.6% of dwt. This seems like a very reasonable occupancy of the dwt, and this is an indication that battery shipping for this length is feasible.

By comparing the results of battery weight for 9 and 10 knots for a set power output with a set speed in any given probability in Table 4.8 the battery weights for similar speeds are slightly higher for set speed. This is a small indication that for a set speed the battery weight is over-predicted. The reason this may occur is because is the size of the increments used in the analysis. Fixed speeds are considered in increments of 1 knot, whereas for the speed probabilities are evaluated at more refined increments of 0.1 knot, seemingly leading to a more refined evaluation.

Power output [kW]	Battery weight [Tons]	% of dwt	Factor
2223	226	4.6	0.8
2779	283	5.8	1.0
3334	340	6.9	1.2
4169	425	8.7	1.5
5002	509	10.4	1.8
5558	566	11.6	2.0

Table 4.9: Battery weight for the different power outputs, factor is the factor between the needed power for 15 knots in calm water and the power output

4.6.3 Comparing the two cases

When comparing the two cases, it is clear that a sailing leg that is 1/4 of the total distance requires roughly 1/4 of the needed battery capacity. This is seen when looking at the cumulative energy consumption probability distributions Figure 4.16 and Figure 4.17 in the same coordinate system.

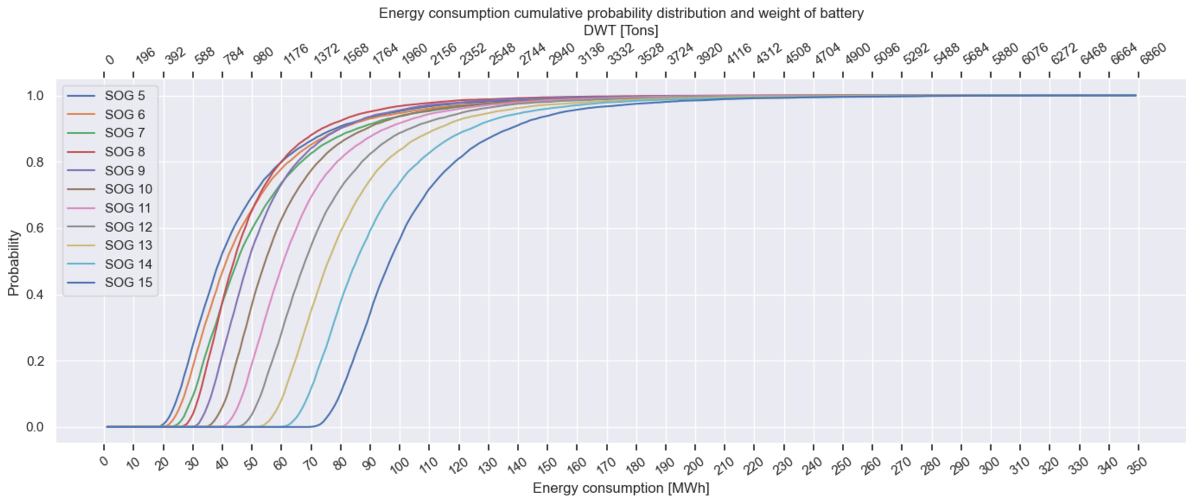

Figure 4.16: Cumulative energy consumption for Tananger - Harlingen, 4 legs

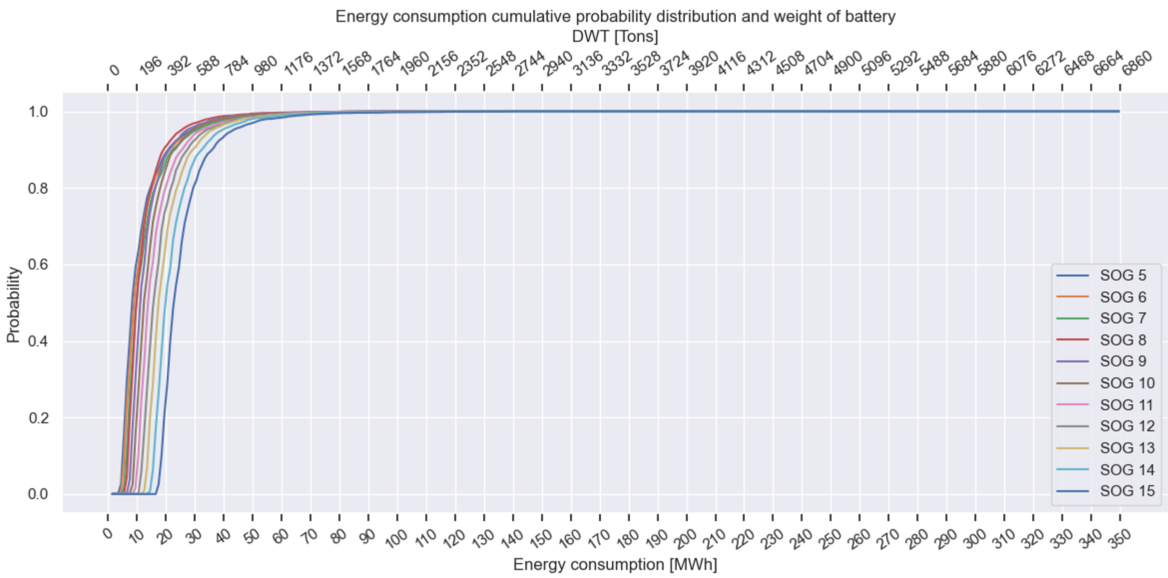

Figure 4.17: Cumulative energy consumption for Kristiansand - Ringkøbing

For the green corridor traversing between Norway and the Netherlands, it is feasible that the vessel could maintain a substantial portion of its payload capacity if the route were to be planned with shorter export stages along the coastlines. In case 2 having the longest export stage is being between Kristiansand and Ringkøbing lowers the battery capacity drastically. This strategy could mitigate the need for big payload compromises, enhancing the ship's operational efficiency and sustainability within this maritime corridor. Also, the shorter route has less difference in energy consumption between the different speeds and will be able to sail at faster speeds without compromising too much payload.

4.7 Case: Range calculation based on payload

By applying the theory from Section 3.7 and Equation 3.7 we find out that when the efficiency is equal between E-diesel and battery ships when the weight of the batteries can be 76% of the dwt.

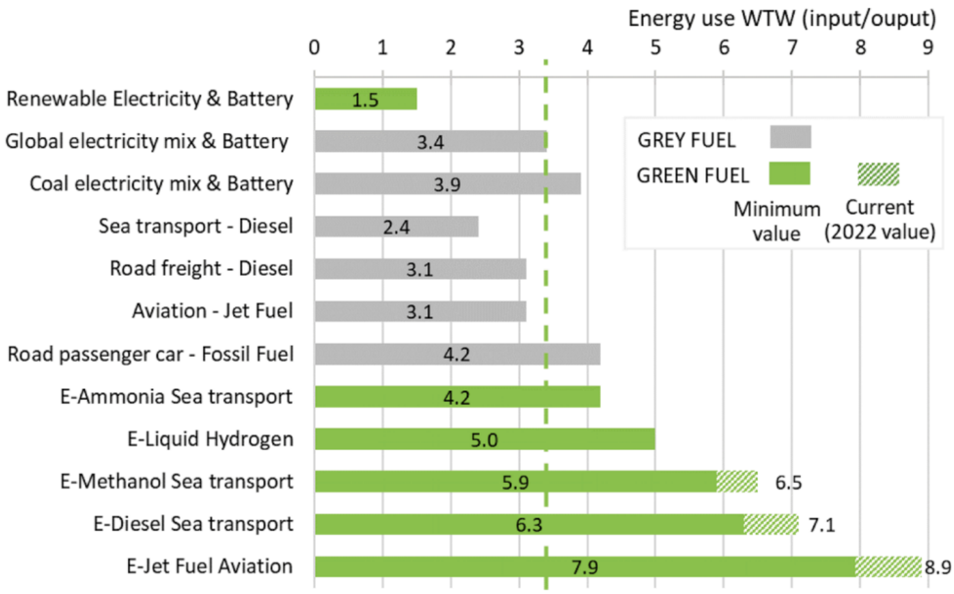

Fig. 5. WTW Energy use as a function of fuel and transport mode.

Figure 4.18: WTW Energy use as a function of fuel and transport mode from (Lindstad et al., 2023)

Using the energy use WTW factors from (Lindstad et al., 2023) and Equation 3.7 the percentage of payload available for equal efficiency for methanol and diesel is calculated compared to battery ships and presented in Table 4.10. Both Methanol and Diesel showcase that the efficiency of electricity is severe compared to other green fuels, and it should be investigated further for where batteries take up more of the payload to achieve zero emissions.

Fuel	WTW Energy use factor	Percentage of payload	Percentage of battery
E - diesel min	6.3	24 %	76 %
E - diesel current	7.1	21 %	79 %
E - Methanol min	5.9	25 %	75 %
E - Methanol current	6.5	23 %	77 %

Table 4.10: WTW Energy use as a function of fuel and transport mode from (Lindstad et al., 2023)

To explore the range, an interactive matrix has been created. This matrix displays the various ranges for the case ship, with ship speed and battery weight, expressed as a percentage of dwt, serving as variable inputs.

Upon examining the range matrix across various speeds, with the battery occupying 76% of the dwt it becomes apparent that more harsh weather conditions gives considerably limited operational ranges, regardless of the vessel's speed. This suggests that certain weather scenarios inherently result in reduced navigational distances due to their significant impact, despite the utilization of substantial battery capacities.

Notably, the instances that correspond to these ranges are characterized by a low probability of occurrence. Therefore, this facilitates the assurance of a high battery capacity being sufficient for the majority of operational conditions.

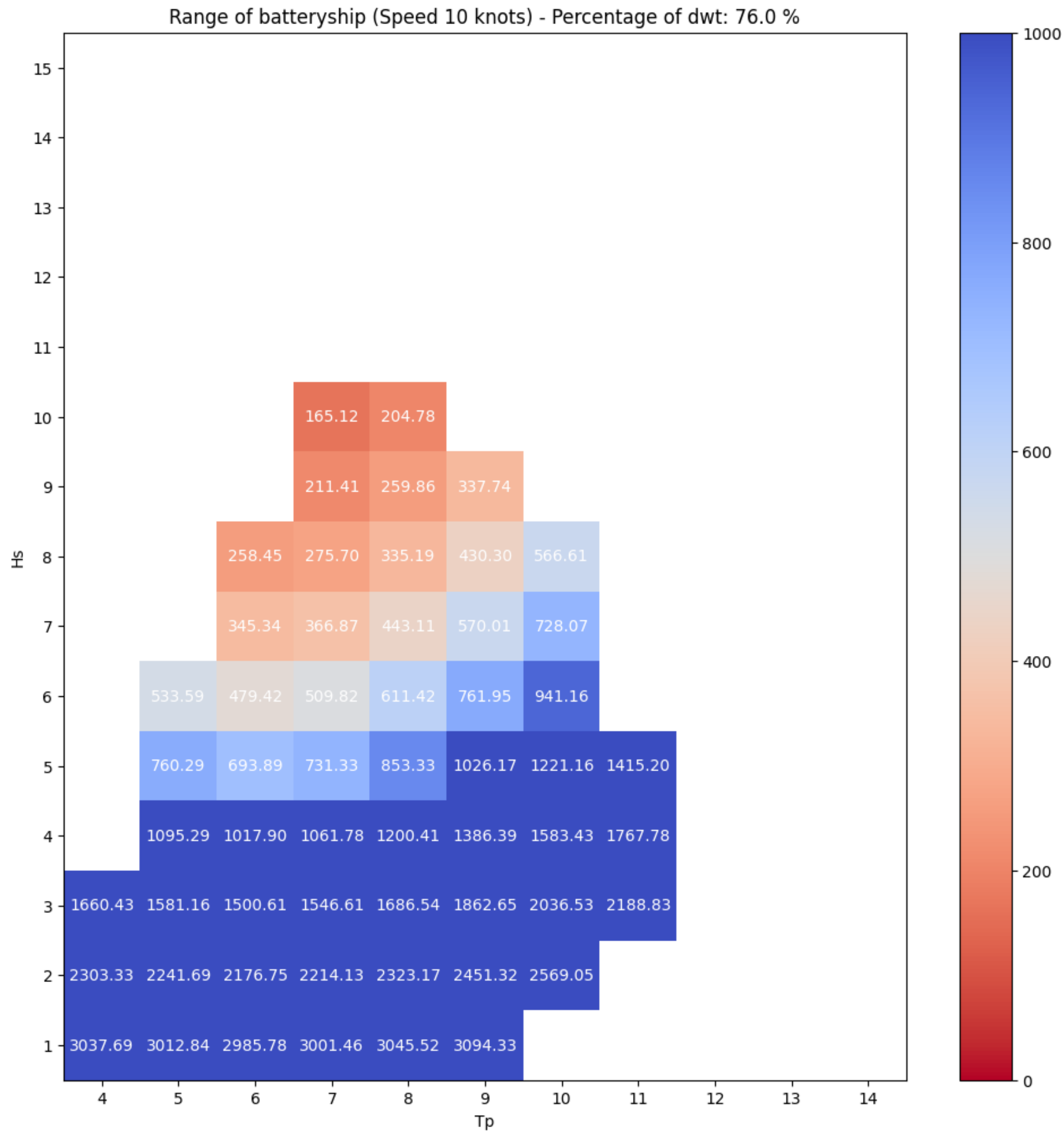

Figure 4.19: Range for a battery ship where battery is 76 % of dwt and speed is 10 knots, head seas

Allocating 76% of the dwt for batteries is an unlikely scenario for a cargo vessel, even if WTW energy assessments suggest it is energy efficient. Hence, later discussions will explore scenarios with a reduced percentage of dwt dedicated to batteries. Specifically, Figure 4.20 presents range calculations for 50% of dwt allocated to batteries, and Figure 4.21 examines the implications of limiting battery occupancy to 25% of dwt. These analyses aim to provide a more realistic perspective on the operational feasibility of battery-powered cargo ships under varying payload constraints.

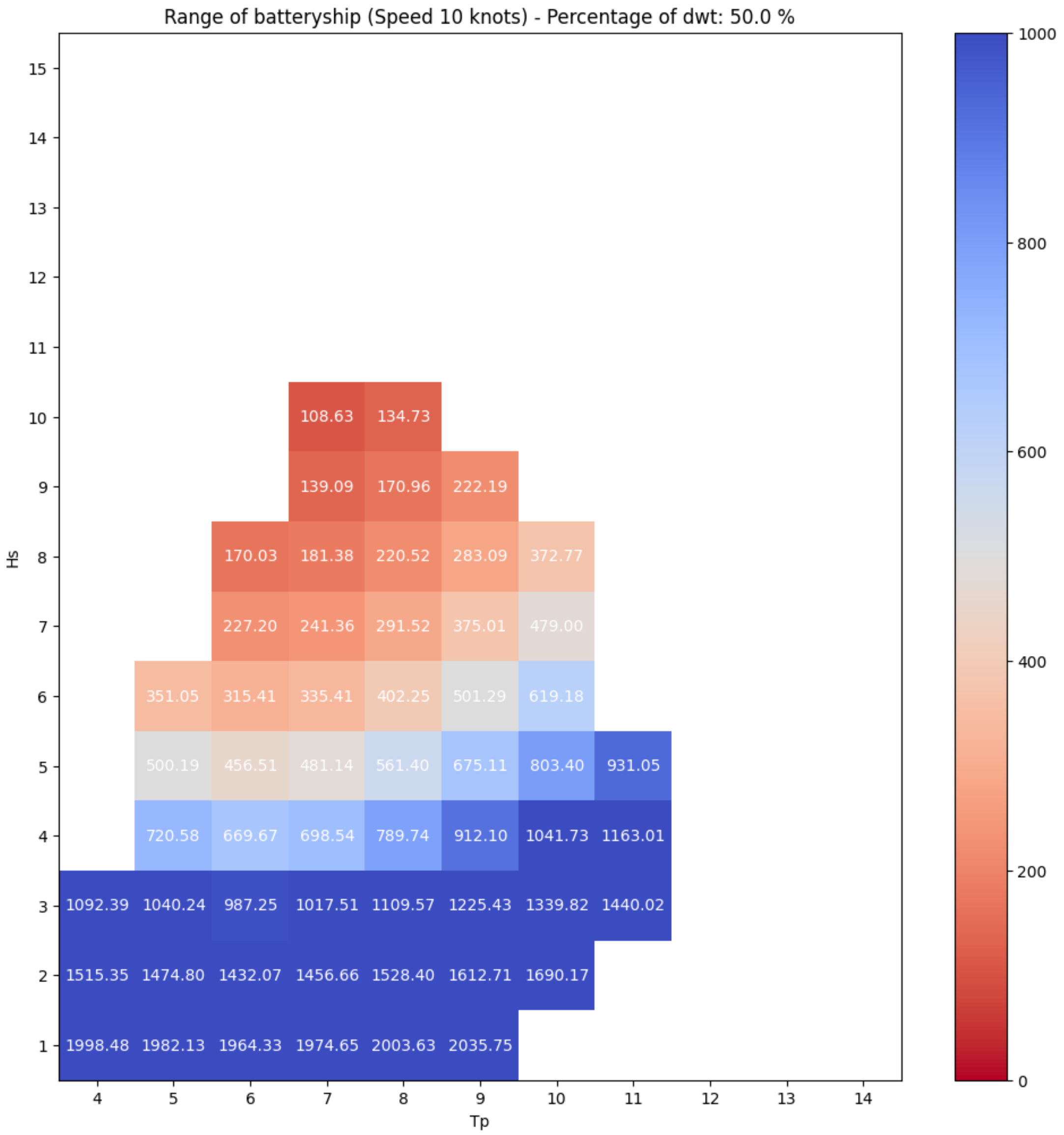

Figure 4.20: Range for a battery ship where battery is 50% of dwt and speed is 10 knots, head seas

In Figure 4.20, a natural decrease in range is observed compared to an allocation of 76% due to the reduced battery capacity. However, it is particularly noteworthy that scenarios with low Hs exhibit long ranges. Further examination of the data in Appendix D, which encompasses a variety of speeds beyond the 10 knots showcased in Figure 4.20, reveals a consistent pattern: High Hs values consistently result in limited ranges, regardless of speed. This trend is in correlation between wind speed and Hs, as high wave conditions are calculated from Hs, leading to increased weather resistance in scenarios with elevated Hs values.

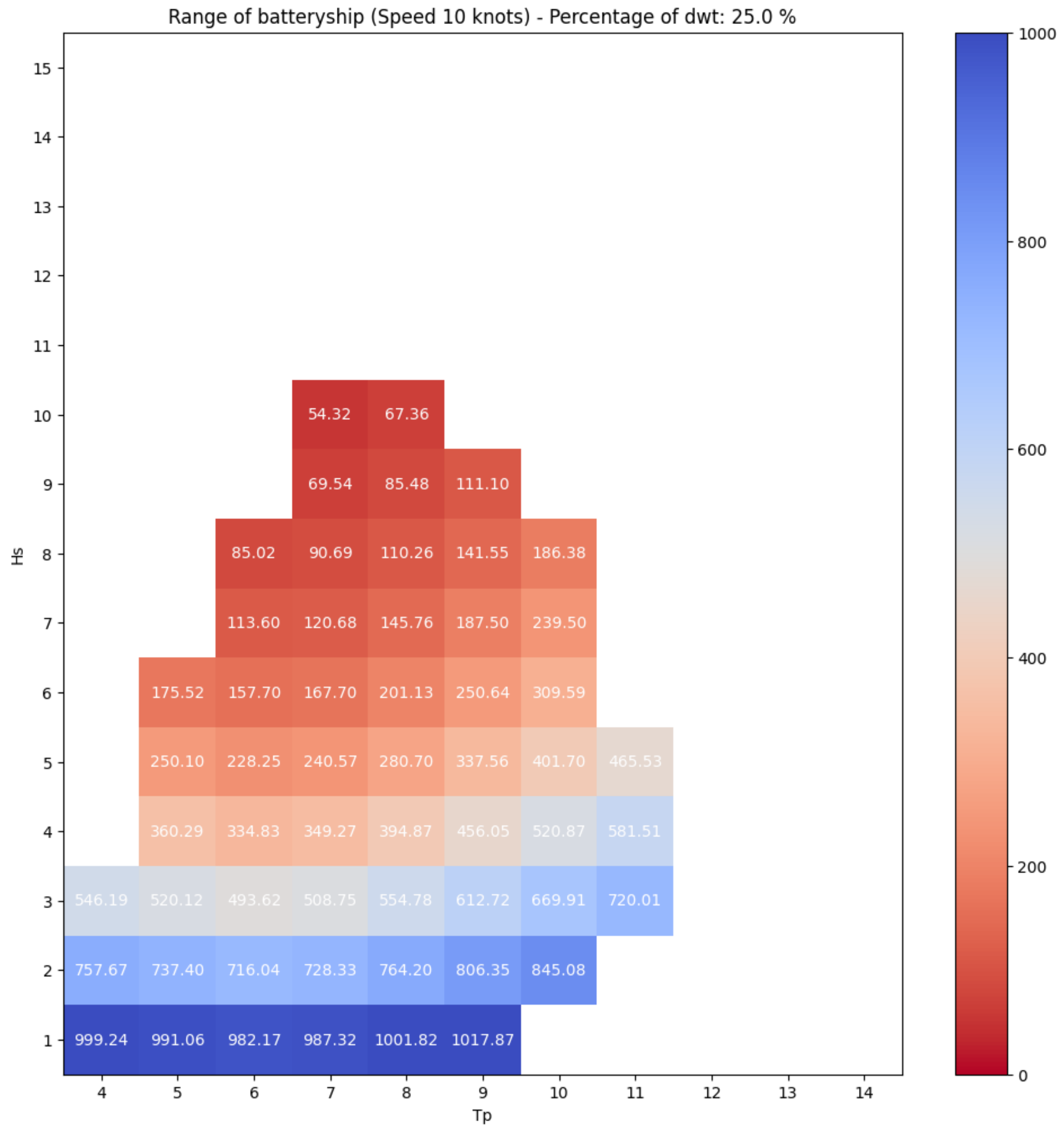

Figure 4.21: Range for a battery ship where battery is 25% of dwt and speed is 10 knots, head seas

In Figure 4.21, a trend of decreasing range is observed at a cruising speed of 10 knots, with batteries occupying 25% of the dwt. Given this allocation of dwt to battery capacity, a strategic shift towards shorter voyage distances becomes imperative. An analysis of the range matrices for a battery allocation of 25% of dwt is found in Appendix C, this reveals a consistent occurrence of weather conditions under which the navigational range falls below 200 km. This pattern suggests that a battery configuration occupying 25% of the dwt is likely to be optimally suited for routes not exceeding 200 km. This aligns well with the observations from the case between Norway - and Denmark where the needed battery capacity never exceeds 25% where the route is 159km.

The interactive matrix can be explored by yourself if the reader wishes to look more into different combinations of speeds and percentages of dwt to estimate the range for different weather conditions for this case ship. By either scanning the QR code in Figure 4.22 or by simply clicking the figure below you will be taken to the interactive matrix.

Figure 4.22: Scan QR code or click on it to go to the interactive matrix

4.8 Summarizing comments

The estimation of battery weight and capacity range has been conducted through multiple of methodological methods.

In the process of estimating the needed battery capacity for a given route under simulated weather conditions, it has been observed that lower speeds, specifically within the range of 5-9 knots, necessitate similar levels of battery capacity. When determining the optimal operational speed for a battery-powered vessel, it is advisable to consider speeds of at least 9 knots. This suggestion is based on the idea that weather conditions mainly affect how much energy is needed. Because of this, the small extra amount of battery needed to go faster from 5 to 9 knots is worth it for the advantage of moving quicker.

In the analysis of required battery capacity for elevated speeds, it becomes evident that shorter voyage distances correlate with reduced battery package weights. Delving into the WTW energy efficiency metrics, it is revealed that battery-powered vessels can achieve parity with e-diesel in terms of energy consumption by allocating merely 24% of the dwt to battery storage. While such a significant dedication of dwt to batteries may not be practically feasible, this finding underscores the imperative for strategic compromises in payload capacity to facilitate the transition towards sustainable maritime operations.

An analysis was undertaken to ascertain the probability of achieving certain speeds and, consequently, the likelihood of specific sailing times, given a predetermined power output and battery capacity. This investigation yielded results that were broadly consistent with those derived from battery capacity estimations for fixed speeds, albeit with a marginally reduced requirement for battery capacity. Given the comparative applicability of establishing a set power output and the similarity in findings, it is rational to consider 9 knots as the minimum operational speed. The selection of higher speeds hinges on the acceptable trade-offs between the vessel's ability to navigate various weather conditions and the proportion of payload capacity that can be allocated to battery storage.

Chapter 5

Conclusion

The objective of this thesis is to investigate if it is feasible to apply battery-powered ships in green corridors. The thesis examines required battery capacities for various speeds, determines the achievable speeds given specific power outputs and battery capacities, and assesses the operational range under different weather conditions and battery weights. This chapter presents the conclusions drawn from this study.

For the Norway-Netherlands route, the analysis reveals that the ship would require heavy batteries. Opting for smaller battery capacities might compromise the ship's ability to complete the journey or maintain operational speed, thereby affecting the reliability of cargo delivery.

In comparing the energy efficiency of battery-powered ships with other low-emission fuels, battery-powered vessels emerge as a viable option for routes where sacrificing a portion of the payload for zero emissions is feasible. The analysis suggests that up to 76% of the ship's deadweight capacity could be allocated to batteries, rather than cargo before its transport efficiency falls below that of using e-diesel. This highlights the significant energy losses associated with the production and use of combustion engines of e-diesel, and thereby the strong motivation for using batteries.

For the route Norway-Denmark, only 1/4 of the capacity is required compared to the Norway-Netherlands route. For this case it emerges that there is more flexibility when reducing the battery capacity without sacrificing too much of either speed or sailing probability. As previously mentioned, when comparing the energy efficiency of e-diesel and electricity, it's understood that some payload capacity can be sacrificed to achieve zero emissions.

With regard to the results regarding different ranges available for different battery capacities and energy efficiency of electricity compared to e-diesel it is concluded that battery-powered ships in green corridors is feasible and should be investigated further. From this study with today's battery technology it seems unlikely that the ship will be able to sail the route between Norway - Netherlands with battery powered ships, but a solution where a ship follows the coastlines and has shorter stretches between ports/charging stations should be feasible.

Looking ahead, the future of battery-powered ships appears promising, especially with ongoing advancements in technology and a growing emphasis on environmental sustainability. However, realizing the full potential of battery-powered ships will require combined efforts in policy development and industry collaboration. It is important that stakeholders in the maritime sector work together to promote the adoption of green shipping corridors and sustainable maritime practices, ensuring a greener future for global shipping.

Chapter 6

Further work

This study is still in the early phase, and further work is needed to achieve more insight and knowledge about the feasibility of applying battery-powered ships for longer sailing distances. This section will provide suggestions for areas that should be further looked into.

In this thesis, the analysis was limited to the weight aspects of the battery packages in the form of available dwt on the case ship. Subsequent studies should examine how battery arrangement, and the space the battery packages will occupy. The placement of the batteries and their space allocation should be further investigated to get a more thorough understanding of how the battery packages will affect the payload capacity on the ship.

An additional study looking into charging of bigger battery packages should be made. Charging big battery packages is a considerable part of why the implementation of battery-powered ships over longer distances is not a given solution. Charging huge battery packages takes a lot of time. It mentioned possible solutions for charging in the theory part, about charging vessels, charging stations at sea, and battery swapping that can make batteries more feasible in the future.

This thesis does not incorporate considerations for safety margins upon port arrival, focusing solely on the energy requirements for transit from one port to another. While the thesis allows for some flexibility in battery capacity, because of a depth of discharge of 0.5 to ensure additional maintenance of the battery. However relying on being able to discharge the battery too much may influence the battery maintenance and overall life cycle, potentially impacting long-term operational efficiency, sustainability and costs.

Future research should include cost analyses comparing batteries with other fuels and a Life Cycle Analysis (LCA) of batteries. This thesis does not cover the cost dimension, and this should be investigated more to be able to find the most profitable solution. Additionally, there should be an LCA study on battery production, looking into the full life cycle of needed energy to produce the batteries.

Bibliography

Corvus-Energy. (2022). Corvus blue whale ess completes sea trials on board seaspan reliant. https://corvusenergy.com/corvus-blue-whale-ess-completes-sea-trials-on-board-seaspan-reliant/

DNV. (2010). *Environmental conditions and environmental loads*. Retrieved 26th January 2024, from https://home.hvl.no/ansatte/tct/FTP/H2023%20Marinteknisk%20Analyse/Regelverk%20og%20standarde/DnV_documents/RP-C205.pdf

DNV. (2020). *Study on electrical energy storage for ships*. Retrieved 26th January 2024, from https://www.emsa.europa.eu/tags/download/6186/4507/23.html

DNV. (2022). *Battery and hybrid ships*. Retrieved 8th May 2023, from https://www.dnv.com/services/battery-and-hybrid-ships-225240

DNV. (2023). *Future fuels*. Retrieved 8th May 2023, from https://www.dnv.com/maritime/hub/decarbonize-shipping/fuels/future-fuels.html

EU, E. U. c. (2021). *Reducing emissions from the shipping sector*. Retrieved 8th May 2023, from https://climate.ec.europa.eu/eu-action/transport-emissions/reducing-emissions-shipping-sector_en

Farguson, L. (2022). *Ports of halifax and hamburg working to decarbonise shipping corridor*. Retrieved 8th May 2023, from https://www.portofhalifax.ca/ports-of-halifax-and-hamburg-working-to-decarbonise-shipping-corridor/

GMF. (2021). *A strategy for the transition to zero-emission shipping*. Retrieved 26th January 2024, from https://www.globalmaritimeforum.org/content/2021/10/A-Strategy-for-the-Transition-to-Zero-Emission-Shipping.pdf

GMF. (2022a). *Annual progress report on green shipping corridors*. Retrieved 8th May 2023, from https://www.globalmaritimeforum.org/content/2022/11/The-2022-Annual-Progress-Report-on-Green-Shipping-Corridors.pdf

GMF. (2022b). *The west australia-east asia iron ore green corridor is within reach*. Retrieved 8th May 2023, from https://www.globalmaritimeforum.org/press/the-west-australia-east-asia-iron-ore-green-corridor-is-within-reach

GMF. (2023). *The shipping industry's fuel choices on the path to net zero*. Retrieved 26th January 2024, from https://www.globalmaritimeforum.org/content/2023/04/the-shipping-industrys-fuel-choices-on-the-path-to-net-zero_final.pdf

gov.uk. (2022). *Cop 26: Clydebank declaration for green shipping corridors*. Retrieved 8th May 2023, from https://www.gov.uk/government/publications/cop-26-clydebank-declaration-for-green-shipping-corridors/cop-26-clydebank-declaration-for-green-shipping-corridors

Hogben, N. (1986). *Global wave statistics*. Published for British Maritime Technology by Unwin Brothers Limited.

Hollenbach, K. U. (1998). Estimating resistance and propulsion for single-screw and twin-screw ships-ship technology research 45. *Schiffstechnik*, *45*, 72.

IBM. (2023). *What is monte carlo simulation?* Retrieved 26th January 2024, from https://www.ibm.com/topics/monte-carlo-simulation

IMO. (2023). *Imo's work to cut ghg emissions from ships*. Retrieved 12th December 2023, from https://www.imo.org/en/MediaCentre/HotTopics/Pages/Cutting-GHG-emissions.aspx

ITTC. (2014). *Ittc – recommended procedures and guidelines*. Retrieved 19th November 2023, from https://ittc.info/media/4210/75-04-01-012.pdf

Joerss, M. (2021). *Green corridors: A lane for zero-carbon shipping.* Retrieved 8th May 2023, from https://www.mckinsey.com/capabilities/sustainability/our-insights/green-corridors-a-lane-for-zero-carbon-shipping

Johansson, J. e. a., L. (2017). *Global assessment of shipping emissions in 2015 on a high spatial and temporal resolution.* Atmospheric Environment.

Kim, Y.-R., Steen, S., Kramel, D., Muri, H., & Strømman, A. H. (2023). Modeling of ship resistance and power consumption for the global fleet: The mariteam model. *Department of Marine Technology, Norwegian University of Science and Technology (NTNU)*, 32.

Kristensen, H. O. (2017). Prediction of resistance and propulsion power of ships. *Work Package 2, 4*.

Lindstad, E., Ask, T. Ø., Carrou, P., Eskeland, G. S., & Rialland, A. (2023). Wise use of renewable energy in transport. *Transportation Research Part D*, 1–12.

Mo, O. (2019). *What's the point of installing batteries on marine vessels if the batteries are charged by electricity from their diesel generators?* Retrieved 26th January 2024, from https://blog.sintef.com/sintefenergy/why-install-batteries-on-ships/

Nationalgrid. (2022). *Decarbonization of shipping – emerging alternative fuels from a us perspective.* Retrieved 8th May 2023, from https://www.nationalgrid.com/stories/energy-explained/what-is-liquefied-natural-gas-lng

Siamak Karimi, M. Z., & Suul, J. A. (2020). Shore charging for plug-in battery powered ships. *IEEE*, 50–57.

Stewart, R. H. (2008). *Introduction to physical oceanography.* Retrieved 25th September 2023, from https://www.colorado.edu/oclab/sites/default/files/attached-files/stewart_textbook.pdf

Twi. (2023). *What is simulation? what does it mean?* Retrieved 26th January 2024, from https://www.twi-global.com/technical-knowledge/faqs/faq-what-is-simulation

Vard. (2013). *Leading the way in the green maritime transition.* Retrieved 26th January 2024, from https://www.vard.com/articles/the-ocean-charger-project-has-officially-started

Appendix A

Energy consumption: Norway - Netherlands

Energy consumption visualized in histograms, each bar representing a 1000 kWh.

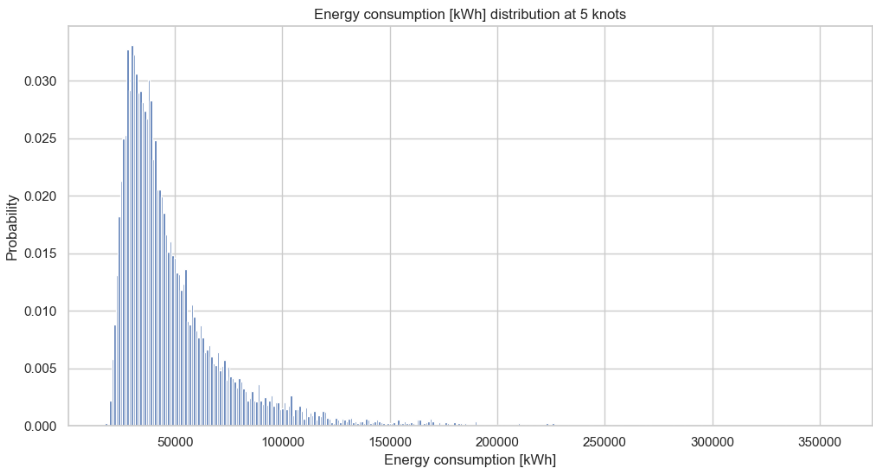

Figure A.1: Energy consumption for ship sailing Tananger - Harlingen with speed 5 knots

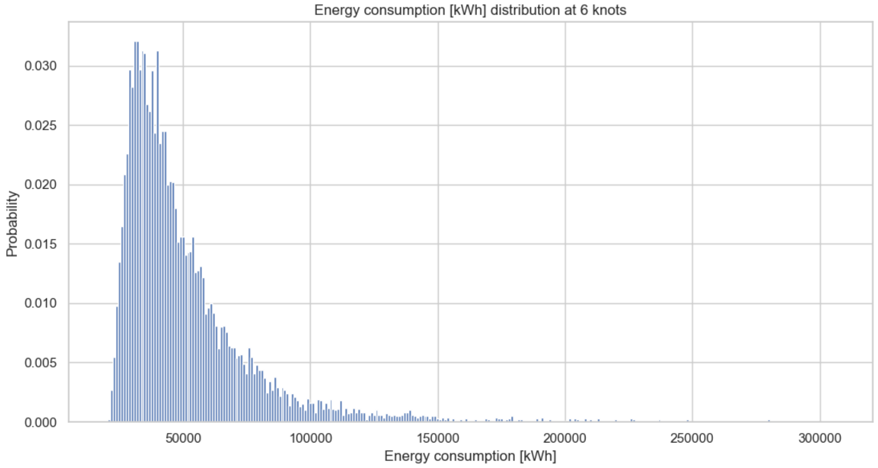

Figure A.2: Energy consumption for ship sailing Tananger - Harlingen with speed 6 knots

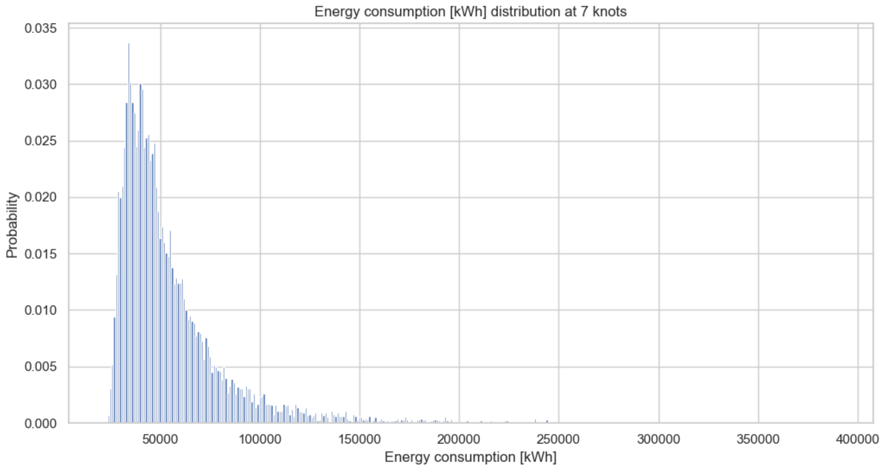

Figure A.3: Energy consumption for ship sailing Tananger - Harlingen with speed 7 knots

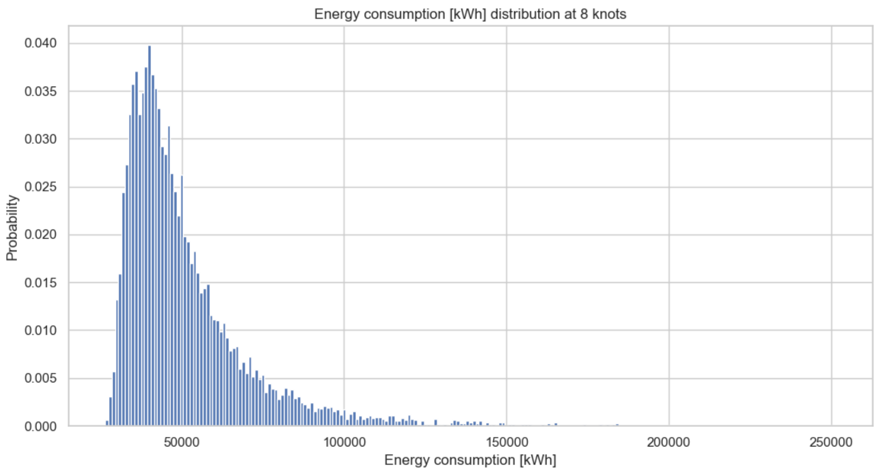

Figure A.4: Energy consumption for ship sailing Tananger - Harlingen with speed 8 knots

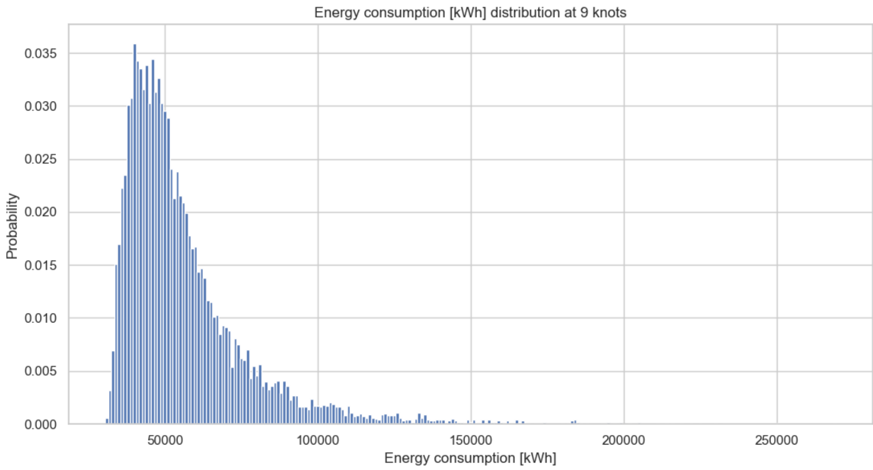

Figure A.5: Energy consumption for ship sailing Tananger - Harlingen with speed 9 knots

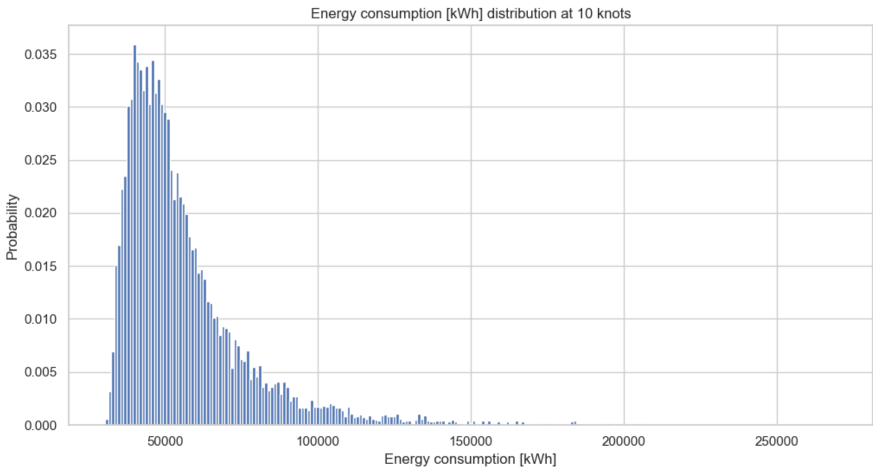

Figure A.6: Energy consumption for ship sailing Tananger - Harlingen with speed 10 knots

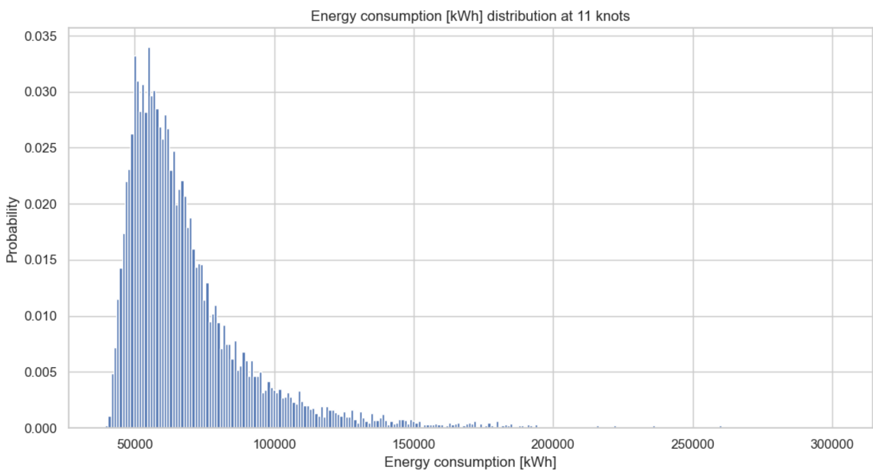

Figure A.7: Energy consumption for ship sailing Tananger - Harlingen with speed 11 knots

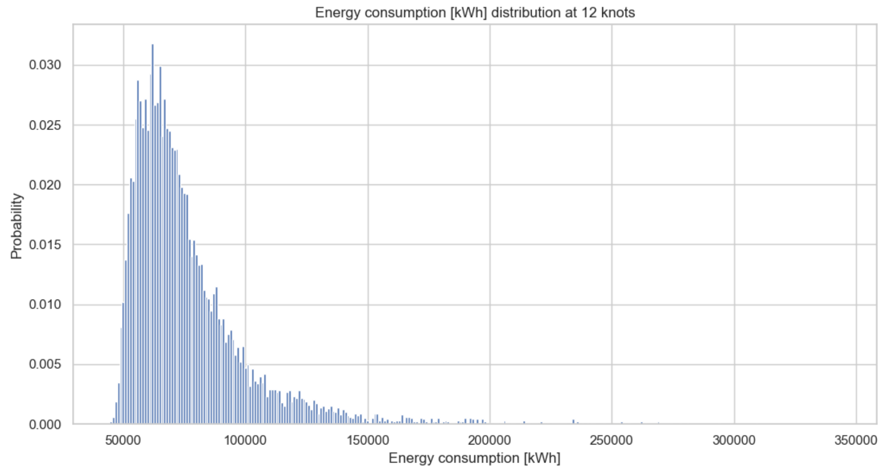

Figure A.8: Energy consumption for ship sailing Tananger - Harlingen with speed 12 knots

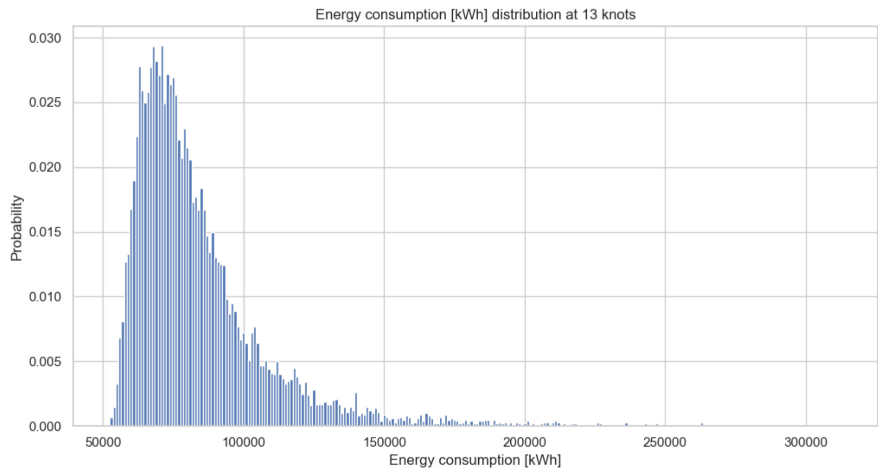

Figure A.9: Energy consumption for ship sailing Tananger - Harlingen with speed 13 knots

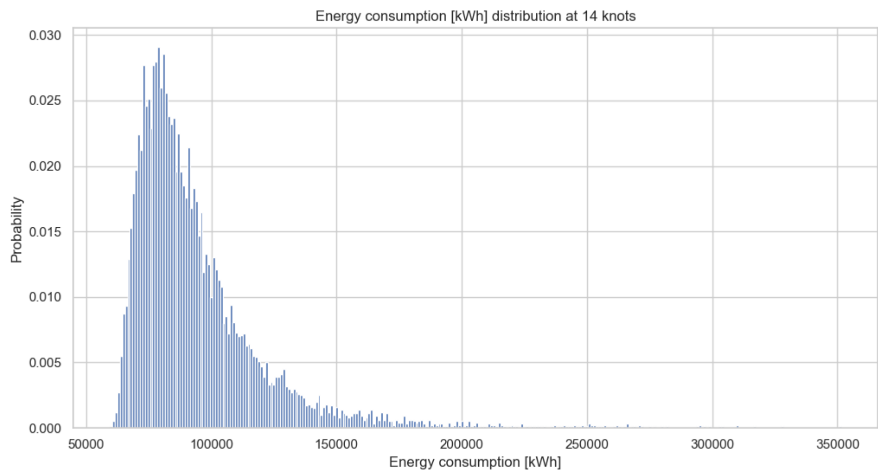

Figure A.10: Energy consumption for ship sailing Tananger - Harlingen with speed 14 knots

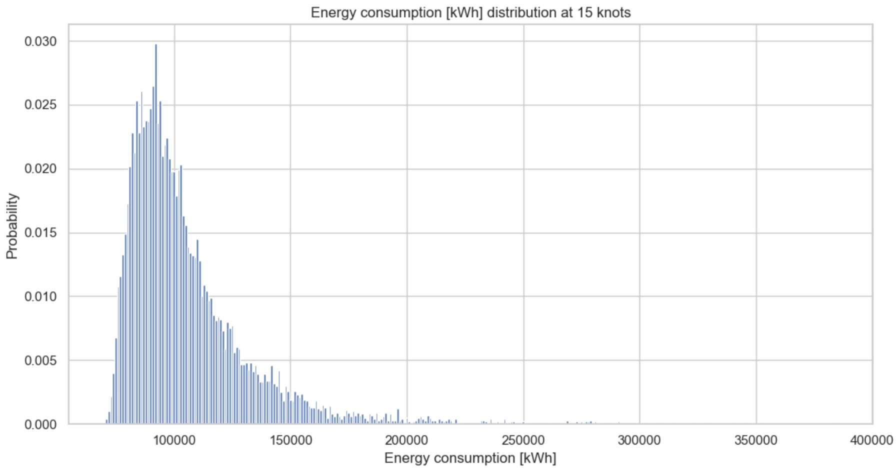

Figure A.11: Energy consumption for ship sailing Tananger - Harlingen with speed 15 knots

Appendix B

Energy consumption: Norway - Denmark

Energy consumption visualized in histograms, each bar representing a 1000 kWh.

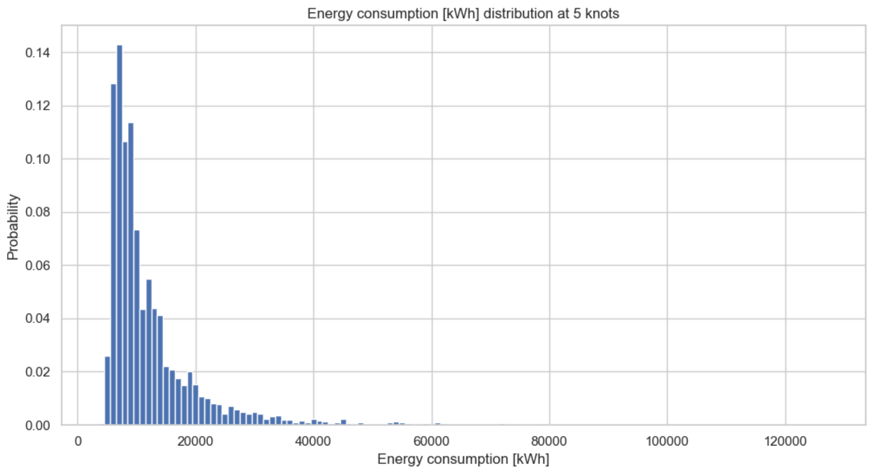

Figure B.1: Energy consumption for ship sailing Kristiansand - Ringkøbing n with speed 5 knots

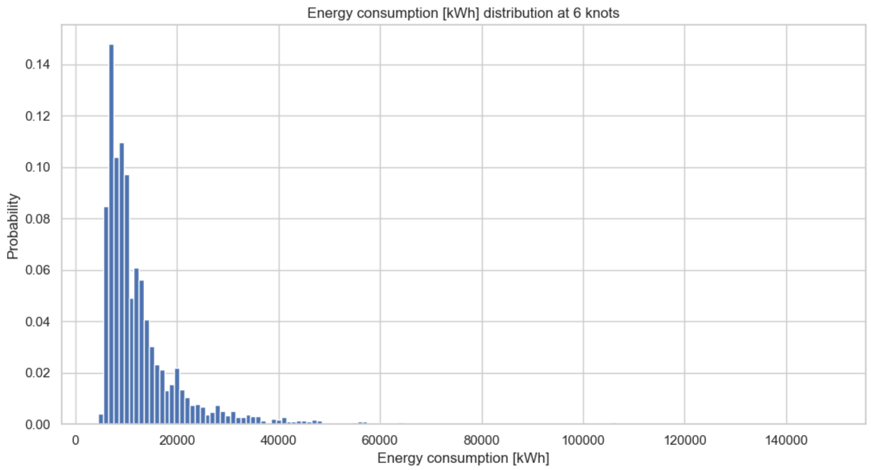

Figure B.2: Energy consumption for ship sailing Kristiansand - Ringkøbing with speed 6 knots

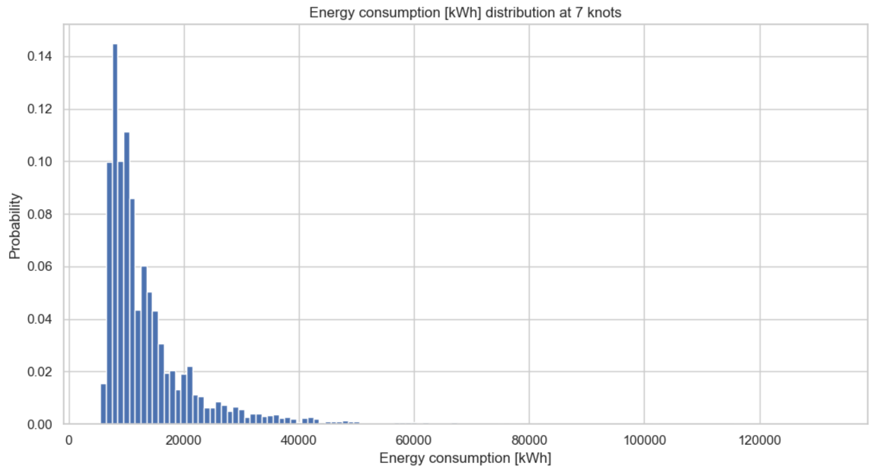

Figure B.3: Energy consumption for ship sailing Kristiansand - Ringkøbing with speed 7 knots

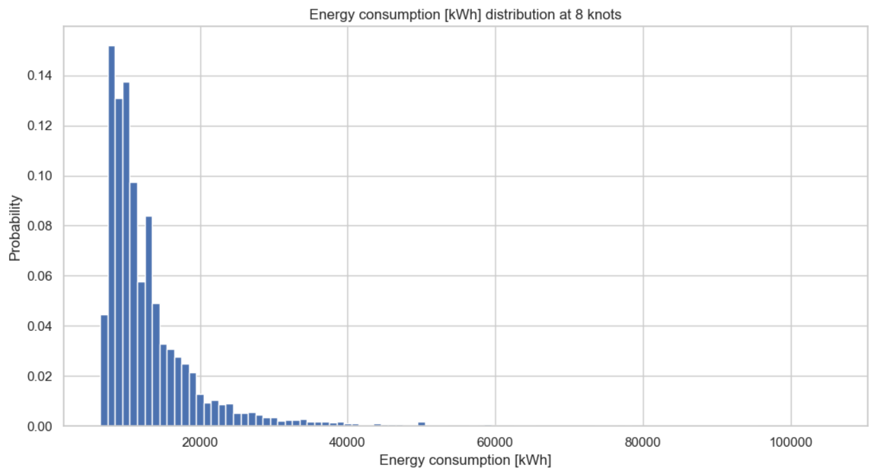

Figure B.4: Energy consumption for ship sailing Kristiansand - Ringkøbing with speed 8 knots

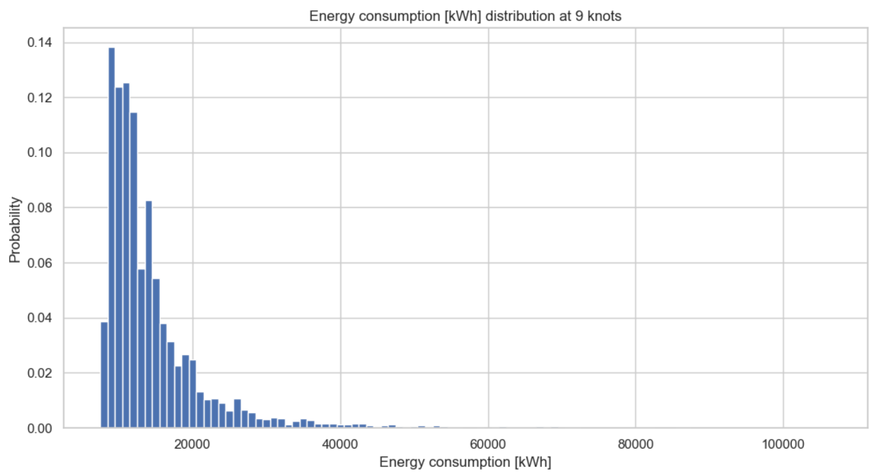

Figure B.5: Energy consumption for ship sailing Kristiansand - Ringkøbing with speed 9 knots

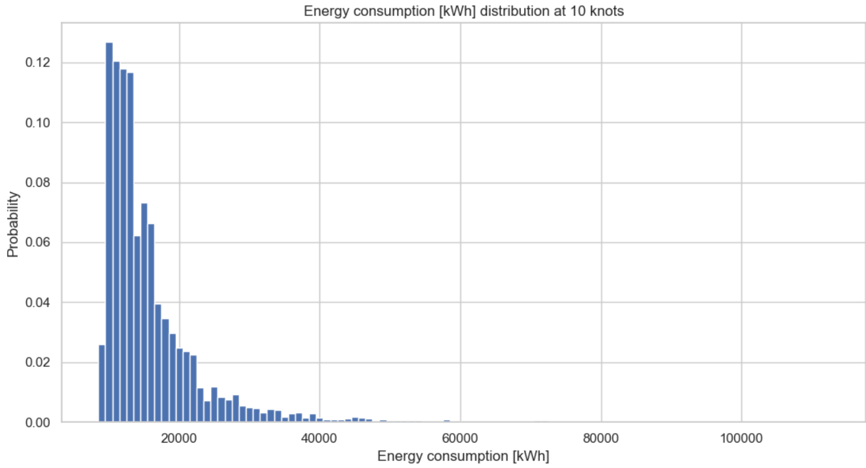

Figure B.6: Energy consumption for ship sailing Kristiansand - Ringkøbing with speed 10 knots

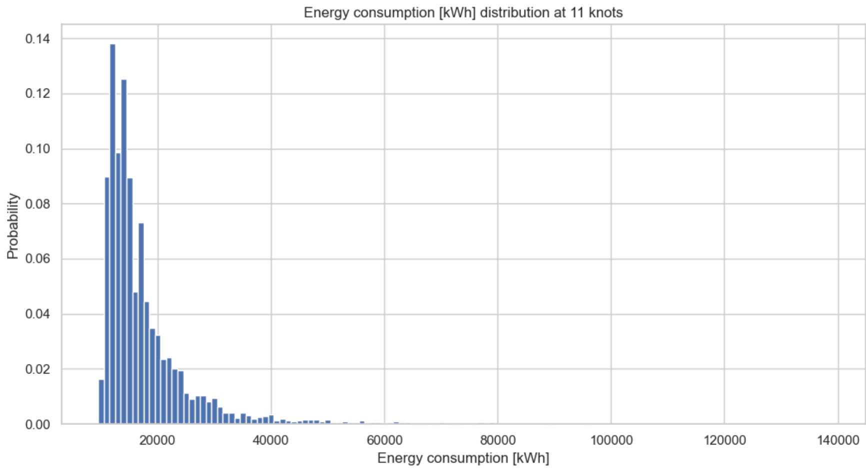

Figure B.7: Energy consumption for ship sailing Kristiansand - Ringkøbing with speed 11 knots

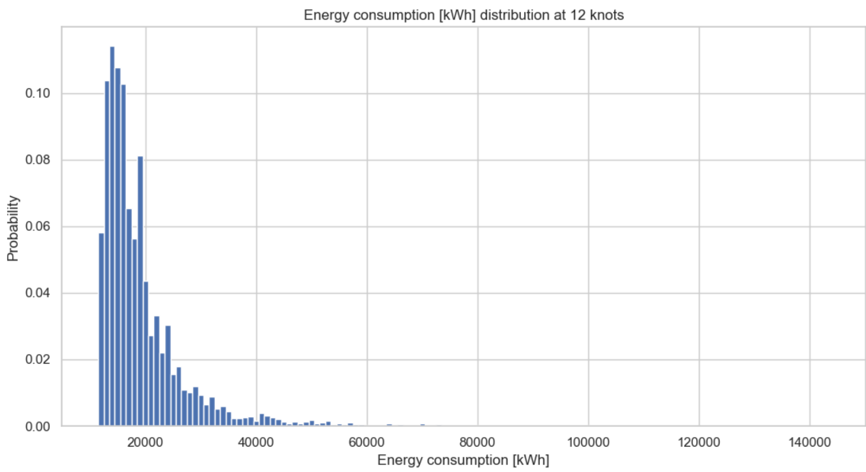

Figure B.8: Energy consumption for ship sailing Kristiansand - Ringkøbing with speed 12 knots

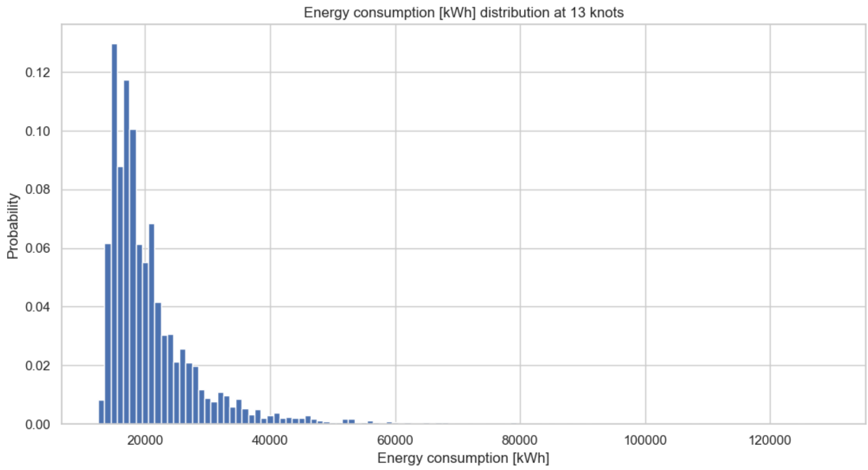

Figure B.9: Energy consumption for ship sailing Kristiansand - Ringkøbing with speed 13 knots

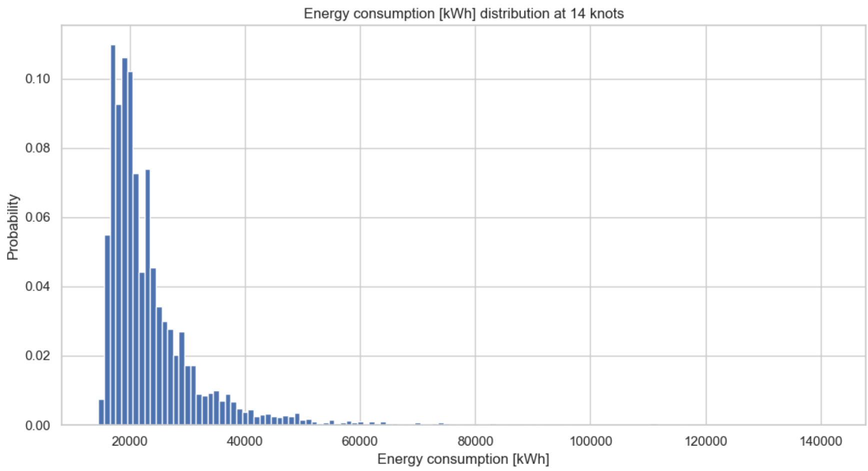

Figure B.10: Energy consumption for ship sailing Kristiansand - Ringkøbing with speed 14 knots

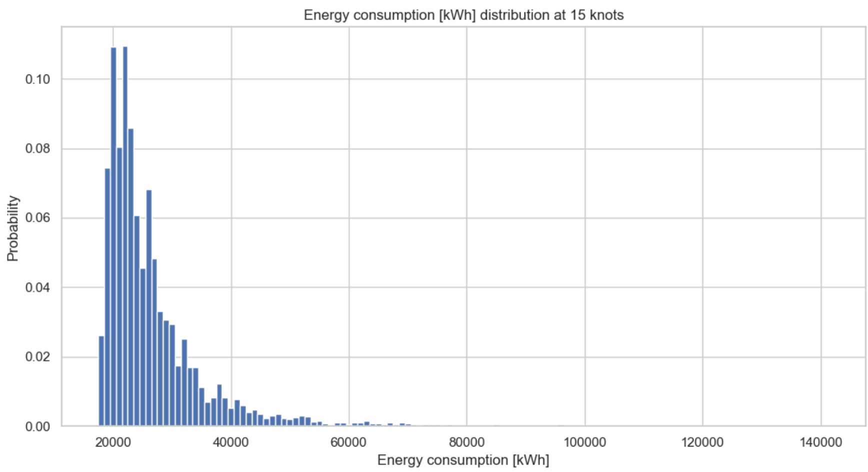

Figure B.11: Energy consumption for ship sailing Kristiansand - Ringkøbing with speed 15 knots

Appendix C

Range calculations where batteries is 25% of dwt

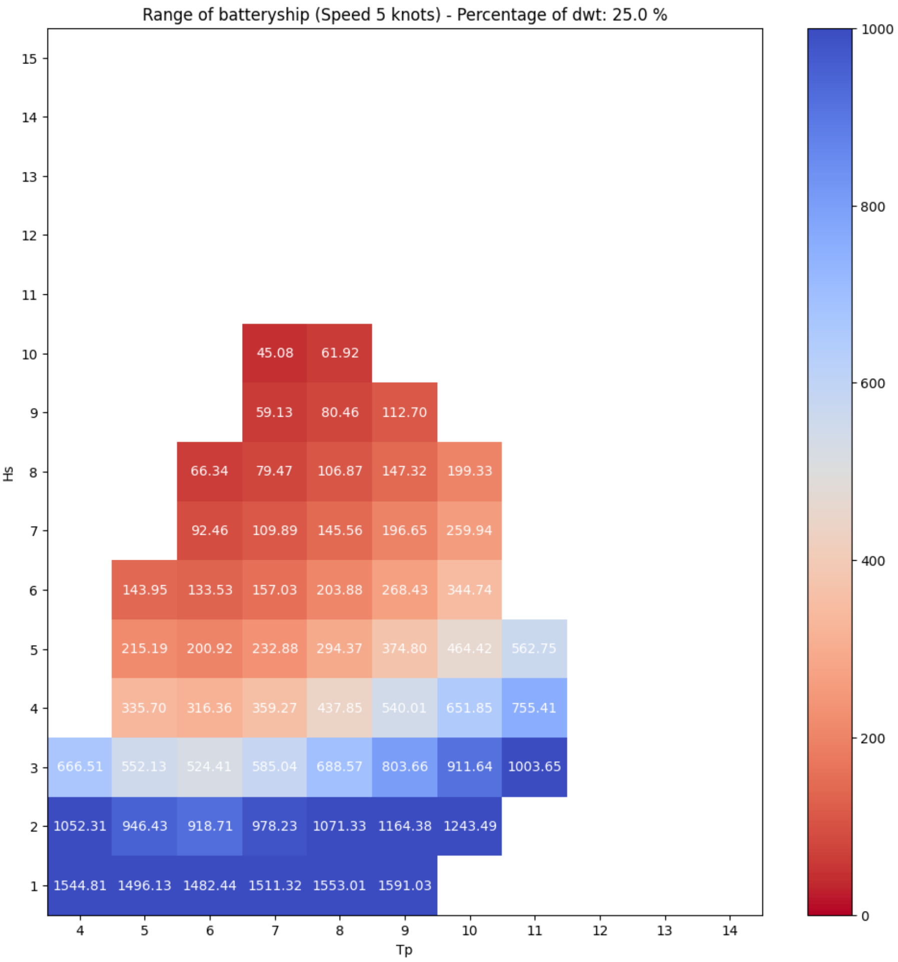

Figure C.1: Range for a battery ship where battery is 25 % of dwt and speed is 5 knots

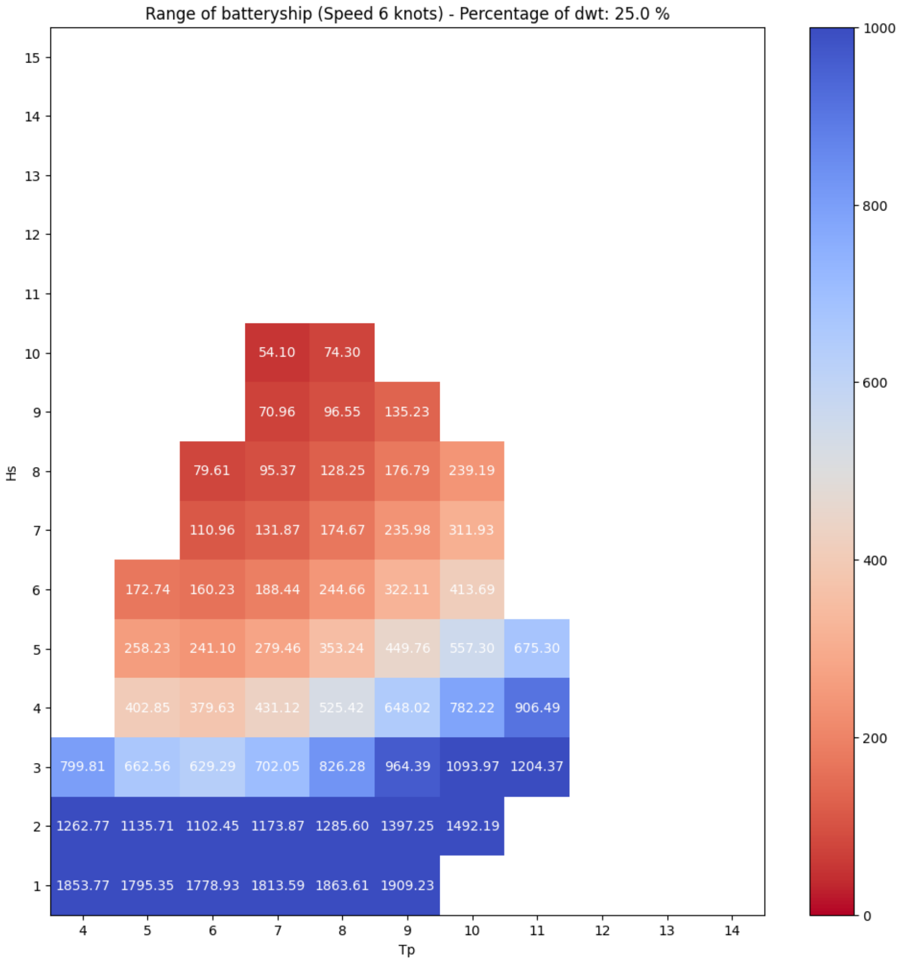

Figure C.2: Range for a battery ship where battery is 25 % of dwt and speed is 6 knots

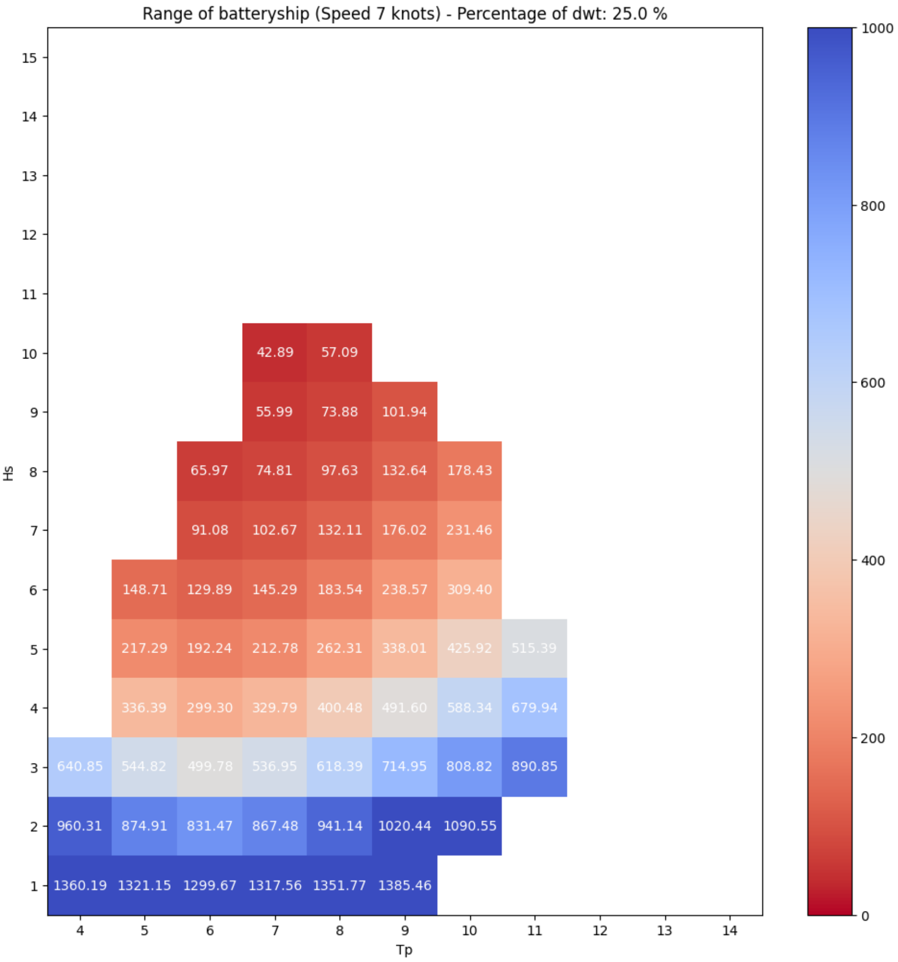

Figure C.3: Range for a battery ship where battery is 25 % of dwt and speed is 7 knots

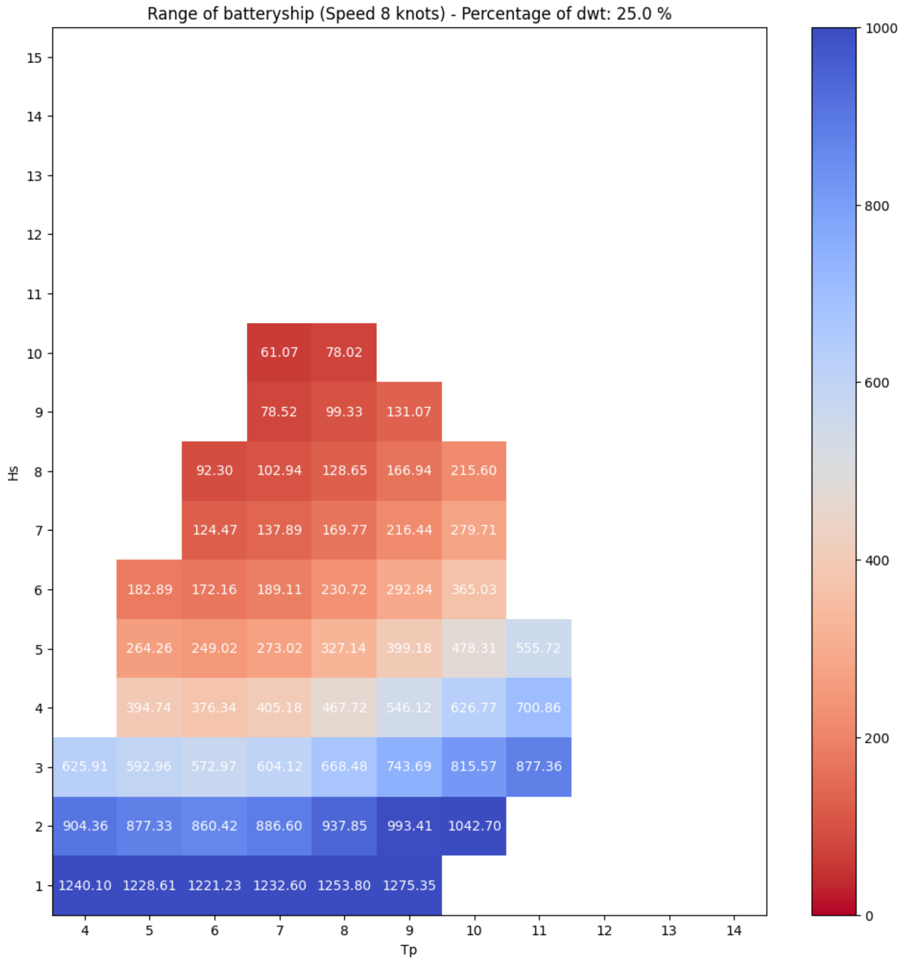

Figure C.4: Range for a battery ship where battery is 25 % of dwt and speed is 8 knots

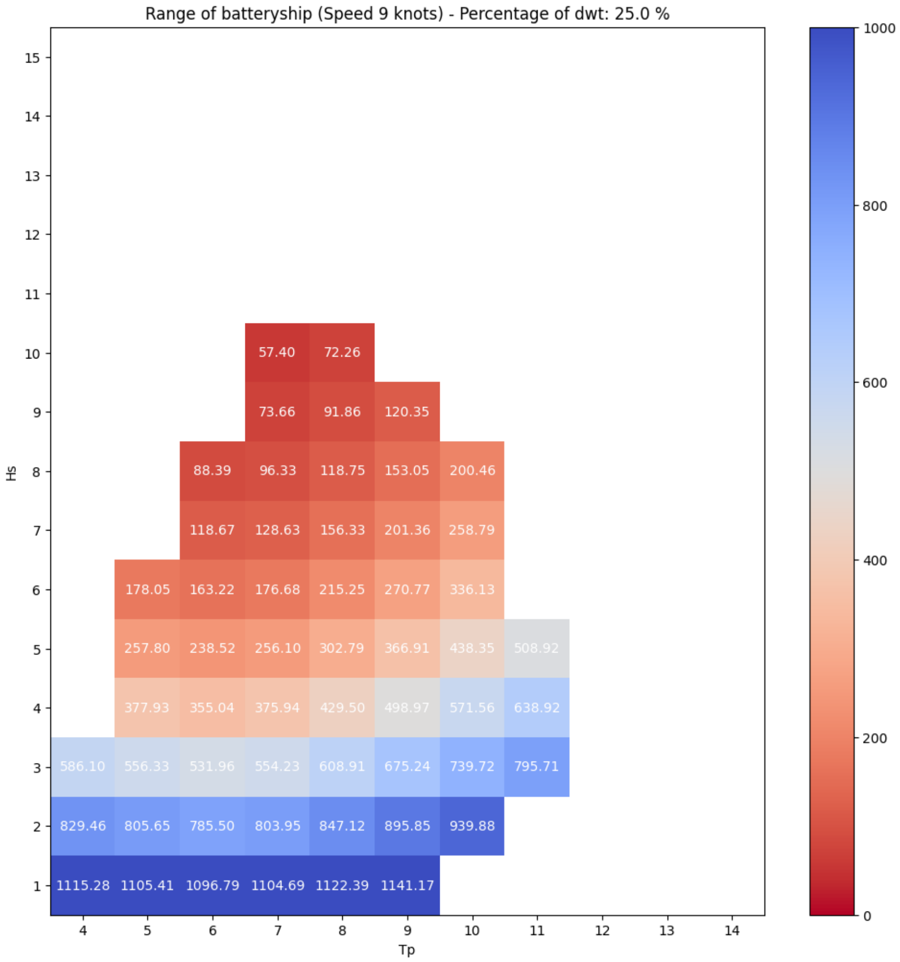

Figure C.5: Range for a battery ship where battery is 25 % of dwt and speed is 9 knots

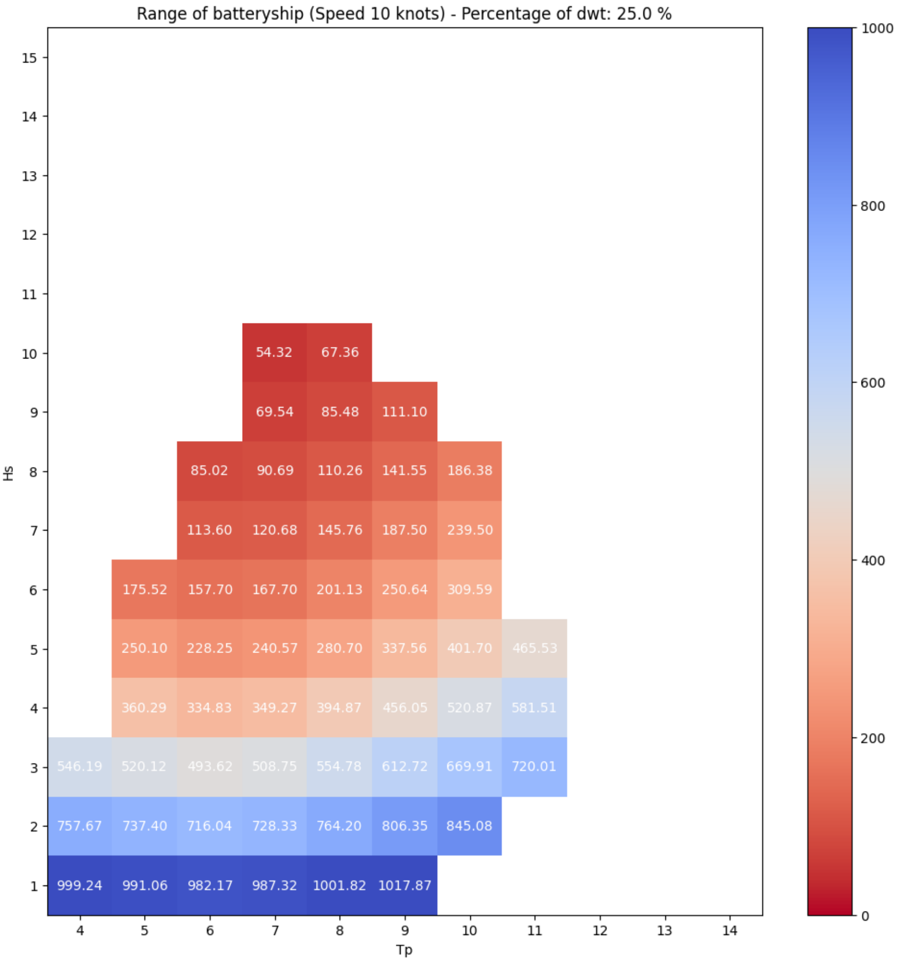

Figure C.6: Range for a battery ship where battery is 25 % of dwt and speed is 10 knots

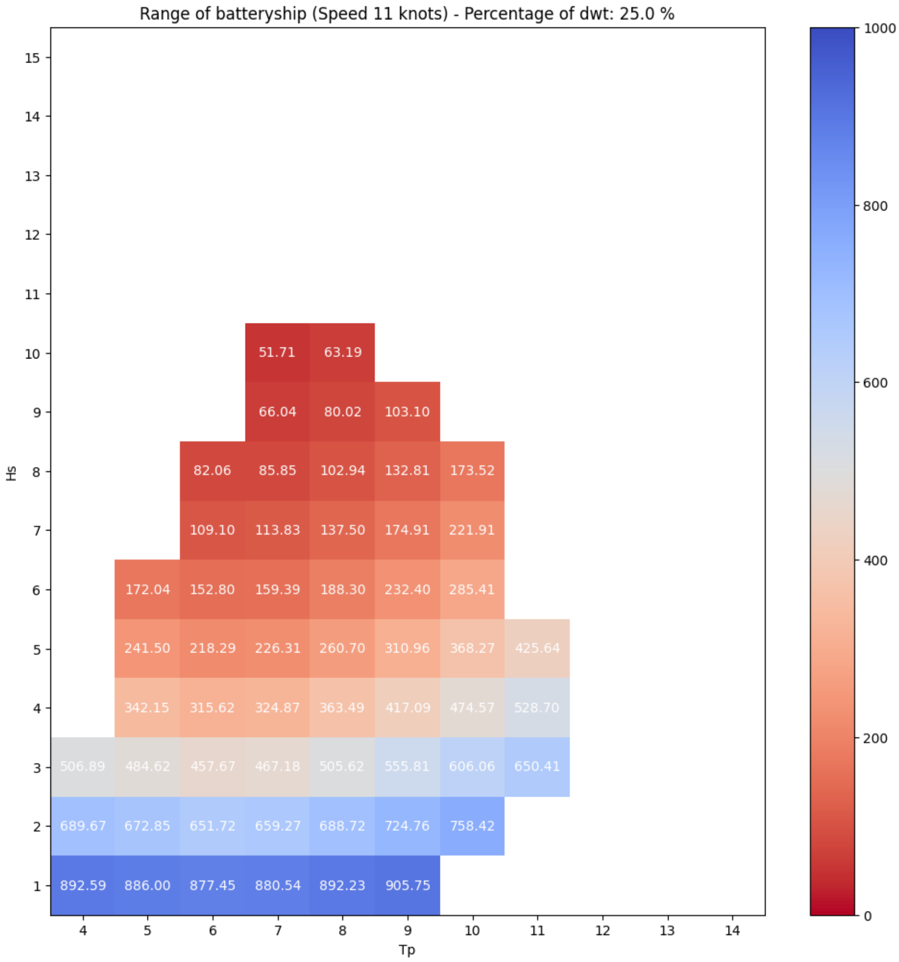

Figure C.7: Range for a battery ship where battery is 25 % of dwt and speed is 11 knots

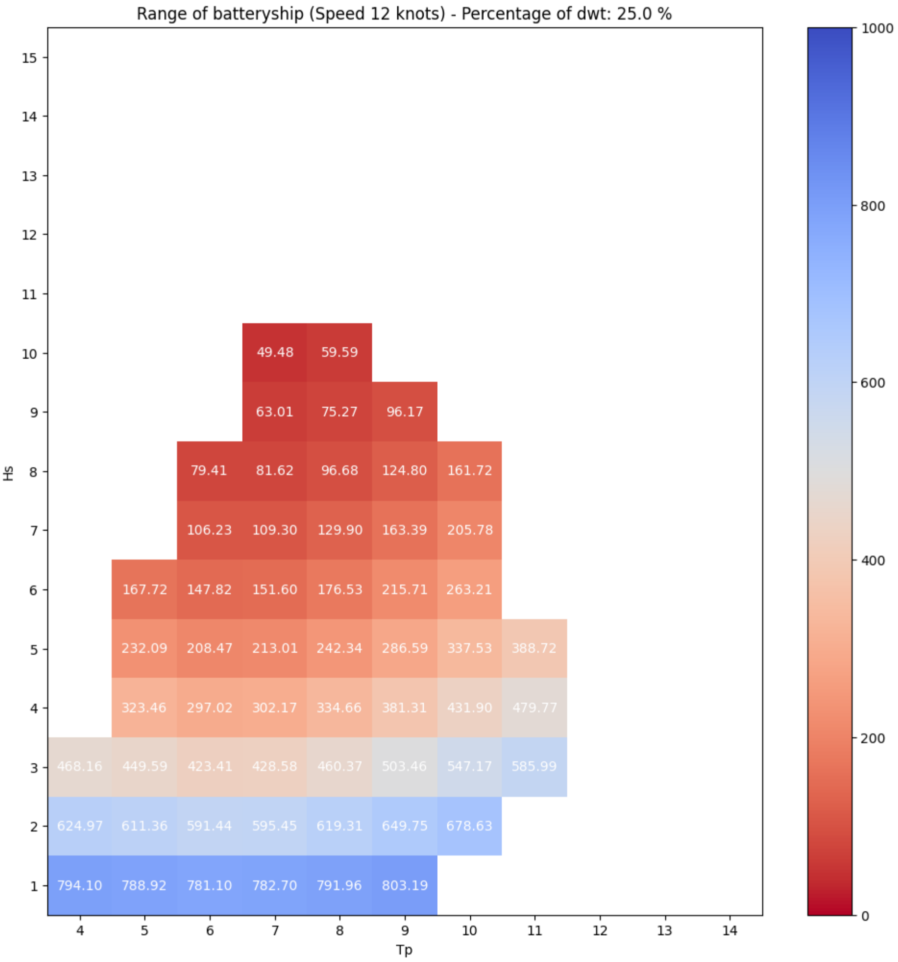

Figure C.8: Range for a battery ship where battery is 25 % of dwt and speed is 12 knots

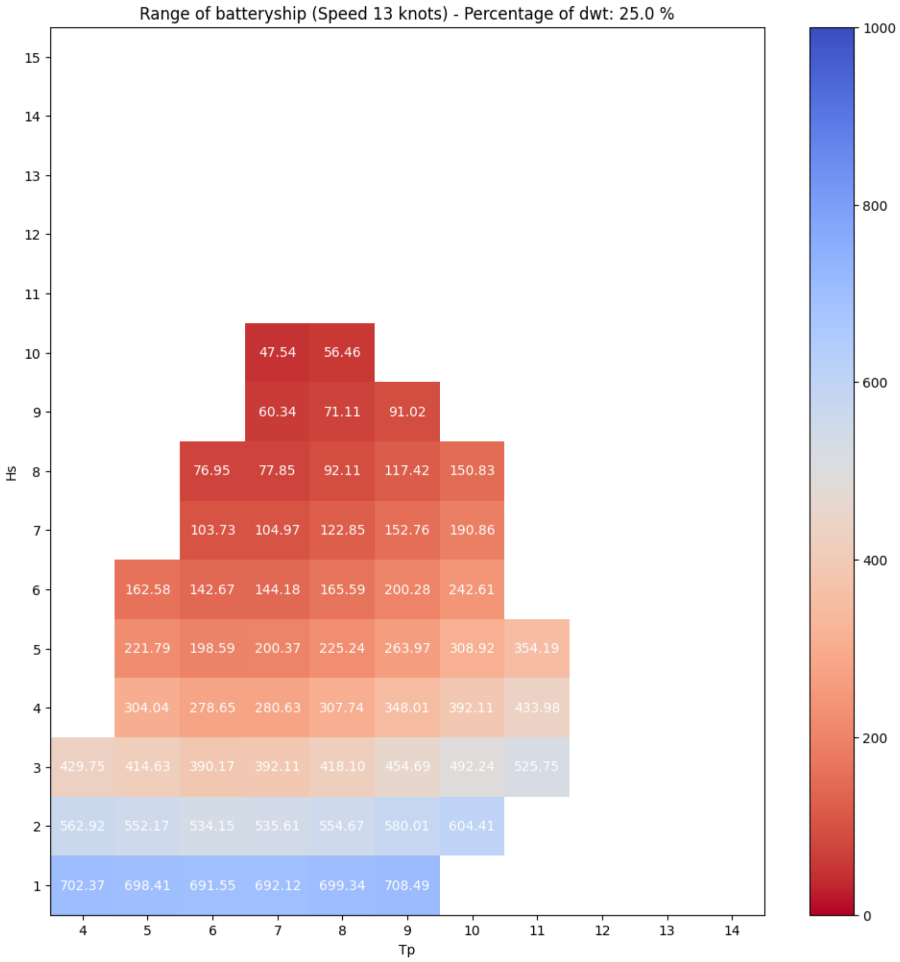

Figure C.9: Range for a battery ship where battery is 25 % of dwt and speed is 13 knots

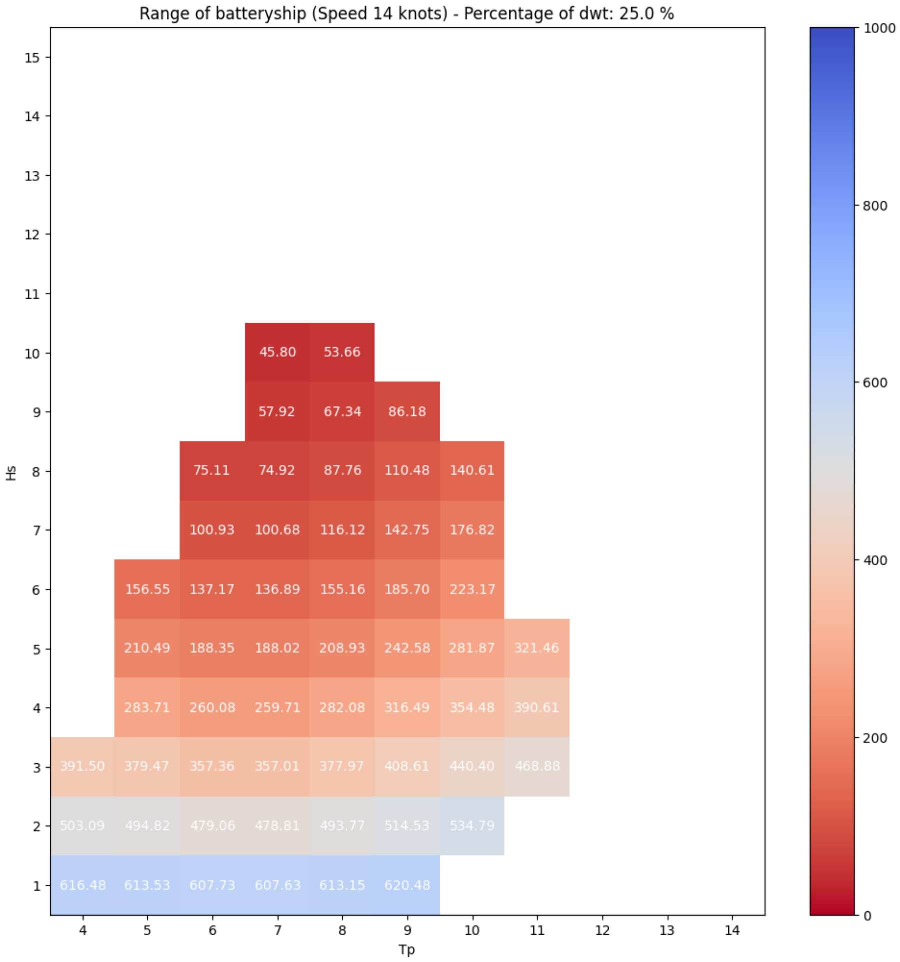

Figure C.10: Range for a battery ship where battery is 25 % of dwt and speed is 14 knots

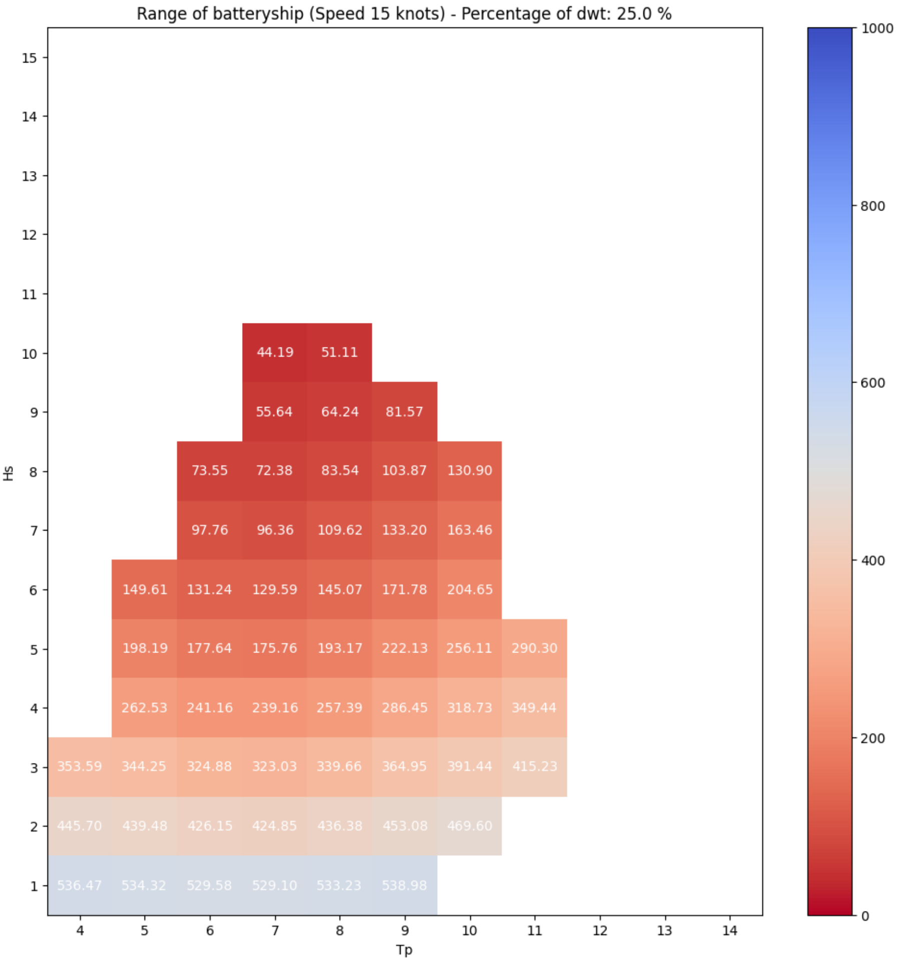

Figure C.11: Range for a battery ship where battery is 25 % of dwt and speed is 15 knots

Appendix D

Range calculations where batteries is 50% of dwt

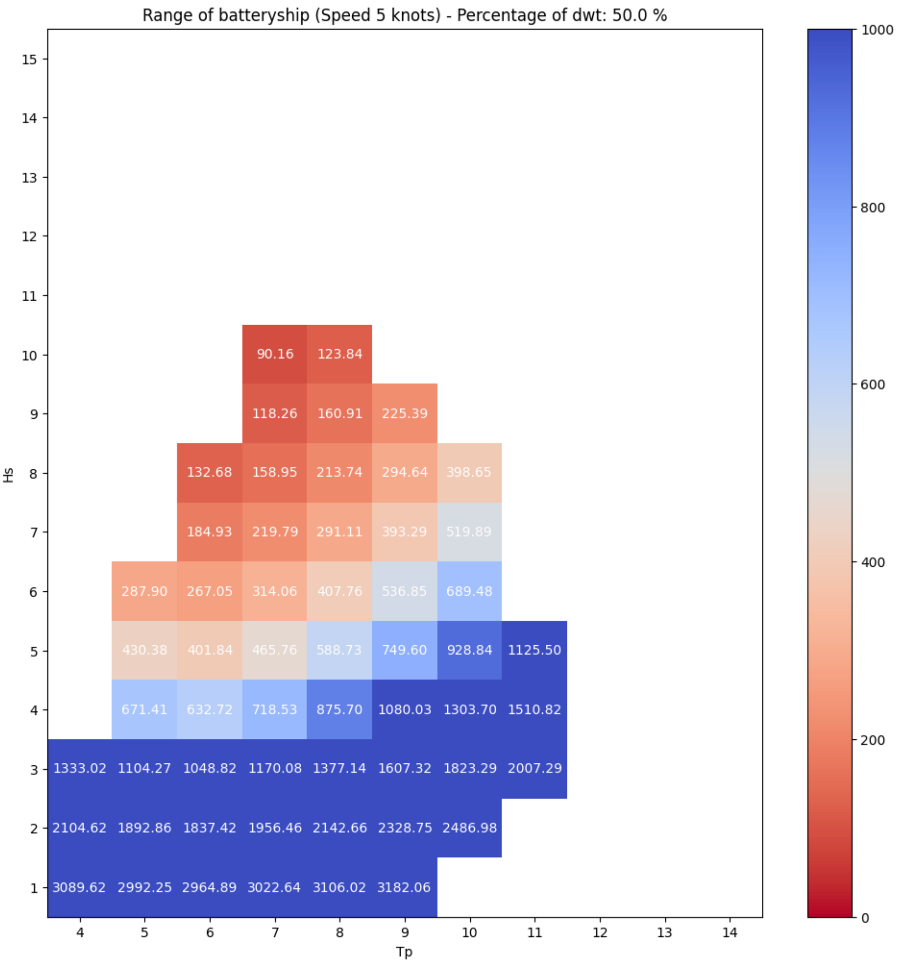

Figure D.1: Range for a battery ship where battery is 50 % of dwt and speed is 5 knots

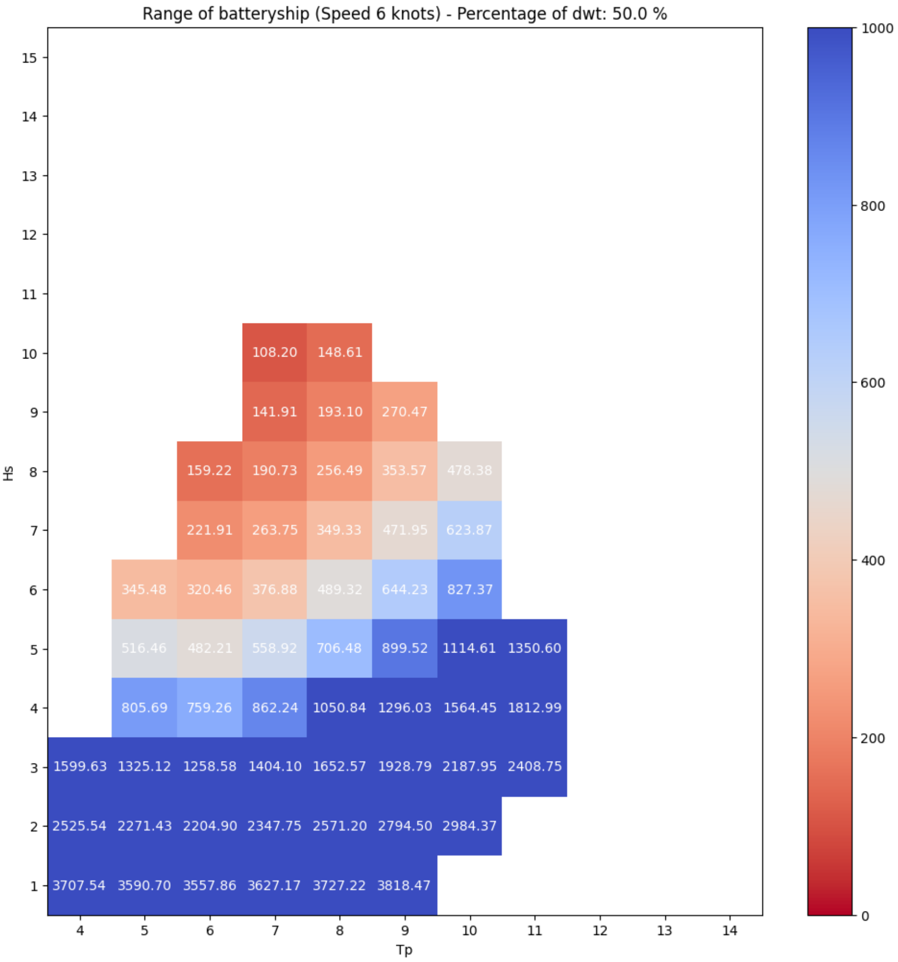

Figure D.2: Range for a battery ship where battery is 50 % of dwt and speed is 6 knots

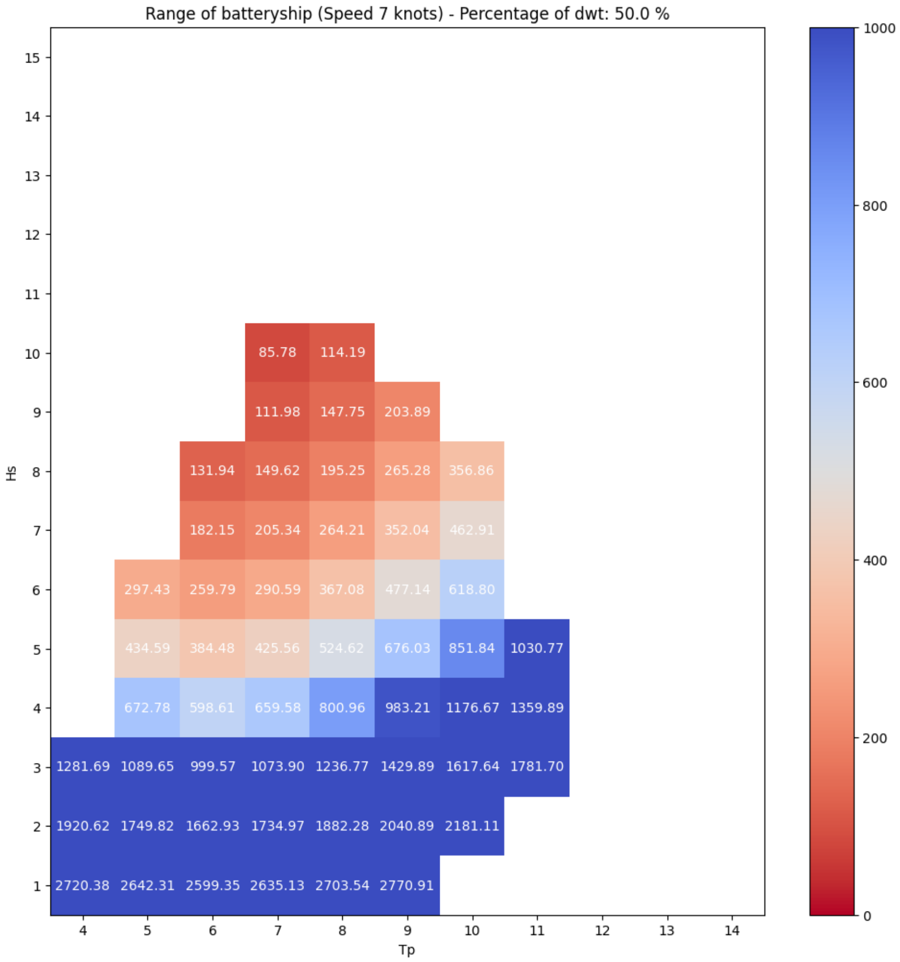

Figure D.3: Range for a battery ship where battery is 50 % of dwt and speed is 7 knots

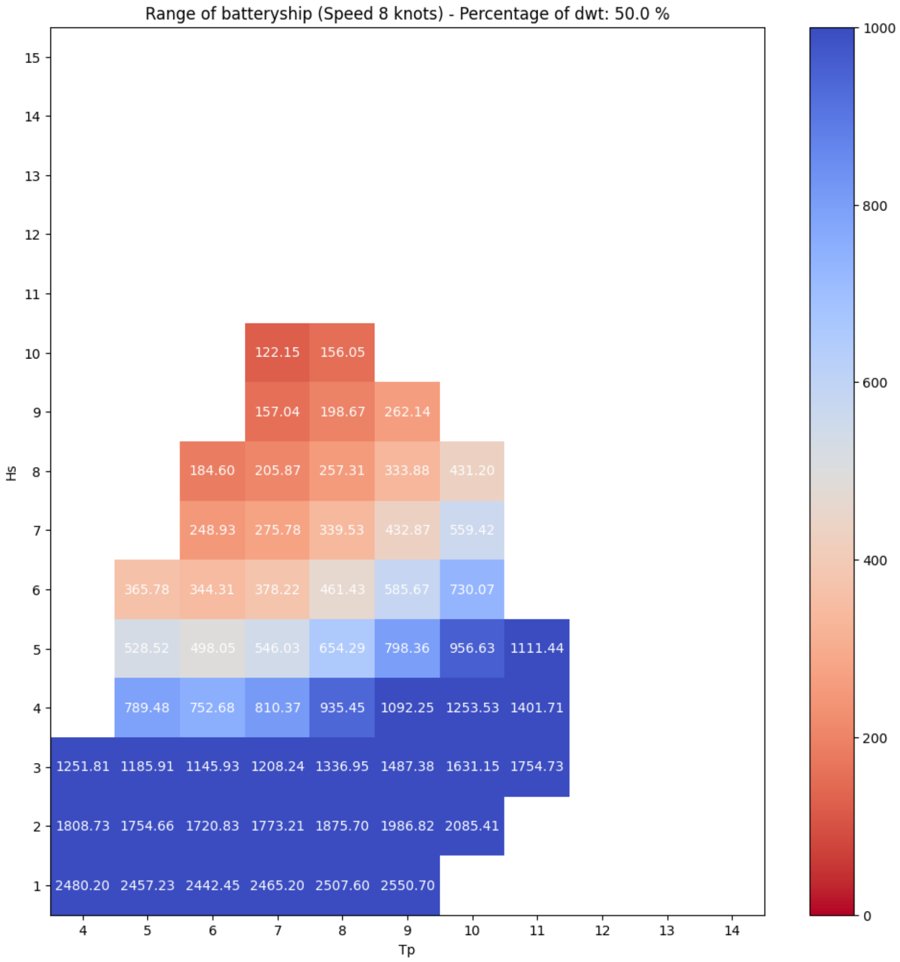

Figure D.4: Range for a battery ship where battery is 50 % of dwt and speed is 8 knots

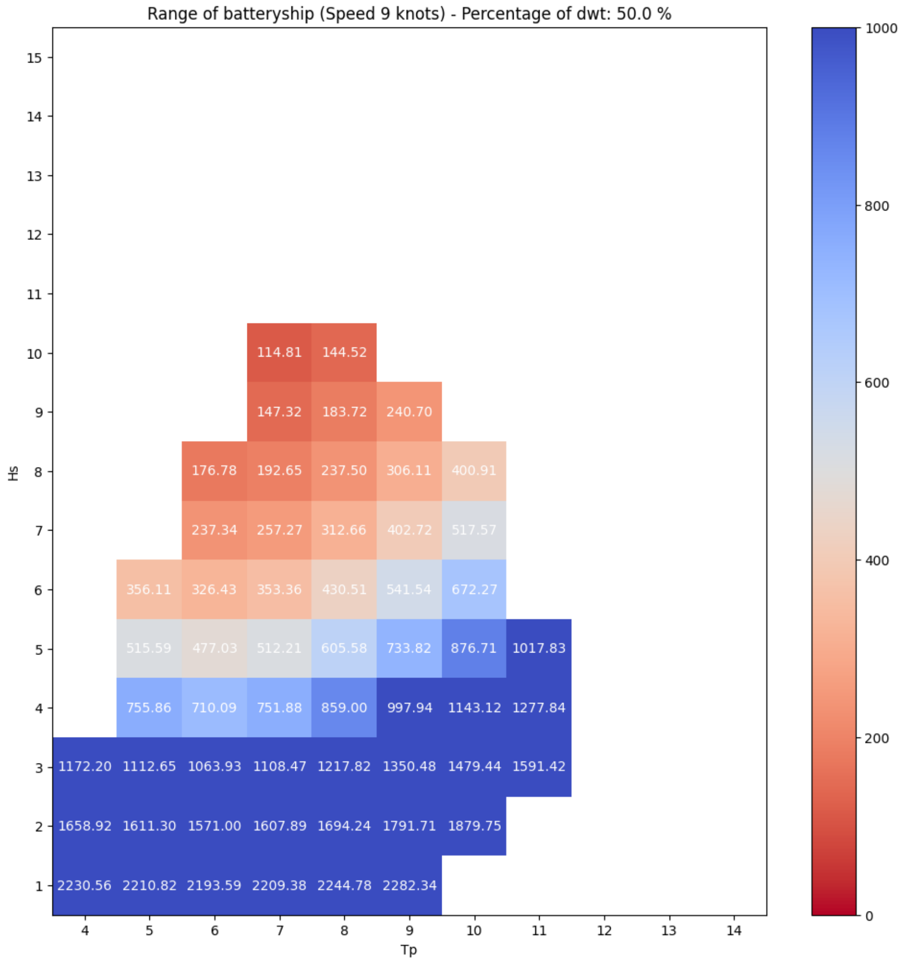

Figure D.5: Range for a battery ship where battery is 50 % of dwt and speed is 9 knots

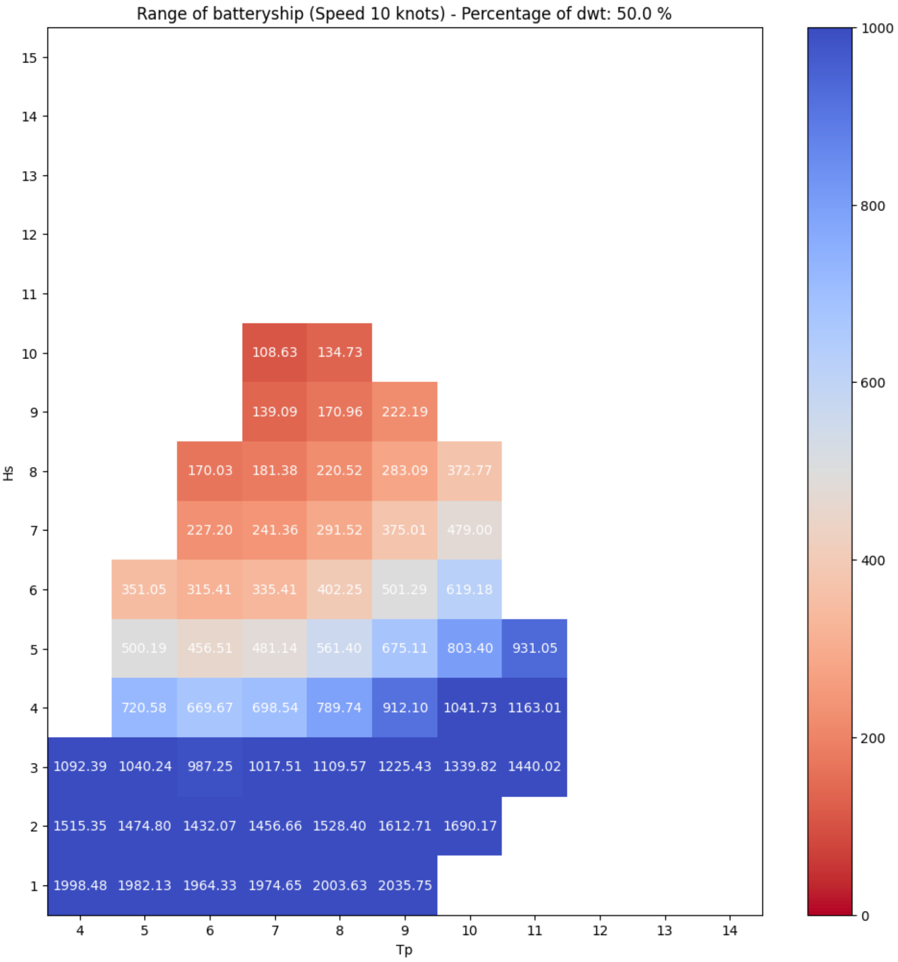

Figure D.6: Range for a battery ship where battery is 50 % of dwt and speed is 10 knots

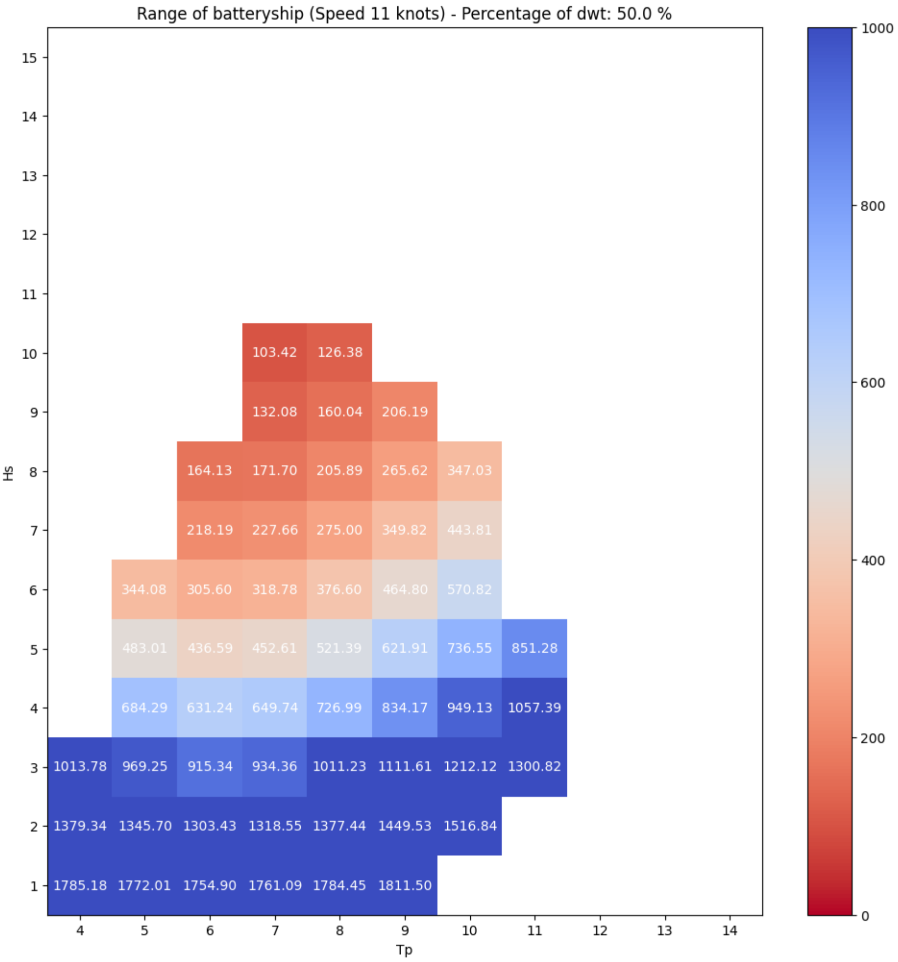

Figure D.7: Range for a battery ship where battery is 50 % of dwt and speed is 11 knots

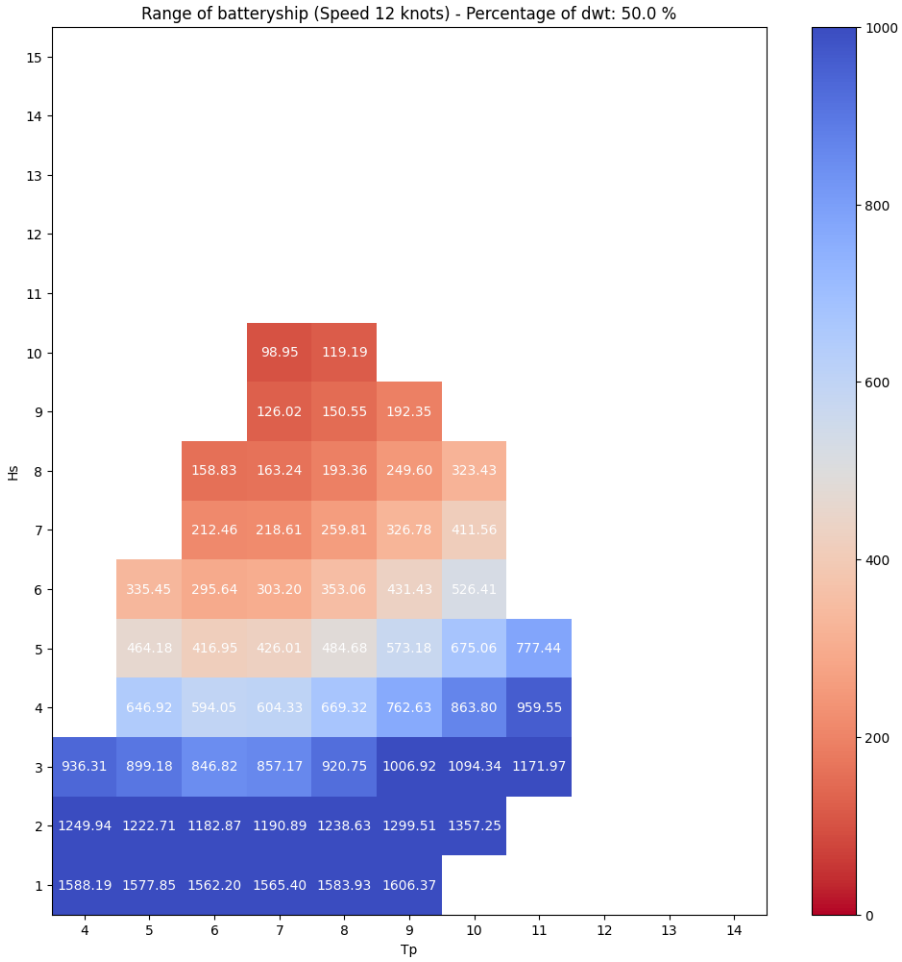

Figure D.8: Range for a battery ship where battery is 50 % of dwt and speed is 12 knots

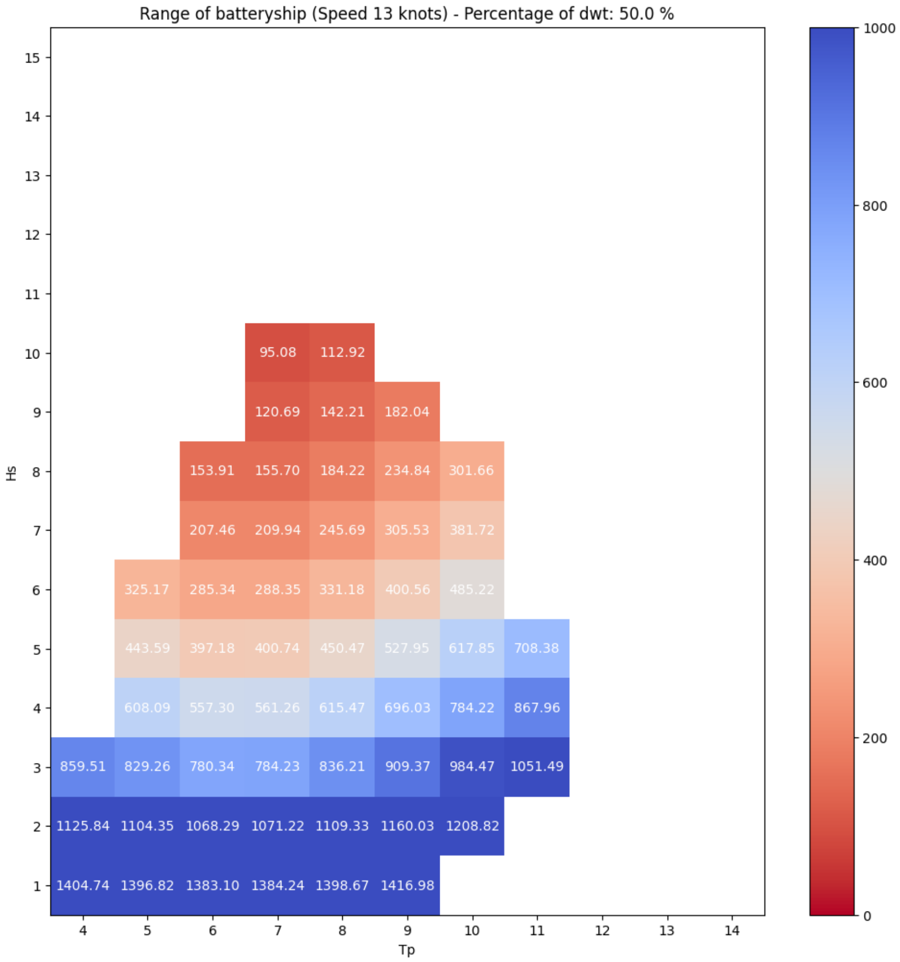

Figure D.9: Range for a battery ship where battery is 50 % of dwt and speed is 13 knots

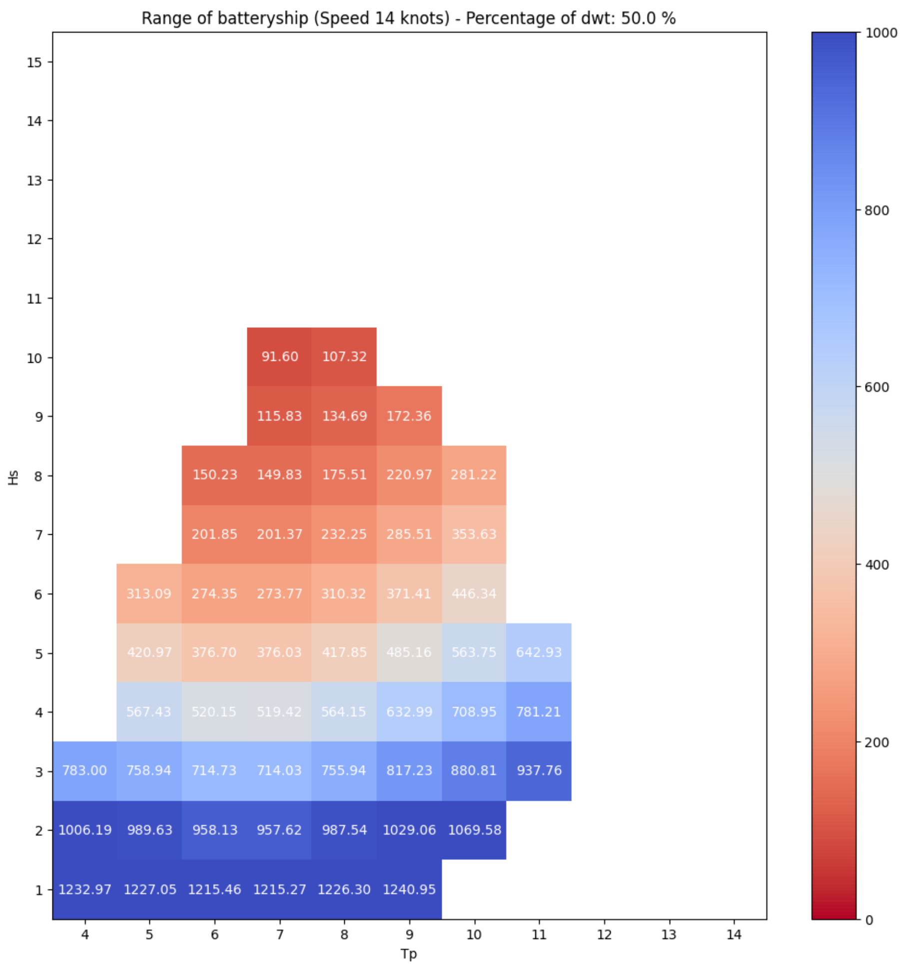

Figure D.10: Range for a battery ship where battery is 50 % of dwt and speed is 14 knots

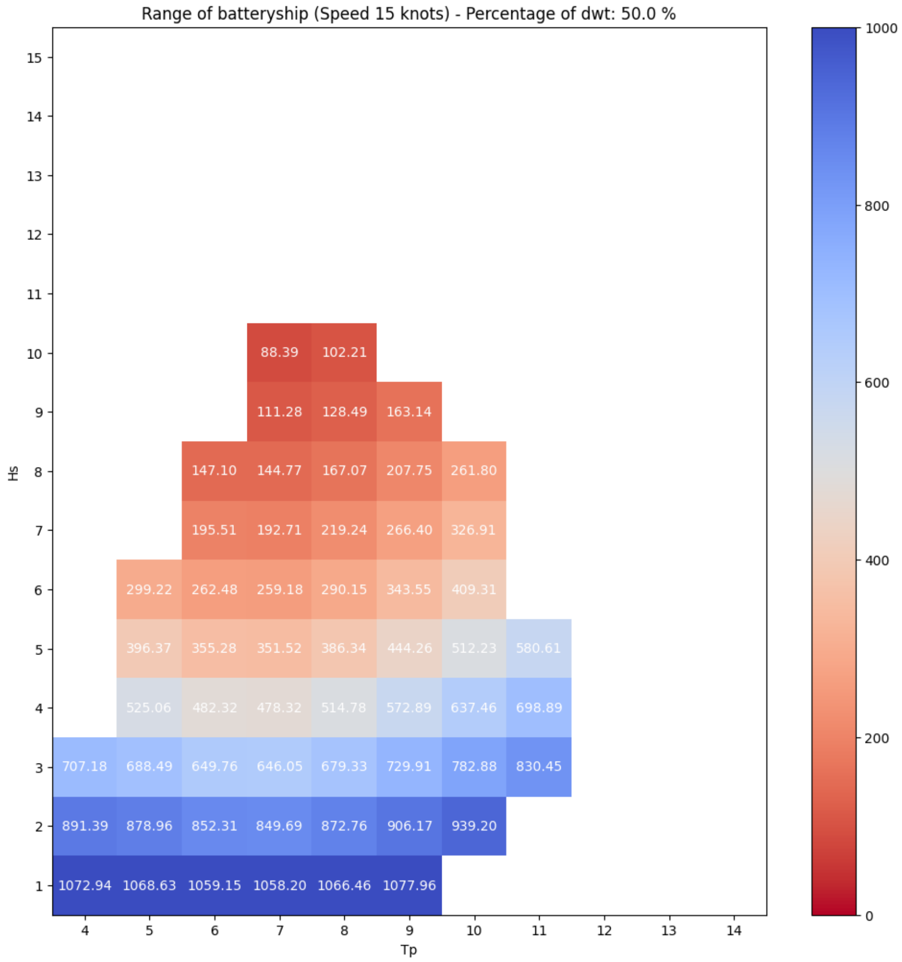

Figure D.11: Range for a battery ship where battery is 50 % of dwt and speed is 15 knots

Appendix E

Range calculations where batteries is 76% of dwt

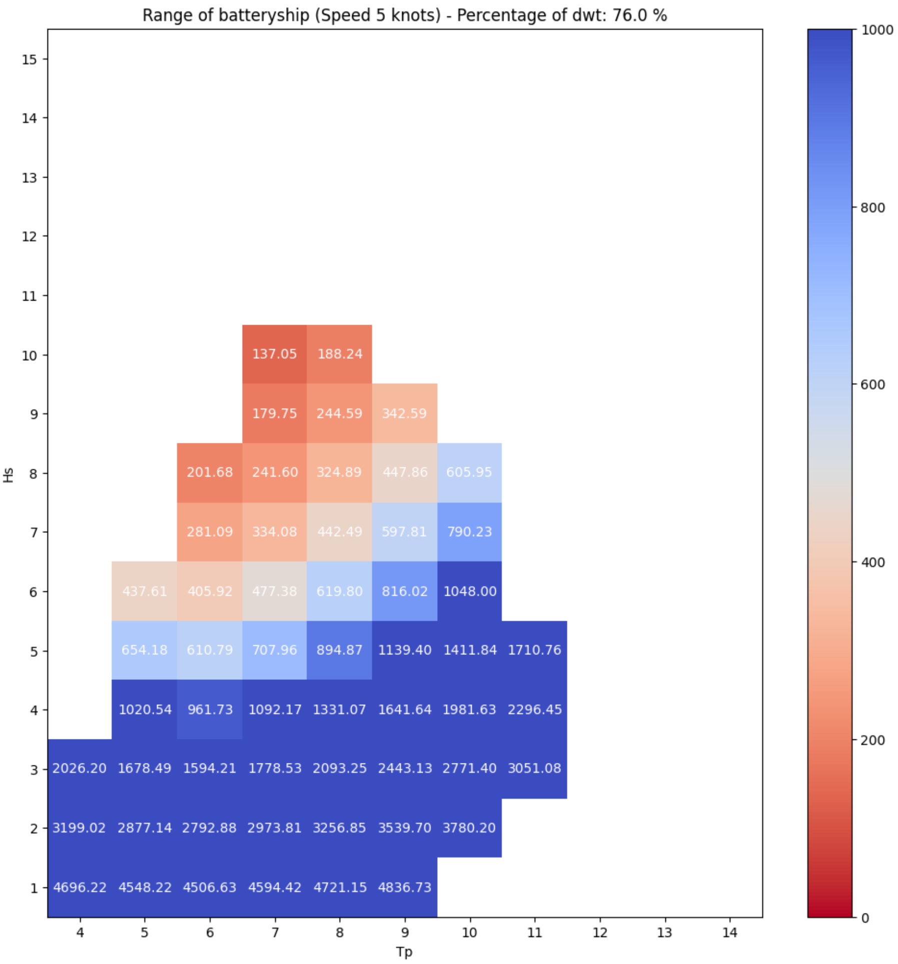

Figure E.1: Range for a battery ship where battery is 76 % of dwt and speed is 5 knots

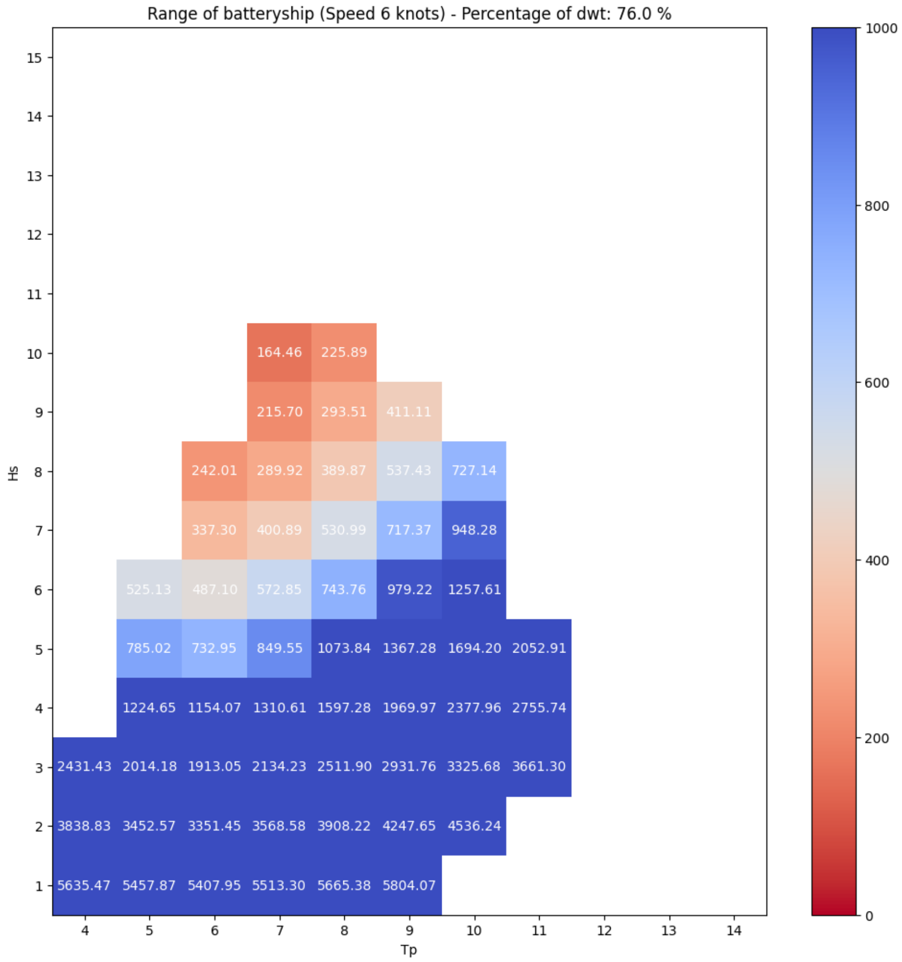

Figure E.2: Range for a battery ship where battery is 76 % of dwt and speed is 6 knots

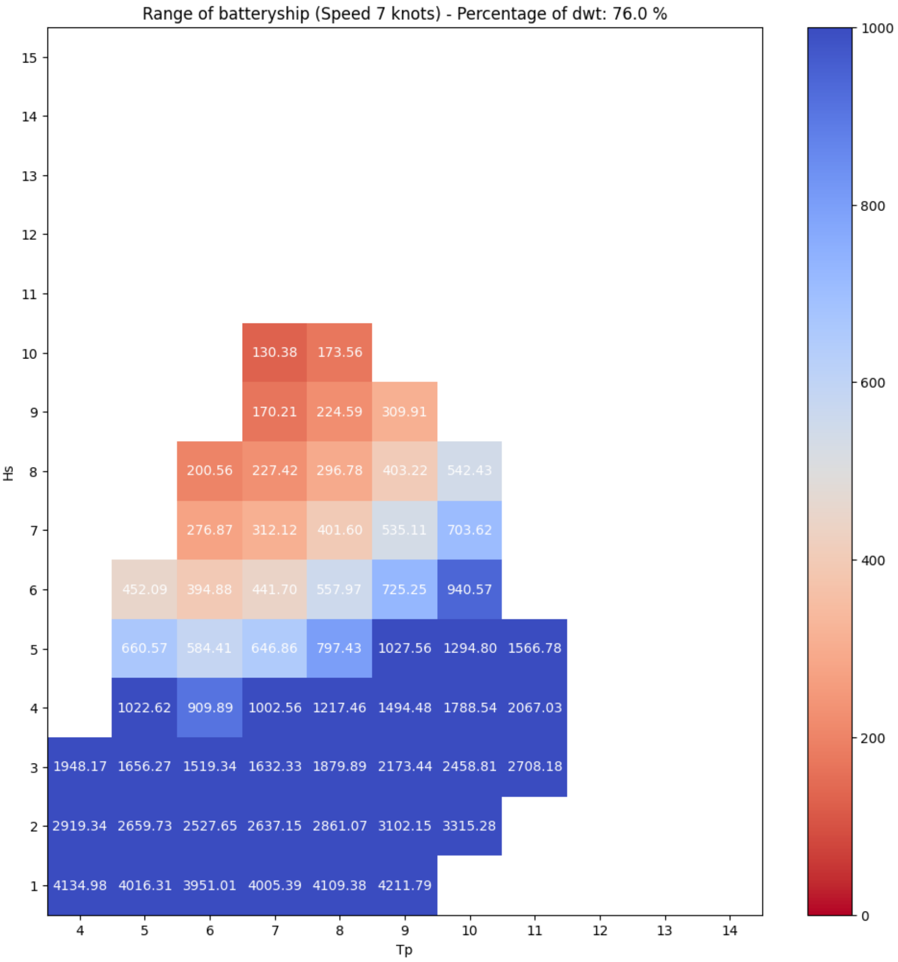

Figure E.3: Range for a battery ship where battery is 76 % of dwt and speed is 7 knots

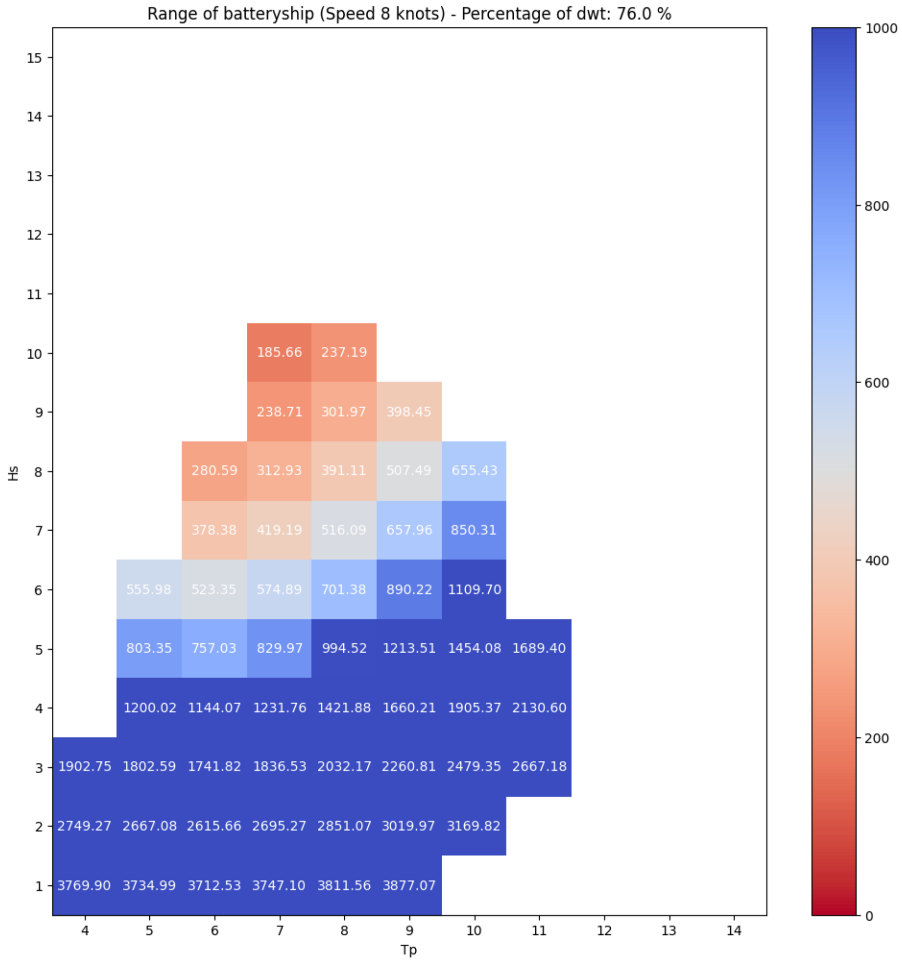

Figure E.4: Range for a battery ship where battery is 76 % of dwt and speed is 8 knots

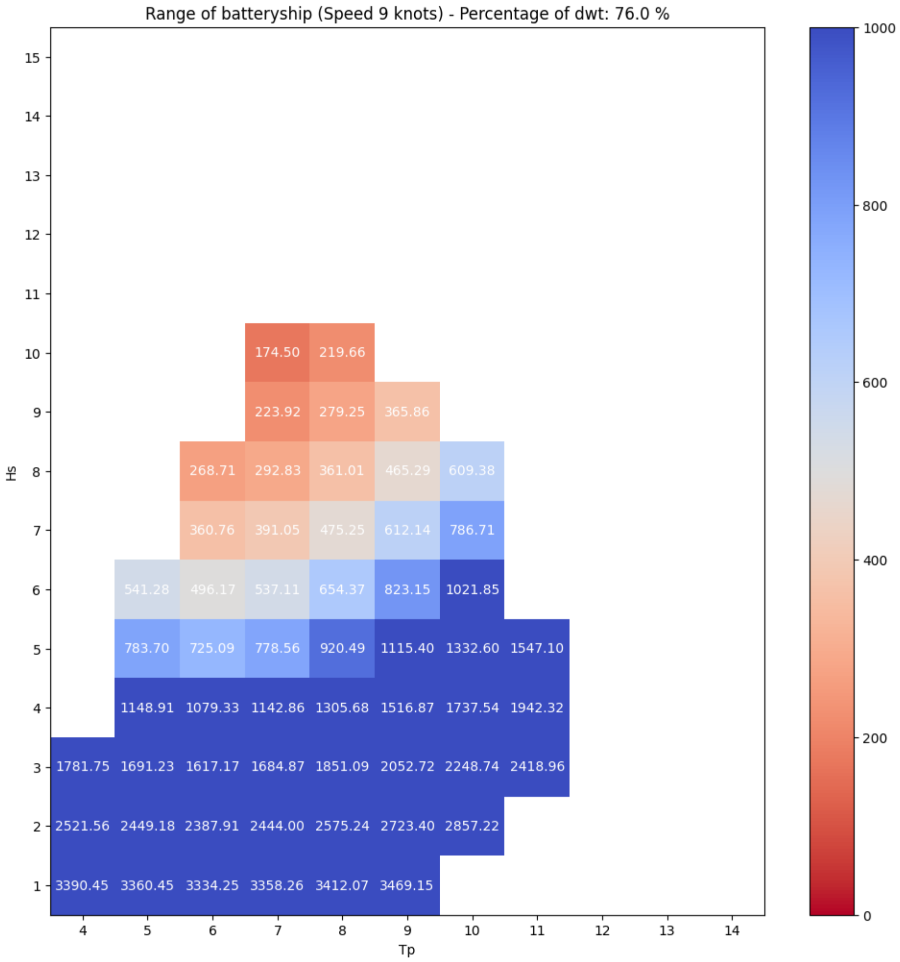

Figure E.5: Range for a battery ship where battery is 76 % of dwt and speed is 9 knots

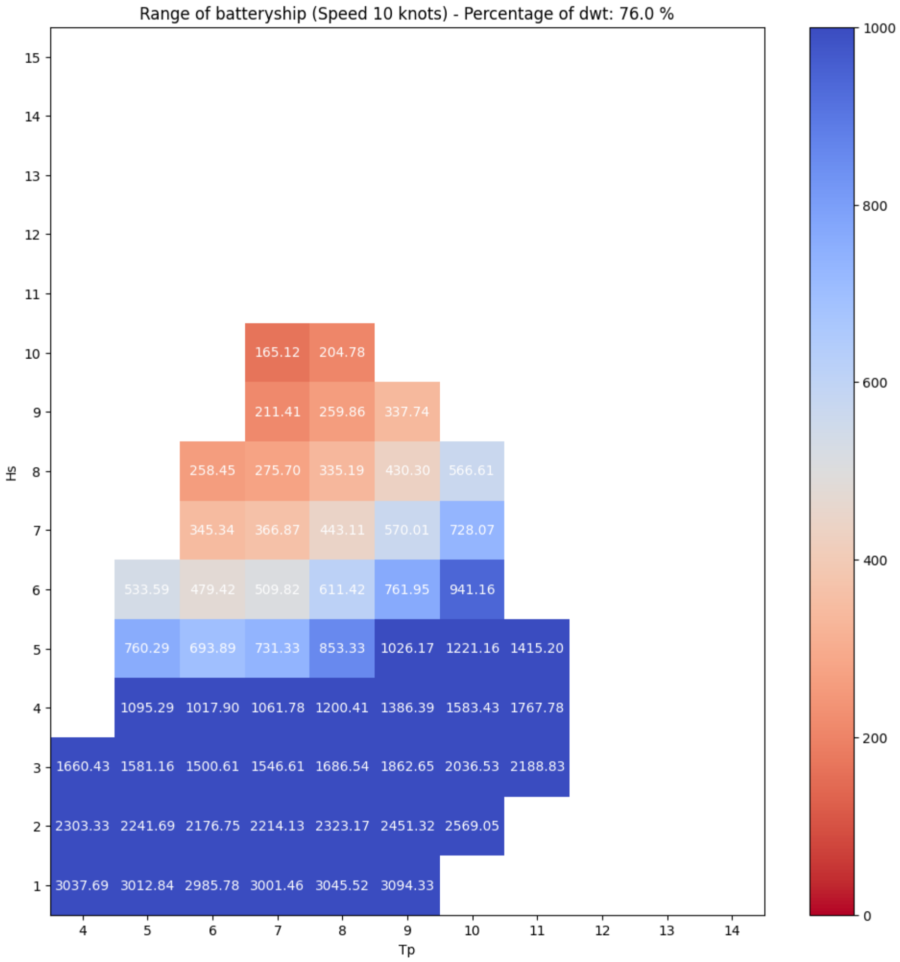

Figure E.6: Range for a battery ship where battery is 76 % of dwt and speed is 10 knots

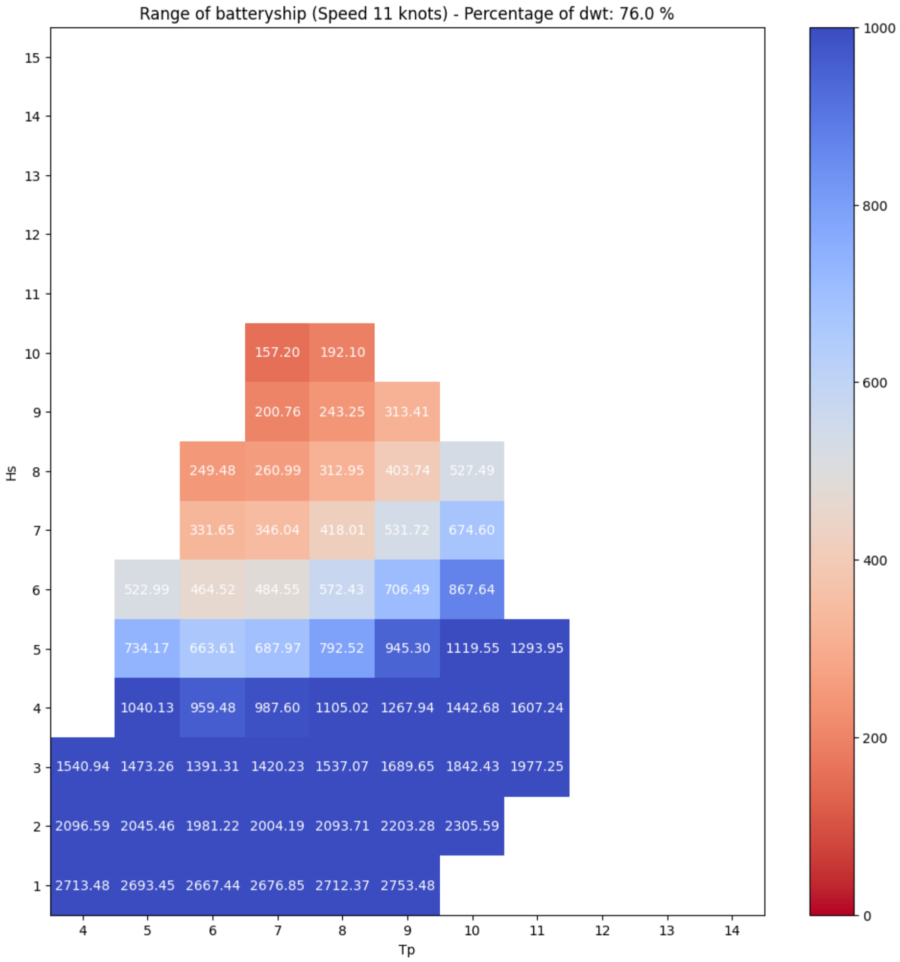

Figure E.7: Range for a battery ship where battery is 76 % of dwt and speed is 11 knots

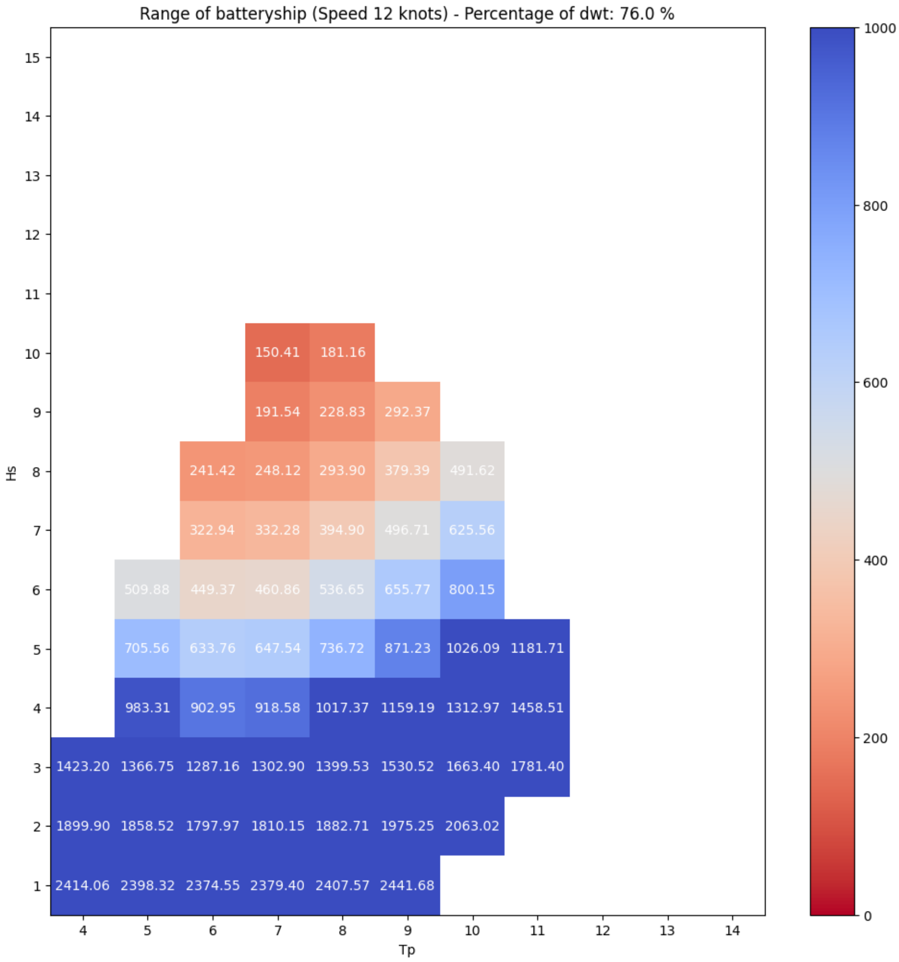

Figure E.8: Range for a battery ship where battery is 76 % of dwt and speed is 12 knots

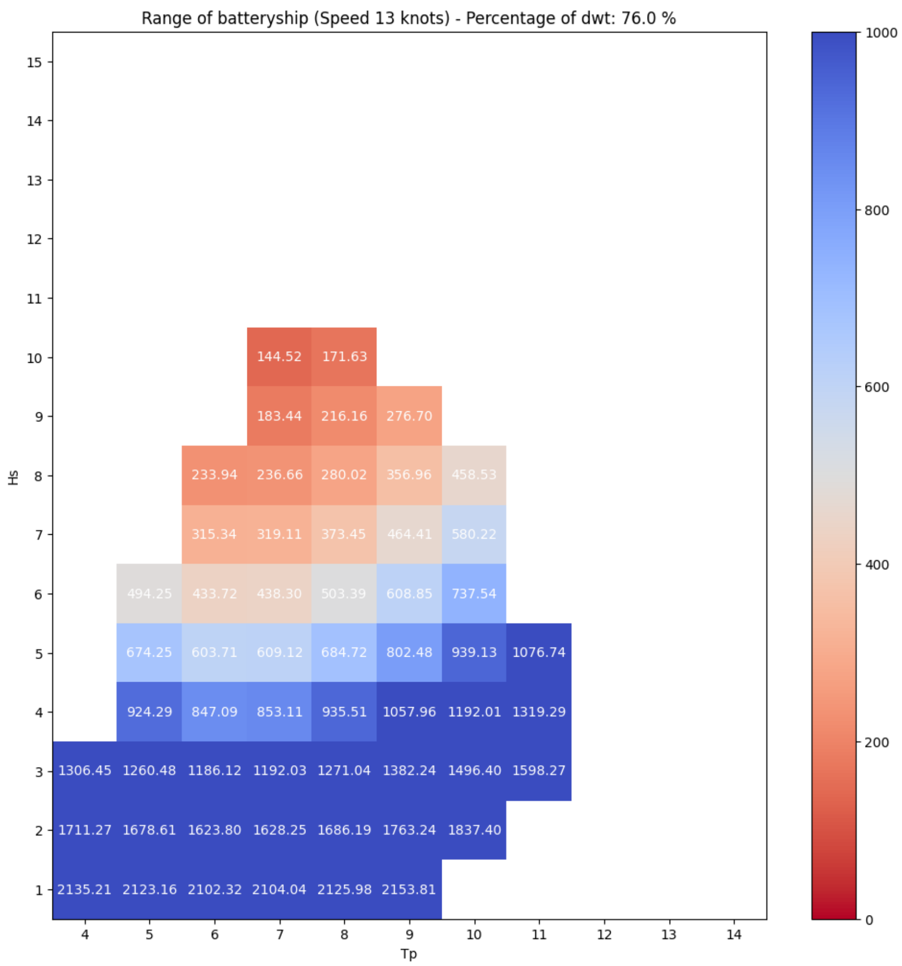

Figure E.9: Range for a battery ship where battery is 76 % of dwt and speed is 13 knots

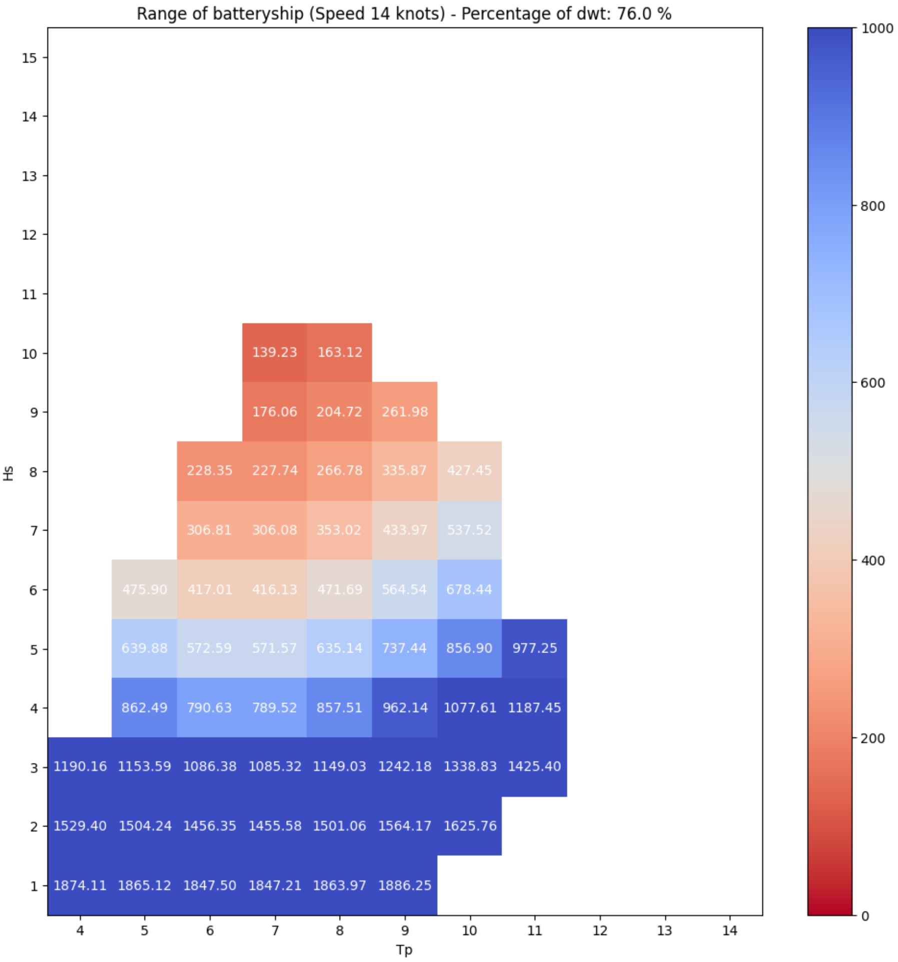

Figure E.10: Range for a battery ship where battery is 76 % of dwt and speed is 14 knots

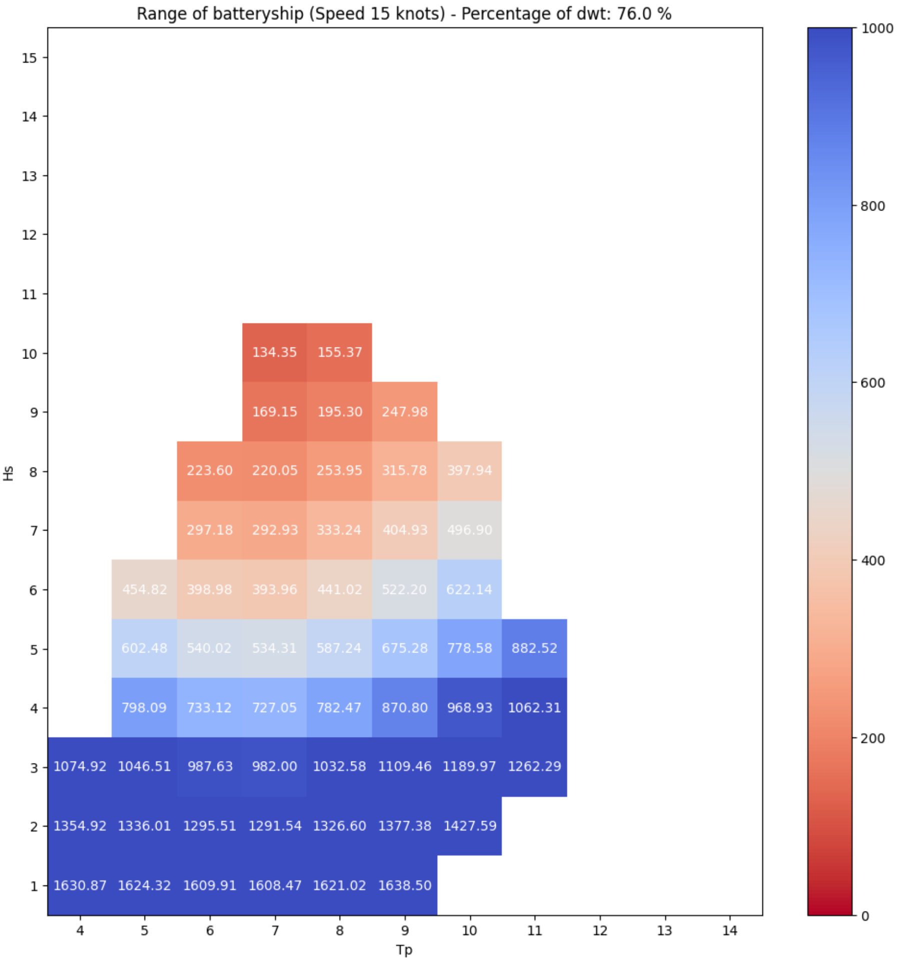

Figure E.11: Range for a battery ship where battery is 76 % of dwt and speed is 15 knots

Appendix F

Hand calculation of power prediction checking the mariTEAM model.

Parameters for Kvitbjørn:

Ship: Kvitbjørn mmsi: 231748000

Ship parametres:

Length ℓ: 120 m Draught T: 6 m

Breadth B: 20.8 m Wetted surface S:

Velocity $V = 10.59$ kn $= 5.44$ m/s

Block coefficient: $C_B = 0.56$

Density of saltwater $\rho = 1025$ g/m³

Viscosity $\nu = 1.1395 \cdot 10^{-6}$

LwL: 119

Number of rudders $N_{rud} = 1$

$H = 150\ \mu$

$S = 2865$

Made with Goodnotes

Figure F.1: Parameters used in hand calculations, ship Kvitbjørn used

Estimate resistance using Hollenbach (1998)

Assume: L_{os} = length, therefore $L_{os}/L = 1 \Rightarrow L_{nf} = L$

Froude number: $F_n = \frac{V}{\sqrt{g L_{fn}}} = \frac{5.44\,m/s}{\sqrt{9.81\,m/s^2 \cdot 120\,m}} = 0.15855$

$$F_{n,crit} = d_1 + d_2 \cdot C_b + d_3 C_b^2 = 0.854 + -1.228 \cdot 0.56 + 0.497 \cdot 0.56^2 = 0.3222$$

$$C_{R,froudecrit} = \left(\frac{F_n}{F_{n,crit}}\right)^{F_n/F_{n,crit}} = \left(\frac{0.15855}{0.3222}\right)^{0.15855/0.3222} = 0.7054$$

Assume propeller diameter is $0.6 \cdot T \Rightarrow D_p = 0.6 \cdot 6.014 = 3.61\,m$

Form factor: $\phi = (C_b/L) \cdot ((B/2) \cdot (TF + TA))^{0.5}$

$$\phi = (0.56/120m) \cdot ((20.8m/2) \cdot (6m + 6m))^{0.5}$$

$$\phi = 0.0624$$

$$k = 0.6 \cdot \phi + 145 \cdot \phi^{3.5} = 0.05213$$

$$C_{R,standard} = b_{11} + b_{12} \cdot F_n + b_{13} \cdot F_n^2 + C_B \cdot (b_{21} + b_{22} \cdot F_n + b_{23} \cdot F_n^2) + C_B^2 \cdot (b_{31} + b_{32} \cdot F_n + b_{33} \cdot F_n^2)$$

$$= (-0.57424 + 13.3893 \cdot 0.15855 + 90.596 \cdot 0.15855^2 + 0.56\,(4.6614 + -39.721 \cdot 0.15855 + -351.483 \cdot 0.15855^2) + 0.56^2 \cdot (-1.14215 + -12.3296 \cdot 0.15855 + 459.254 \cdot 0.15855^2))\;/\;10$$

(/ 10: correcting for mistake in hollenbach paper)

$$= 0.0610956$$

$$K_L = e_1 L^{e_2} = 2.1701 \cdot 120\,m^{-0.1602} = 1.00785$$

Residual resistance coefficient

$$C_{R\_hb} = C_{R,standard} \cdot C_{R,froudecrit} \cdot K_L \cdot \left(\frac{T}{B}\right)^{a_1} \cdot \left(\frac{B}{L}\right)^{a_2} \cdot \left(\frac{L_{os}}{L_{wL}}\right)^{a_3} \cdot \left(\frac{L_{wL}}{L}\right)^{a_4} \cdot \left(\frac{D_p}{TA}\right)^{a_6} \cdot \left(1 - ((TA - TF)/L)^{a_5}\right)$$

$$\cdot (1 - N_{rud})^{a_7} \cdot (1 - N_{Brac})^{a_8} \cdot (1 - N_{boss})^{a_9} \cdot (1 - N_{Thr})^{a_{10}}$$

($TA - TF = 0$)

Assume: $N_{Brac} = 0$, $N_{Boss} = 0$, $N_{Thr} = 0$, $TA = TF$

$$C_{r\_hb} = 0.0610956 \cdot 1 \cdot 1.00785 \cdot \left(\frac{6m}{20.8m}\right)^{-0.3382} \cdot \left(\frac{20.8m}{120m}\right)^{0.8086} \cdot \left(\frac{120m}{120m}\right)^{-6.0258} \cdot \left(\frac{119m}{120m}\right)^{-3.5632}$$

$$\cdot \left(\frac{0.65 \cdot 6m}{6m}\right)^{0.0146} \cdot (1-1)^0 \cdot 1^0 \cdot 1^0 \cdot 1^0$$

$$C_{r\_hb} = 0.02327$$

Reynold number $R_n = \frac{VL}{\nu} = \frac{5.44\,m/s \cdot 120\,m}{1.1395 \cdot 10^{-6}} = 572882843.4$

ITTC '57 friction line $C_F = \frac{0.075}{(\log_{10}(R_n) - 2)^2} = \frac{0.075}{(\log_{10}(572882843.4) - 2)^2} = 1.6422 \cdot 10^{-3}$

Made with Goodnotes

Figure F.2: Hand calculations of calm water resistance, ship Kvitbjørn used

Increase of friction due to hull roughness ITTC '78

$$\Delta C_F = ((100 \cdot (H \cdot V)^{0.21} - 403) \cdot C_F^2 = ((100 \cdot (100 \cdot 5.44\,m/s)^{0.21} - 403) \cdot 1.6422 \cdot 10^{-3} = \underline{1.5500 \cdot 10^{-5}}$$

$$\phi = \frac{C_b}{L} \cdot \sqrt{B \cdot (TA + TF)} = \frac{0.56}{120m} \cdot \sqrt{20.8\,m\,(6m + 6m)} = \underline{0.0737}$$

$$k = 0.6 \cdot \phi + 145 \cdot \phi^{3.5} = 0.6 \cdot 0.0737 + 145 \cdot 0.0737^{3.5} = \underline{0.059978}$$

Total residual coefficient $C_R = C_{R\_hb} \cdot B \cdot \frac{T}{S} - k \cdot C_F$

$$C_R = 0.02327 \cdot 20.8\,m \cdot \frac{6\,m}{2865\,m^2} - 0.059978 \cdot 1.6422 \cdot 10^{-3} = \underline{9.152 \cdot 10^{-4}}$$

Total resistance coefficient:

$$C_{TS} = (C_F + \Delta C_F) \cdot (1 + k) + C_R$$

$$= (1.6422 \cdot 10^{-3} + 1.55 \cdot 10^{-5})(1 + 0.059978) + 9.152 \cdot 10^{-4} = \underline{2.672 \cdot 10^{-3}}$$

Total resistance of ship

$$R_{TS} = \frac{1}{2} \cdot \rho \cdot V^2 \cdot S \cdot C_{TS} \;/\; 1000$$

divide by 1000 to get kN

$$= \frac{1}{2} \cdot 1025 \cdot 5.44\,m/s^2 \cdot 2865\,m^2 \cdot 2.672 \cdot 10^{-3} / 1000 \approx \underline{116\,kN}$$

From the MariTEAM code the calmwater resistance is $\approx 113\,kN$, it uses Holtrop method.

Figure F.3: Hand calculations of calm water resistance, ship Kvitbjørn used

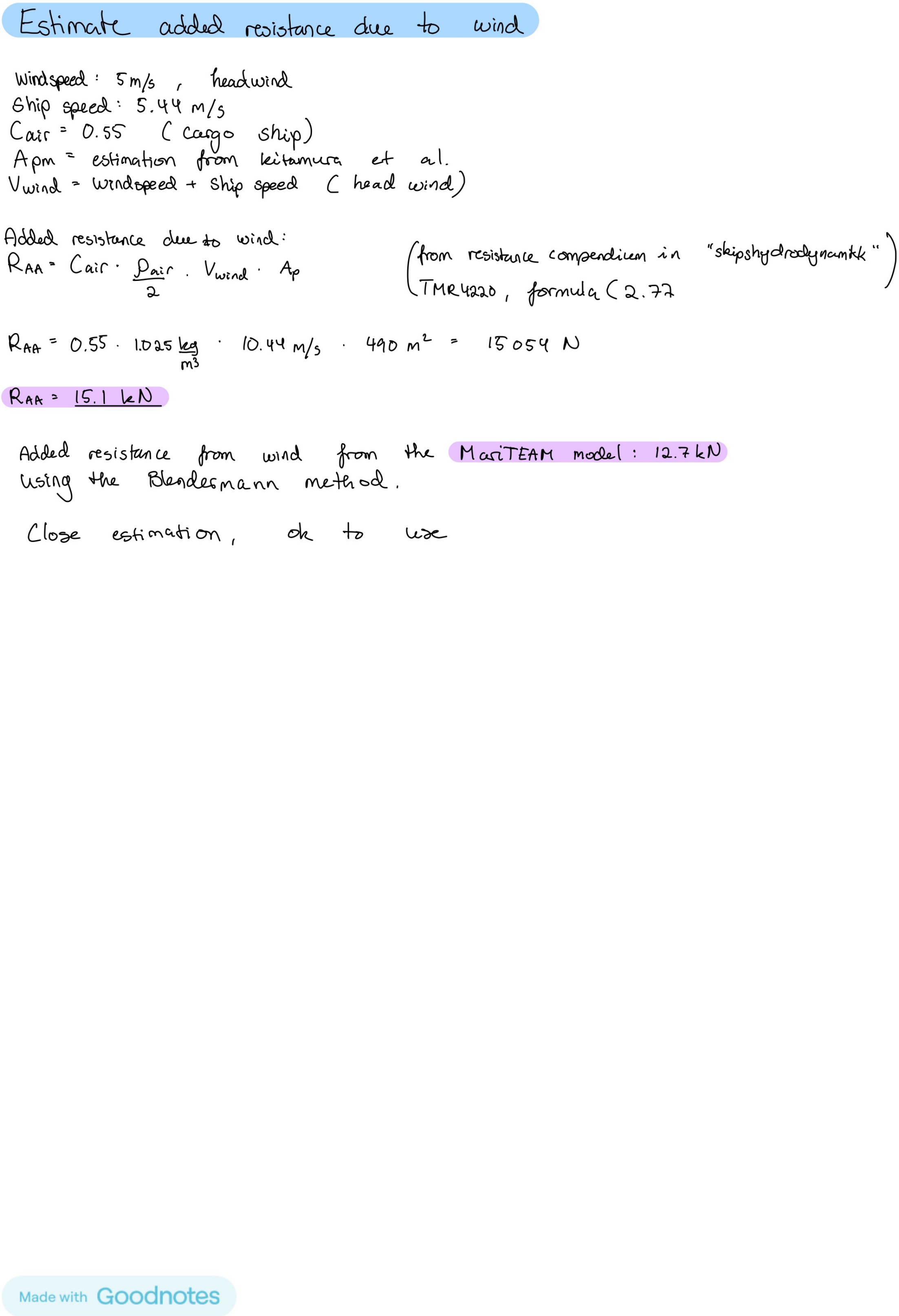

Estimate added resistance due to wind

Windspeed: 5 m/s, headwind
Ship speed: 5.44 m/s
C_{air} = 0.55 (cargo ship)
A_{pm} = estimation from kitamura et al.
V_{wind} = windspeed + ship speed (head wind)

Added resistance due to wind:

$R_{AA} = C_{air} \cdot \frac{\rho_{air}}{2} \cdot V_{wind} \cdot A_p$

(from resistance compendium in "skipshydrodynamikk" TMR4220, formula (2.77)

$R_{AA} = 0.55 \cdot 1.025 \frac{kg}{m^3} \cdot 10.44\ m/s \cdot 490\ m^2 = 15\,054\ N$

R_{AA} = 15.1 kN

Added resistance from wind from the MariTEAM model: 12.7 kN using the Blendermann method.

Close estimation, ok to use

Made with Goodnotes

Figure F.4: Hand calculations of added wind resistance, ship Kvitbjørn used

Estimate added resistance from waves

STAWAVE-1 : $R_{wave} \approx R_{AWL} = \frac{1}{16} \cdot \rho g H_{1/3}^2 \cdot B \sqrt{\frac{B}{L_{BWL}}}$

$L_{BWL} = 0.95 \cdot L = 0.95 \cdot 20.8m = \underline{19.76\,m}$

$H_s = 2$

$R_w = \frac{1}{16} \cdot 9.81 \frac{m}{s^2} \cdot 1025 \frac{kg}{m^3} \cdot 2m^2 \cdot 20.8m \cdot \sqrt{\frac{20.8m}{19.76m}}$

$R_w = 53641\,N \approx \underline{53.6\,kN}$

The MariTEAM model gives 46.8 kN, since Stawave-1 is a rough estimate this is within reasonable difference

Made with Goodnotes

Figure F.5: Hand calculations of added wave resistance, ship Kvitbjørn used

Power prediction

Using STEM 3 by (Johansson 2017)

↳ $P_{tot} \approx \frac{1}{\eta_D} (R_T + R_{weather}) \cdot V$

$\eta_D = 0.84 - \frac{n\sqrt{L_{pp}}}{1000}$ $\quad n = 750/60 \approx 12.5$

$\eta_D = 0.84 - \frac{12.5 \cdot \sqrt{120m}}{1000} = 0.703$

$R_T = R_{calm} + R_{wind} + R_{waves}$

$R_T = 116kN + 12.7kN + 53.6kN$

$R_T = 182.3kN$

$P_{tot} = \frac{1}{0.703} \cdot (182.3\ kN) \cdot 5.44\ m/s$

$P_{TOT} = 1410.7\ kW$

The MariTEAM model gives 1506 kW, so the conclution is that the calculations from the MariTEAM model is correct.

Figure F.6: Hand calculations of total power prediction, ship Kvitbjørn used

Appendix G

Corvus Blue whale Battery Specifications

Corvus Energy

Corvus Blue Whale

The Corvus Blue Whale Energy Storage System is a ground-breaking ESS specifically designed to meet the large energy requirements of emission free operation over longer periods of time.

The Corvus Blue Whale design is a result of the knowledge gained from having the largest global installed base of ESS solutions combined with our industry leading research and development capabilities. Low weight and low total system volume have been key design criteria, along wth keeping the unsurpassed Corvus energy safety features from Orca resulting in world leading energy density in a battery room with minimal service aisle requirements.

The Corvus Blue Whale ESS differs from other ESS technologies available in the market in that it is specifically designed for use in vessels such as Cruise, Ro-Pax, Ro-Ro, Mega Yachts and other large vessels where the operational profiles calls for slow charge and discharge rates and a product that enables emission free sailing over longer periods of time and/or emission free port stays. The system has been developed with larger installations (>10MWh total system energy) in mind.

Applications

Blue Whale is ideal for applications that are in need of a large amount of energy at a cost effective kWh price. Typical vessel-types are:

- Cruise ships
- Ro-Ro/Pax
- Yacht
- Merchant
- Sightseeing/Workboats
- Inland Vessels

Features

- Low C-Rate – for slow charge and discharge
- Industry leading volumetric and gravimetric room energy density
- Designed for voltages up to 1140 VDC
- Low installation and commissioning time
- Very cost-efficient for large installations
- Enhanced reliability with contained power connections
- Weight and volume reduced ~30% and ~50 % compared to Orca Energy
- Flexible and modularised design
- No service aisles required
- Passive single-cell Thermal Runaway protection
- Scalable capacity and voltage according to vessel requirements
- Industry-proven Battery Management System (BMS)
- Remote monitoring capabilities
- Enhanced EMI immunity design for maritime environments

Figure G.1: Information about Corvus blue whale

Corvus Energy

Technical Specifications | Corvus Blue Whale

Performance Specifications	
C-Rate - Peak (Discharge / Charge)	1C / 1C for 20 minutes
C-Rate - Continuous (Discharge / Charge)	0,7C /0,7C

System Specifications	
Single Module Size / Increments	43 kWh / 80 VDC
Single Pack Range	301-4816 kWh / 571 - 1142 VDC
Max Gravimetric Density - **Room**	112 Wh/kg | 8,9 kg/kWh
Max Volumetric Density - **Room**	77 Wh/l

Example Pack - 6 Strings	
Energy	3612 kWh
Voltage	Max: 1142 VDC | Nom: 1075 VDC | Min: 1008 VDC
Dimensions	Height: 2850 mm I Width: 1390 mm I Length: 10 565 mm
Weight	30 550 kg

Example System - 4 Packs of 6 Strings	
Energy	14 448 kWh
Voltage	Max: 1142 VDC | Nom: 1075 VDC | Min: 1008 VDC
Dimensions	Height: 2850 mm | Width: 5560 mm | Length: 10 565 mm
Weight	122 200 kg

Safety Specifications	
Thermal Runaway Anti-Propagation	Passive cell-level thermal runaway isolation with exhaust gas system
Fire Suppression	Per SOLAS, class and Corvus recommendation
Disconnect Circuit	Hardware-based fail-safe for over-temperature and over-voltage
Short Circuit Protection	Fuses included on the module and string level
Emergency Stop Circuit	Hard-wired
Ground Fault Detection	Integrated
Disconnect Switchgear Rating	Full load

General Specifications	
Class Compliance	DNV GL, Lloyds Register, Bureau Veritas, ABS
Type Approval	Pending
Ingress Protection	System: IP44
Cooling	Forced air
Vibration and Shock	UNT38.3, DNVGL-CG-0339, IEC 60068-2-6
EMC	IEC 61000-4, IEC 60945, CISPR16-2-1

2021-04-06

Figure G.2: Battery specification about Corvus Blue whale

Appendix H

Functions

Explanation of functions, everything is coded in pyhton. There are several libraries used within Python such as: Numpy, matplotlib, pandas, math, widgets.

H.1 realistic_hs_tp_combinations()

Function to find the binary matrix for the realistic sea conditions (Hs and Tp combinations) for a range matrix for battery ship. Combining the observed Hs and Tp combinations

Input	Type	Description
Hs	List	List of significant wave heights
Tp	List	List of wave periods
zone	Numpy array	Numpy array as matrix with the observations for given nautic zone

Table H.1: Input for python function realistic_hs_tp_combinations()

Output: numpy array with a binary matrix of which hs and tp combinations are realistic to occur.

H.2 wind_wtref(Hs)

Function to estimate the wind speed from a given hs, from Equation 3.1.

Input	Type	Description
Hs	int	Significant wave height

Table H.2: Input for python function wind_wtref()

Output: Wind speed

H.3 wind_decomp(Hs)

Function to decompose the wind into eastward and northward components

Input	Type	Description
wind_vel	int	velocity of the wind
deg	int	degree of angel the wind blows

Table H.3: Input for python function wind_decomp()

Output: u10, v10

H.4 beaufort_scale(wind_speed)

Function to define where on the Beaufort scale the wind is

Input	Type	Description
winds_speed	int	Wind speed in m/s

Table H.4: Input for python function beaufort_scale()

H.5 wave_direction()

Function to get a random wave direction with the probabilities for nautic zone 11.

Output: wave direction

H.6 sims(sogs, simulations, legs, dist)

Function to run one simulation of the Monte Carlo simulations.

Input	Type	Description
sog	int	speed over water in knots
simulations	int	number of simulations
dist	int	distance of leg

Table H.5: Input for python function for sims()

Output: DataFrame with power for machinery and auxiliary machinery for one simulation

H.7 multiple_sims(sogs, simulations, legs, dist)

Function to run multiple simulations.

Input	Type	Description
sogs	list	list with speed over water in knots
simulations	int	number of simulations
legs	int	number of legs
dist	int	distance of leg

Table H.6: Input for python function for multiple_sims()

Output: CSV with the different power consumption simulations for the different speeds

H.8 range_calculations(sogs)

Function to find the power consumption for the Hs and Tp diagram for zone 11, this will be used in the interactive matrix.

Input	Type	Description
sogs	list of int	List of integers

Table H.7: Input for python function range_calculations()

Output: DataFrame with the power prediction for different weather conditions

H.9 energy_consumption_bars(csvfile, sogs)

Function to divide the power consumption into bars of 1000 kWh, and counting the numbers inside the bars.

Input	Type	Description
Csvfile	CSV filename	CSV file with energy consumption data
sogs	list of int	List of integers

Table H.8: Input for python function energy_consumption_bars()

Output: CSV file for each individual speed with their power consumption bars and their probability.

H.10 energy_c_histogram(csvfile, sog)

Function to visualize of energy consumption where the consumption is split into bars of 1000 kWh and with a corresponding probability.

Input	Type	Description
Csvfile	CSV filename	CSV file with energy consumption data in 1000 kWh bars
sogs	list of int	List of integers

Table H.9: Input for python function energy_c_histogram()

Output: Visualization

H.11 cumulative_prob(csvfile, sogs)

Function to calculate the cumulative probability for the energy consumption.

Input	Type	Description
Csvfile	CSV filename	CSV file with energy consumption data
sogs	list of int	List of integers

Table H.10: Input for python function cumulative_prob()

Output: CSV file with the cumulative probability of energy consumption for the different sogs (speed over water).

H.12 all_speed_plots_prob(csvfile, y_val)

Function to visualize the cumulative probabilities for the different speeds, and finding the needed battery weight for a given sailing probability.

Input	Type	Description
Csvfile	CSV filename	CSV file with energy consumption data and their cumulative probability
y_val	float	Probability of reaching destination

Table H.11: Input for python function all_speed_plots_prob

Output: Visualization of the cumulative probability distribution with the needed battery weight for the given probability.

H.13 plot_probability_speed(csvfile, energy_limits)

Function visualizing the probability of being able to reach destination for a given speed .

Input	Type	Description
Csvfile	CSV filename	CSV file with energy consumption data
energy_limits	int	maximal energy consumption on trip

Table H.12: Input for python function plot_probability_speed()

Output: Visualization of probability of reach destination for a given speed

H.14 cumulative_speed_prob(csv, power_limit, capacity)

Function to find cumulative probability of reaching destination.

Input	Type	Description
csv	CSV filename	CSV file with energy consumption data
power_limits	int	maximal power consumption on trip
capacity	int	maximum battery capacity

Table H.13: Input for python function cumulative_speed_prob()

Output: Array with the count of the optimal speeds with given power limit and battery capacity.

H.15 cumulative_prob_speeds()

Function to visualize the cumulative probability of optimal speed reaching destination.

Output: Visualization of the cumulative probability of optimal speed reaching destination

NTNU
Norwegian University of
Science and Technology